UNIVERSITY OF TROMSØ UIT

FACULTY OF SCIENCE AND TECHNOLOGY
DEPARTMENT OF GEOLOGY

Relationships between metamorphism and deformation in the Nordmannvik nappe, south of Lyngseidet: a focus on high grade relics

Thomas HIBELOT

GEO-3900 Master's Thesis in Geology
May 2013

UNIVERSITY OF TROMSØ UIT

FACULTY OF SCIENCE AND TECHNOLOGY
DEPARTMENT OF GEOLOGY

Relationships between metamorphism and deformation in the Nordmannvik nappe, south of Lyngseidet: a focus on high grade relics

Thomas HIBELOT

GEO-3900 Master's Thesis in Geology
May 2013

AKNOWLEDGMENTS

I would like to thank my supervisors Holger Stünitz and Synnøve Elvevold for their great advices thoughout this work. Their knowledges and involment in this work have been a precious help and I am really glad to have been part of this project. I am also grateful toward Luca Menegon and Steffen Bergh for their useful suggestions about field work. The Geology Department of the University of Tromsø is also warmly acknowledged for the great opportunitites and facilities that are proposed, and provided to international students.

Livia thank you so much for your company during this project. It was a real pleasure to work with you. I am feeling lucky and honoured that we could work together.

Marishka, you have been supporting me a lot during all this time, despite the hard time you had yourself. I am indebted toward you for that. Thank you so much.

Tanya, Potato, Masha, Nioky, Sophie, Sacha, Irina, Darina, Anna, Aleksander, Thibaud, Alexey, Andrey and many others; thank you guys. Your good mood and energy have been very important and supportive to me. It's essential to have good friends like you to keep on running.

Bon et toi JB je t'oublie pas. Tu es un peu comme mon petit frère dingo (mais vraiment dingo !). Merci pour toute l'aide, les discussions et les delires de cette année; ça fait du bien d'être idiot des fois! Flo, maman, papa ainsi que toute ma famille et amis, merci d'être toujours present quand j'en ai besoin. Vous êtes en or (ce qui tombe bien pour un géologue)!

Tromsø, May 2013,
Thomas Hibelot

ABSTRACT

The Nordmannvik nappe (Lyngen fjord, northern Norway) is a high grade tectonic unit dominated by mylonitic garnet-kyanite-mica gneisses, with additional calc-sillicates, mafics and high grade relics. The unit was principaly deformed during the Scandian event of the Caledonian orogeny, reaching at least an upper amphibolite facies. A metamorphic peak, set at a minimum of 750°C / 0.9 GPa, has been recorded in both metapelites and mafic bodies. Petrographic evidences have shown that Scandian garnet-kyanite-mica gneisses evolved by dehydratation reactions before their subsequent decompression in a late stage, coevally with the implementation of a mylonitic fabric. A main aspect of this work concerned the identification of high grade lenses in which the Scandian mylonitic fabric was not observed. Some of these lenses composed of weakly deformed garnet-sillimanite gneisses have reached a granulite facies identified by the assemblage Qtz + Kfs + Grt + Sil + melt. Such high grade rocks with some mafic lenses have shown evidences for a pre-Scandian metamorphic event most likely composed of a prograde orogenic path followed by a subsequent decompression of the high grade assemblages. Because pre-Scandian pelitic rocks are observed in the area, it is concluded that the Nordmannvik nappe must not be included in the oceanic rocks composing the Upper Allochton, as it is usually presented in the literature. Instead, petrographic similarities between rocks from the Nordmannvik nappe and from the lower units suggest that the Nordmannvik nappe belongs to the upper Middle Allochton, made of metasediments from the outermost Baltica margins. In addition and based on petrographic and structural elements, the phyllite unit which outcrops along the upper contact of the Nordmannvik nappe is suggested to have derived from the garnet-kyanite-mica gneisses rather than from the overlying mafics of the Lyngen Nappe Complex. Eventually, structural features support the Scandian character of the Nordmannvik nappe. Westward dipping foliation planes and a general SE transport of the nappe match the regional settings usually attributed to the nappe stacking episode of the Caledonian orogeny. Temperature ranges of quartz dynamic recrystallization, yet poorly constrained, have not given any results which may conflict with the petrography.

Key worlds: Caledonian orogeny, Nordmannvik nappe, mineral reactions, basement tectonics, partial melting, migmatite, mylonitization, fluid-rock interactions**.**

CONTENTS

1 INTRODUCTION

1.1 GOAL OF THE PROJECT

The present thesis is a metamorphic study of high-grade rocks from the Nordmannvik Nappe outcropping in the surroundings of Lyngseidet. Along the western Lyngen fjord, the Nordmannvik Nappe occurs as a thin elongated metamorphic body sandwiched between the Lyngen Nappe Complex and the Kålfjord Nappe. Rocks of the Nordmannvik nappe are exposed along the Lyngen fjord and good outcrops occur along the coastal road. Literature is not extensive about this area and the unit has been poorly investigated when compared to the surrounding ones.

The main purpose of this work is to study structural features and metamorphic mineral reactions which characterize the area. Retrogression processes and partial melting notably, have been under the scope of petrological studies and their occurrences documented. In addition, the northern part of the peninsula extending from Lyngseidet to Koppangen has been mapped in collaboration with Livia Nardini, MSc student working on the same project. Phyllites, which are found at the contact between the Nordmannvik Nappe and its overlying unit have also been studied. Eventually, correlation between the large scale data, and the detail mapping performed in the peninsula are done.

The study of the Nordmannvik Nappe unit relates to works carried out by H. Stünitz and L. Menegon, from the University of Tromsø who have been investigating rocks from the Kalak Nappe Complex in order to study processes such as melt segregation and retrogression in lens shaped rock bodies. The discovery of similar settings within the Nordmannvik nappe has been the trigger of our present investigations.

1.2 GEOGRAPHICAL DESCRIPTION OF THE AREA

The Nordmannvik Nappe crops out along a north-south directed belt. The rocks studied herein occur in an area localized between Furuflaten and Koppangen (Troms county, northern Norway) where the coastal road is ending (Fig. 1.1). The road section extending between these two points shows good quality outcrops and is propitious to sampling. The investigated area is topographically

low, dominantly between the sea level and about 150 meters but the relief increases dramatically as we approach the steep flanks of the Lyngen Alps. The most important town in the area is Lyngseidet, reached in 1.5 hours driving from Tromsø. In addition, two peninsulaes lie along the coastal road. The southern peninsula, north of Furuflaten has been poorly investigated, the focus beeing done on the northern peninsula (north of Lyngseidet) which appeared far better when it comes to outcrop abundance. Most of the work has been focusing on the coastal road crossing this peninsula.

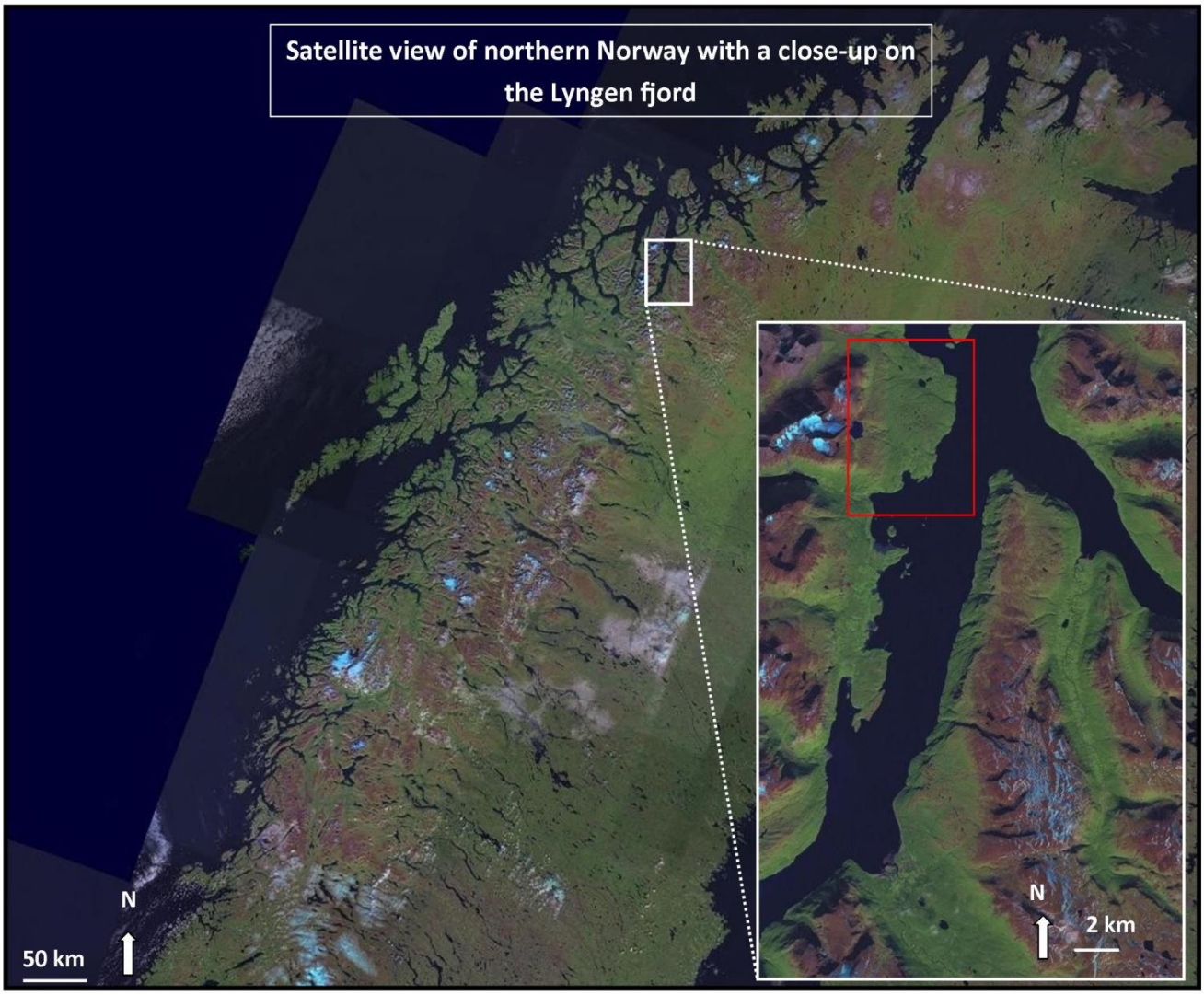

Figure 1.1 Geographical location of the Lyngen fjord in northern Norway. The red frame delimits the northerm peninsula which has been mapped. Satellite images are from http://kart.finn.no/.

1.3 ABBREVIATIONS AND CONVENTIONS

Abbreviations used in this thesis are listed in table 1. In mapping, conventional signs have been used, based on Mc Clay (1987).

Table 1.1 Abbreviations used in the thesis.

Minerals	Localities and structural units	Technical abbreviations
Amph = amphibole	LNC = Lyngen Nappe Complex	BLG = grain boundary bulging
Bt = biotite	TNC = Tromsø Nappe Complex	CPO = c-axis preferred orientation
Cal = calcite	KNC = Kalak Nappe Complex	GBM = grain boundary migration
Cpx = clinopyroxene	WGR = Western Gneiss Region	HP = high pressure
Czo = clinozoisite		HT = high temperature
Ep = epidote		Fig = figure
Grt = garnet		SGR = subgrain rotation
Hbl = hornblende		MP = medium pressure
Kfs = K-feldspar		MT = medium temperature
Ky = kyanite		UHP = ultra high pressure
Ms = muscovite		UHT = ultra high temperature
Sil = sillimanite		
Pl = plagioclase		
Qtz = quartz		
Rt = rutile		
Tur = Turmaline		
Ttn = titanite		
Zo = zoisite		
Zr = zircon		

1.4 REGIONAL SETTINGS

1.4.1 INTRODUCTION

This part of the report aims to present and provide guidance throughout the different events which made up the Caledonian orogeny. Focus is done on the main tectonometamorphic events (phases), the resulting tectonostratigraphy and the characteristics of each of the tectonic units. Available geochronology and former work dealing with the investigated area are presented. A general map of the Scandinavian Caledonides is shown in Figure 1.2.

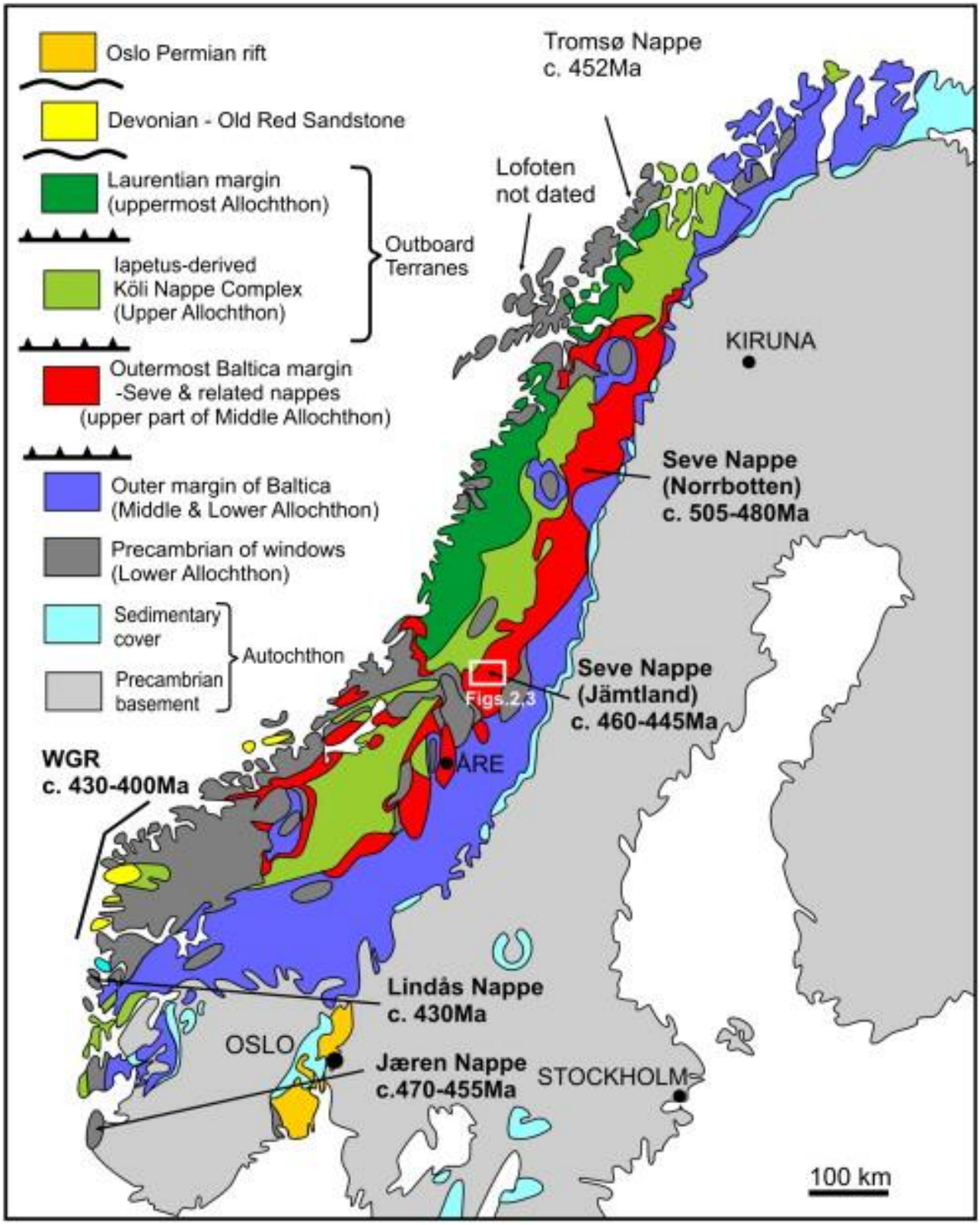

Figure 1.2 Tectonic map of the Scandinavian Caledonides with eclogite occurrences, modified from Gee et al. (2008). The white frame is not relevant for this work. From Janák et al. (2013).

1.4.1.1 GEOLOGICAL FRAMEWORK

The Caledonian orogeny spanned from the Neoproterozoic to the early Paleozoic, and involved Baltica and Laurentia (Andreasson, 1993 ; Torsvik et al., 1996 ; Roberts, 2003 ; Gee et al., 2008 and others). The Baltican margin notably comprises most of the actual Norwegian territory whereas Laurentia is well evidenced on the eastern margin of Greenland. Both margins arose from the initial break-up of Rodinia (Torsvik et al., 1996; Andreasson et al., 1998) and are broadly dominated by Paleoproterozoic and Archean crystalline crust (Gee et al, 2008). Caledonian rocks north of 66°N are referred to as the Arctic Caledonides where rich exposure and deep erosional level are propitious to rewarding investigations (Andreasson, 1993).

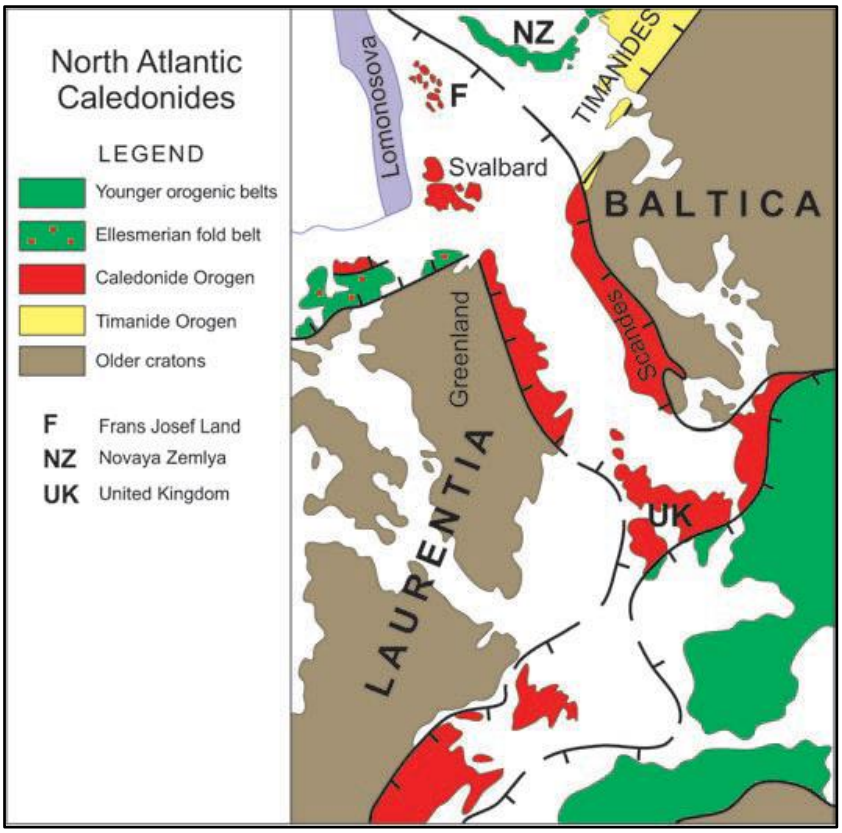

Figure 1.3 Outline of the North Atlantic Caledonides and relationship between Laurentia and Baltica. From Gee et al. (2008).

The Laurentian platform margin, from eastern Canada to Eastern Greenland and Svalbard is defined by a thick Cambrian to mid-Ordovician carbonate bank which is covered by Cambrian siliclastics from late Vendian to early Cambrian. On the other side, the Baltican platform comprises siliclastics ranging all over the Cambrian, with black shale deposition during the middle/late Cambrian to early Tremadocian (Bergh and Andresen, 1985; Gee et al., 2008).

An overall description of the Caledonian orogeny relates the merger process of Baltica and Laurentia through several minor collisional events before ultimately ending by the main NW directed subductional event of Baltica underneath Laurentia in Mid Silurian-Early Devonian time (Scandian event). This collision has been on a par with the closure of the Iapetus Ocean (initially located between the two continental blocks), and accounted for the main event of the Caledonian orogeny, eventually leading to the creation of the Pangea supercontinent.

It has to be kept in mind that this short description is a simplication of the plate reconstruction settings. Though this thesis does not focus on the Pre-Caledonian paleogeography, the tectono-history is no longer a matter of only two continents and margins (Baltica, Laurentia) with a single ocean between. These facts won't be detailed more herein and the interested reader can refer to Andreasson et al. (1998).

1.4.1.2 Synthetic review of Caledonian tectonic events

Three distinct phases / events compose the Caledonian orogeny. Three arcs related collisions led to the main subductional event in the Silurian to Early Devonian, when most of the nappes and macrostructures have been emplaced. A fouth event of extensional nature was also recorded partially coeval with the main thrusting event and the occurrence of a sinistral transpressive shear, with upright folding in some areas (Roberts, 2003).

According to old publications, a metamorphic event older than the terminal Silurian, (main Caledonian or Scandian) has been recognized within some of the Caledonian nappes (Gee, 1975; Roberts, 2003). Though this event is not considered anymore, K-Ar and Rb-Sr based datings have given birth to the term *Finnmarkian* (Sturt et al., 1978; Roberts, 2003) for a tectonothermal event in Northern Norway which ranges from Late Cambrian to Earliest Ordovician time. This event, would have restricly concerned tectonic units from the Baltican margin (Andreasson et al., 1998) and was assumed to have resulted from the collision of the Baltican margin with an inferred magmatic arc above a seaward facing subduction zone (Roberts, 2003 and references therein).

In a recent publication, Corfu et al. (2007) suggested that the term "Finnmarkian" is not appropriate and its original definition bearing on incorrect basis. Geochronology carried out at the time of the emergence of the "Finnmarkian" concept was based on relationship between structural and intrusive elements which are not any longer applicable. Arguments supporting this assumption are to be found in Corfu et al. (2007). The different phases of the orogeny are now reviewed.

TRONDHEIM EVENT

The Trondheim event is recognized in parts of the Upper Allochton and accounts for a principal phase of deformation and metamorphism. Eide and Lardeaux (2002) described ophiolite obduction and blueschist facies metamorphic paragenesis from ophiolites. U-Pb zircon ages in the range c. 493-482 Ma have been obtained in plagiogranite dykes and sheets from some of these supra-subduction-zone ophiolites (Roberts, 2003 and references therein). This obduction/metamorphic event has been inferred to occur in the Lower Ordovician accordingly with fossil datations. In addition, both Baltican and Laurentian affinities are inferred out of faunas and lithological concordances but the general dominance of Laurentian faunas in the central Caledonides led to consider a model in which the ophiolites have been generated in a peri-Laurentian situation (Roberts, 2003 and references therein). Torsvik et al. (1996) proposed that an incipient anticlockwise rotation of Baltica away from Siberia and toward Laurentia, occurred during the Trondheim event. The Iapetus Ocean, initially located between the two continental blocks, started to be contracted at this time (Roberts, 2003).

TACONIAN EVENT

During the Mid-to-Late Ordovician occurred a Taconian equivalent tectonothermal phase. This event mainly concerned the Uppermost Allochton but some parts of the Upper Allochton experienced it as well (eg. Smøla Island, central Norway) (Roberts, 2003). In the Ordovician-earliest Silurian, the Smøla-Hitra batholith (Smøla Island) consists in deformed and weakly metamorphosed sedimentary rock from the Early to Middle Ordovician which were intruded by evolved-arc plutons (Roberts, 2003 and references therein). A Mid Ordovician tectonothermal activity has also been identified in the southern part of the Uppermost Allochton where comparable Late Ordovician-Early Silurian pluton cut earlier mylonitic foliations (Roberts, 2003 and references therein).

According to Roberts (2003 and references therein), accretions onto a continental margin are inferred to have occurred around 470-465 Ma. Eclogites, yielding a Caradocian metamorphic age (449,5 – 460,9 Ma) have been discovered, indicating that the metamorphism locally reached an eclogite facies. This Taconian event is thought to have been followed by a rapid exhumation (Roberts, 2003 and references therein) which has been upperly constrained in northern parts of the Uppermost Allochton by latest Ordovician-Early Silurian aged faunas (Bjørlykke and Olaussen, 1981).

SCANDIAN EVENT

As the principal tectonometamorphic event, the Scandian event gave rise to the current characteristic distribution of Caledonian allochtons in Norway and Sweden (Gee, 1975; Roberts, 2003). An oblique Silurian collision between Baltica and Laurentia led to the subduction of the Baltican margin underneath Laurentia sometimes reaching eclogite facies at depth of 125 km at 407 Ma (Roberts, 2003 and references therein). Several evidences demonstrate that the timing of the Scandian event varies widely depending upon the investigated locations. In this work, an age of 425-426 Ma proposed by Dallmeyer and Andresen (1992) is considered. It is believed that the rapid subduction was followed by a very fast exhumation and the entire Scandian event is assumed to have been of a really short duration, perhaps 10 Ma. This major event affected all the main allochtons to greater or lesser extents (Roberts, 2003).

The Caledonian eclogites in western Norway were formed in a subduction zone. However, the high pressure rocks in Greenland that were formed at the same time demonstrate that West Norway could not have been subducted underneath present-day Greenland (which belongs to Laurentia).

A recent theory carried out by Elvevold and Gilotti (2000) states that crustal thrust-imbrication and thickening may have dominated on the Laurentian side during the Scandian collision. Their research in northeast Greenland has shown that the Laurentian crust may have experienced pressure great enough to double its thickness but not more. Also lacking is evidence of garnet-peridotites that would indicate crustal interactions with mantle material, typically occurring in subduction zone (Elvevold and Gilotti, 2000). High grade eclogites have been found in Greenland as well as ultrahigh-pressure metamorphism (Gilotti and Ravna, 2002). This eclogite facies metamorphism (in Greenland) has been further documented by Gilotti et al., 2004; Mc Clelland et al., 2006; and Gilotti and Mc Clelland, 2007.

LATE-TO-POST SCANDIAN EVENT

An extensional episode has been recorded during and after the principal Scandian orogenic event. This late stage extensional deformation have led to several discussions since the 70's when pinch and swell structures were found in the Seve Nappe Complex (Sweden), and assumed to result from a gravity-driven nappe displacement (Andreasson et al., 1998 and references therein). A 60% vertical shortening has then, been inferred out of boudins structures by Ramberg and Sjostrom (1973). A different interpretation of these structures came up later, asserting that the gravitational collapse has occurred onto the assembled nappe pile (Gee, 1978).

Since the late 80's, kinematic analysis have been performed and theories evolved again. Nowaday, the extensional event is thought to partly arise from gravitational collapse of the orogenic wedge (Roberts, 1983; Andersen 1998) but is also assumed to have been accomodated by divergent driving forces as a back sliding along a metasedimentary decollement zone or some west dipping shear zones (Fossen, 1992). In the Ofoten-Tysfjord area, orientation of cross folds suggests a sinistral shear affecting the orogeny from the Early Silurian to the Late Devonian (Steltenpohl, 1988) and may support the extensional shearing-related episode theory.

1.4.2 CALEDONIAN UNITS ARCHITECTURE

1.4.2.1 PRESENTATION

The Scandinavian Caledonides are made up of several thrust nappes composed of various lithologies which underwent a large range of metamorphism grades (Roberts, 2003). This stack of thin, but far-travelled, thrust nappes were emplaced onto the Baltican outer platform during the mid-late Silurian collision of Baltica and Laurentia (Andresen and Steltenpohl, 1994).

An eastward translation of the Baltican passive margin remnants (formerly detached from Baltica) and some Iapetus ocean pieces onto the Fennoscandian shield resulted in four distinctive allochtons (Roberts, 2003). The resulting tectonostratigraphy has been divided into a Lower, Middle, Upper and Uppermost allochtons, all involving nappes translation up to several hundreds of kilometers (Roberts and Gee, 1983; Roberts, 2003). These allochtones lay onto parautochtonous units and autochtonous sediment covers that coat the crystalline Precambrien basement.

In a recent paper Gee et al (2008) suggests that the Lower and Middle Allochton represent the telescoped pre-collisional continental margin of Baltica. The Upper Allochton then, is mostly composed of sedimentary and igneous rocks derived from the Iapetus Ocean which include ophiolites and Island Arc complexes (Gee et al, 2008 and references therein). The Uppermost Allochton terminates the nappe sequence with ophiolites and arc complexes from both the Baltican and the Laurentian margin. This nappe complexe therefore includes the most exotics elements in the Scandinavian Caledonides.

Based on the observations made further in this thesis, the Nordmannvik nappe investigated in the present work is most likely part of the Middle Allochton and not the Upper Allochton as the literature usually describes this unit. In our study area, the discovery of pre-Scandian granulite facies metapelites is incompatible with the presumed oceanic floor composition of the Upper

Allochton. This point is further discussed in chapter 4. A more detailed description of the units layout in the Troms County is now given.

1.4.2.1 Review of the Caledonian units in Troms

The Scandinavian Caledonides are well represented in Troms, Northern Norway (Fig. 1.4). Their evolution is rather complex and geochronologic studies carried out support a polymetamorphic evolution (Dallmeyer and Andersen, 1992). A detailed description of all the different units and their subdivisions has been achieved by Andresen (1988). A simple geologic map of the Scandinavian Caledonides of northern Norway is presented below.

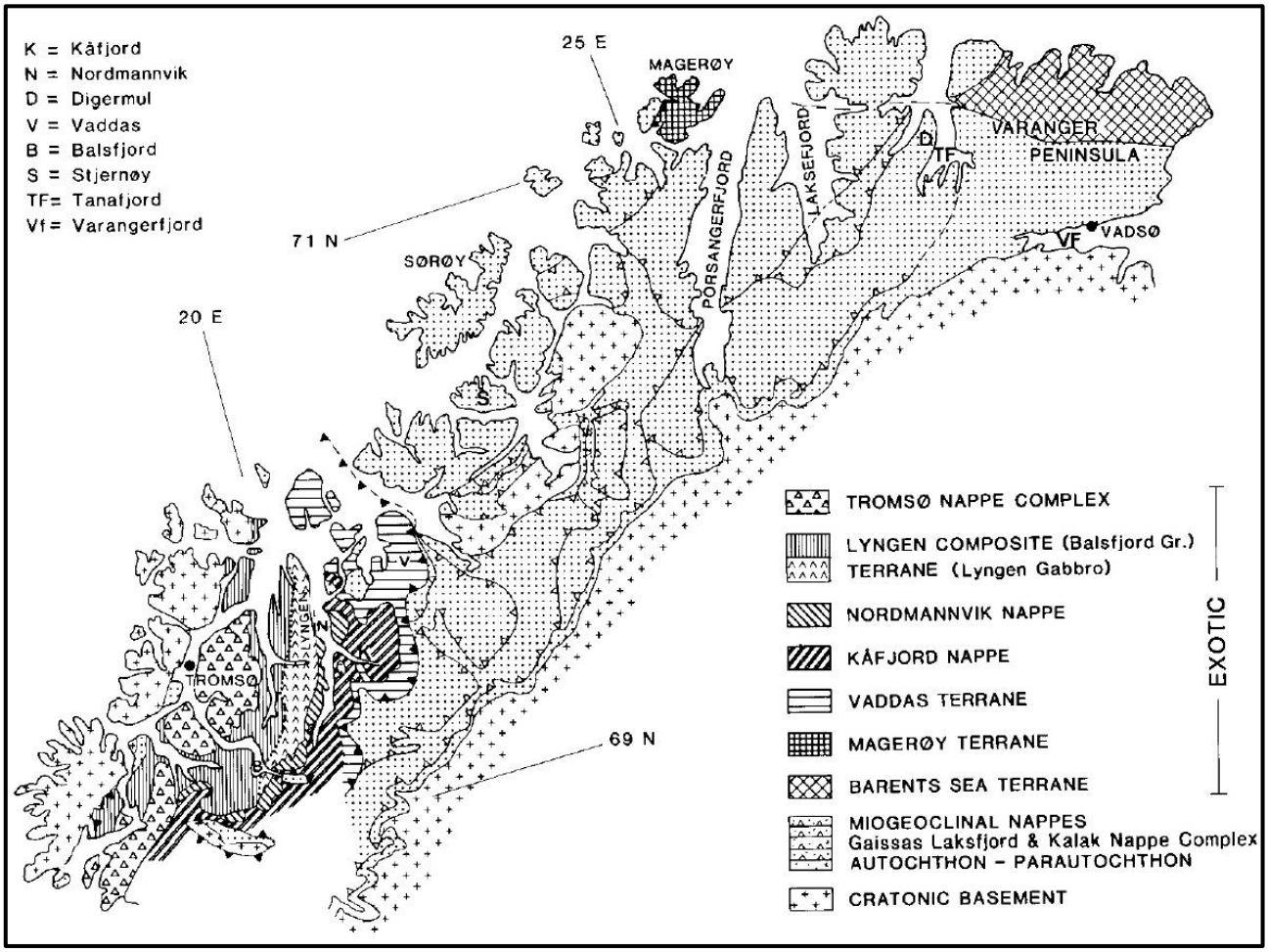

Figure 1.4 Simplified geological map of the Scandinavian Caledonides in Finnmark and northernmost Troms showing the main tectonic units and terranes. From Andresen (1988).

Except for the Lower Allochton which is absent, all allochtons, autochtons and parautochtons are observable in Troms. They are in ascendant order, the Dividal Group, The Kalak Nappe Complex, the Vaddas Nappe, the Kålfjord Nappe, the Nordmannvik Nappe, the Lyngen Nappe Complex and the Tromsø Nappe Complex.

The Dividal group comprises the autochton and the parautochtone sequences which both acts as a base for the Middle Allochton comprising the Kalak Nappe Complex. In the literature, the Vaddas Nappe, the Kålfjord Nappe, the Nordmannvik and the Lyngen Nappe Complex (Lyngen Ophiolite and Balsfjord Group) form the Upper Allochton (Fig. 1.5). Nevertheless and considering the results obtained in this thesis another tectonostratigraphy is proposed (cf. chapter 4) in which the Nordmannvik nappe is part of the Middle Allochton.

Concerning the exotic terranes (those comprised in the Upper Allochton and above), little is known about the absolut timing of their orogenic evolution. Nevertheless these terranes are observed in an area supposed to be a transitional zone between a Finnmarkian and a Scandian related orogenic zone (Lindstrøm and Andresen, 1992). The boundary between both of these orogenic events is suggested at the base of the Vaddas Nappe.

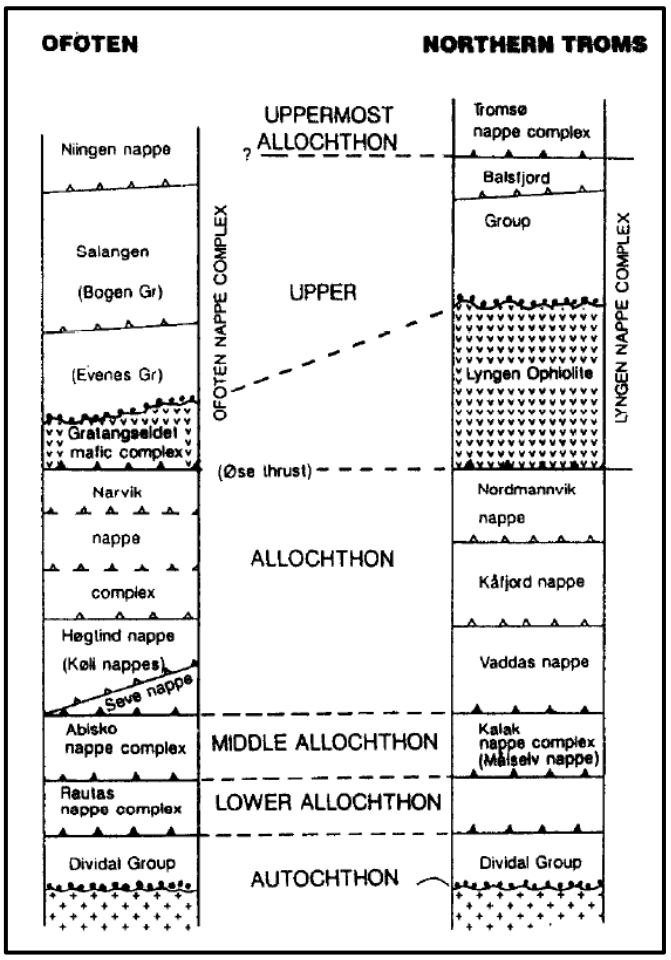

Figure 1.5 Proposed tectonostratigraphic correlation of the Ofoten and Troms (Balsfjord) nappe stacks. Relative thickness of the tectonic units is highly schematic and not to scale. From Andresen and Steltenpohl (1994).

Figure 1.5 presents and compares the stratigraphy in the Ofoten area (Nordland) and in Troms. The figure aims to be a reminder of the unit layout but the proposed similarities between both the Ofoten and Troms region won't be detailed herein. Thought, it has to be kept in mind that some structures clearly linked both regions. The Øse thrust, for instance is a post-thermal peak thrust marking very steep metamorphic gradients separating the Lyngen Nappe Complex (LNC) from the underlying amphibolite to granulite facies Nordmannvik nappe (Bergh and Andresen, 1985). The different stratigraphic units are now described following an ascendant order.

The *Precambrian basement rocks* are exposed in three structurally different settings. The east part of the orogeny belt shows undisturbed crystalline foreland basement (1) whereas the middle of the orogeny displays large and small tectonic windows (2). In the Western Basement Complex (coastal basement region), Precambrian basement rocks showing various degrees of surimposed Caledonian structures are observed (3). The basement rocks range in age from Archean to Mid Proterozoic (Andresen, 1988).

The *Kalak Nappe Complex* (KNC) is made up of eight nappes or thrust sheets (Ramsay et al., 1985; Andresen, 1988). The unit has undergone two dominant deformation stages, up to five locally (Corfu et al., 2007). The main differences with the underlying units are a higher metamorphic grade, a more complex deformational style, the frequent occurrence of mafic dikes and other type of intrusives and large volumes of basement rocks occurrence (Andresen, 1988). Schists, basement rocks and psammites account for the main rock type encountered in this unit.

It has been at first, widely accepted that the KNC is derived from the western margin of Baltica as the lithology and ages of rocks from this unit match those of the autochtonous basement (Andersen, 1988 and references therein).

In a recent paper, Corfu et al. (2007) demonstrated that the KNC did not evolve on the margin of the Baltic craton. Based on granites and migmatites datations, the authors asserted that the KNC must have been derived from outside of Baltica prior to the Scandian event during the Silurian. Accordingly to geological and geochronological analogies, they suggested a potential Laurentian origin for the KNC.

Anyhow, regarding the previously mentioned unit, it has to be pointed out that a general upward and westward increase in metamorphic grade is observed toward the upper parts of the KNC (Andresen, 1988).

Exotic terranes are divided in two groups defined by their tectonic settings. In Troms, they are observed as a sequence of composite flat-lying nappes on top of the KNC, and are the units composing the Upper and Uppermost Allochtons. In Finnmark, a distinct block forming the northeastern half of the Varanger Peninsula has a thrust contact against the overlying KNC towards the west (Andresen, 1988). This "Barent Sea terrane" will not be discussed more herein but a detailed review is available in Andresen's publication (1988).

The *Vaddas nappe* is a relatively undisturbed right way up stratigraphic and magmatic succession (Lindahl et al., 2005) basally composed of interbedded marbles and schists which are conformably overlain by a quartzite dominated sequence (Padget, 1955; Dallmeyer and Andresen, 1992). A sequence of marble and mafic metavolcanic rock makes up the upper levels of the Vaddas nappe. Metamorphic grade in the Vaddas Nappe goes from upper greenschist facies to locally lowermost amphibolite facies (Lindhal et al., 2005; Andresen, 1988; Binns, 1978) and a single tectonothermal event is inferred (Dallmeyer and Andresen, 1992). An extensive description of this nappe is beyond the scope of this thesis but an comprehensive description of rocks present in the Vaddas Nappe has been made by Padget (1955) who separated the non-granitized rock (currently part of the Vaddas Nappe) and the granitized rock, structurally bellow and now part of the Middle Allochton (Andresen, 1988). The Vaddas Nappe has undergone a complex intrusion history with gabbro and amphibolite occurences (Lindahl et al., 2005).

It is interesting to highlight the close link existing between the Kalak Nappe Complex, the Vaddas Nappe and the so called Seve-Kalak Superterrane (in Sweden) often cited in the literature. A simple explanation is that the stratigraphic contact between the Kalak and Vaddas Nappe rocks is assumed to be a northern extension of the contact between the Seve and Koli Nappe Complexes in Sweden (Lindahl et al., 2005). This unit will not be detailed herein but it shares lithotectonical similarities with both the Kalak and the Vaddas Nappe. The concept of "Superterrane" then, arose from the amalgamation of all nappes composed of Baltican rift basin infill and rift magmatism in one single structural body (Andreasson et al., 1998). Morover, it is thought that the actual KNC structural settings are possibly linked to the thrusting of the Vaddas Nappe to its current position, and is

somehow related to the Scandian event (Lindahl et al., 2005 and references therein). Evidences for this are based on structural works which have shown that the tectonographic succession now exposed in the Vaddas area has undergone a late to post Scandian W- to the SW directed collapse of the outer margin of the orogeny (Lindhal et al., 2005).

Separated from the Vaddas nappe by the Cappis thrust is the *Kåfjord nappe*, which continues the lower Upper Allochton (Dallmeyer and Andresen, 1992 and references therein). Marbles, metapsammites and garnet mica schists composed the lower part of this unit whereas upper parts of it are made of mylonitic gneisses with locally boudinaged amphibolite layers. The given metamorphic grade is middle amphibolite facies throughout the Kåfjord Nappe but it appears difficult to establish a lithostratigraphy because of the high strain, the extensive mylonitization and the development of several internal faults in this unit (Andresen, 1988). Bergh and Andresen (1985) recognized three distinct episodes of deformation (all part of the same global metamorphic event) which resemble those affecting the overlying Nordmannvik Nappe. The metamorphic grade of the Kålfjord Nappe remains nevertheless lower than in the Nordmannvik Nappe.

The *Nordmannvik Nappe* is a high grade tectonic unit sandwiched between the Kåfjord Nappe and the Lyngen Nappe (Zwann and Roberts, 1978; Andresen, 1988). The Nappe is mainly composed of polymetamorphic rocks which include pervasively mylonitic mica schist, amphibolite bearing gneisses, marbles and local ultramafic lenses (Dallmeyer and Andresen, 1992 and references therein). It has been proposed that an “early” Caledonian metamorphism locally reached the granulite facies (Andresen et al., 1985; Bergh and Andresen, 1985; Dallmeyer and Andresen, 1992). A consequence of this is that the Nordmannvik Nappe may have constituted a metamorphic basement for the overlying Lyngen Nappe Complex (LNC). The metamorphic grade has been defined as middle/upper amphibolite facies with granulite relicts occurring in some mega-porphyroclasts (Lindstrøm and Andresen, 1992; Andresen, 1988). This unit has a particular interest since it recorded a polyphase metamorphic evolution (Bergh and Andresen, 1985 and others) but also because of the occurrence of some high grade relics wrapped in the lower grade mylonitic fabric.

The *Lyngen Nappe Complex* is divided in three distinctive lithotectonics units (Dallmeyer and Andresen, 1992) which are namely the Koppangen formation, the Lyngen Gabbro and the Balsfjord Group (Andresen, 1988).

The *Koppangen formation* is composed of conglomerate-bearing schist metasandstone and accounts for the lower part of this unit. A thrust separates this upper green schist facies unit from the upper amphibolite facies underlying Nordmannvik Nappe (Andresen, 1988).

The *Lyngen Ophiolite* accounts for most of the LNC thickness and is composed of intensely deformed dolerite dike swarms followed by deformed metagabbros. Most of the Lyngen peninsula is thus made of this layered gabbro and some large or small serpentinized ultramafic bodies occur within (Andresen, 1988).This unit is called the Lyngen Ophiolite since the gabbro which composes it is assumed to be part of an ophiolitic complex.

The uppermost unit of the LNC is the *Balsfjord Group*, located west of the Lyngen Ophiolites and has a depositional contact with the gabbros (Minsaa and Sturt, 1985; Andresen, 1988). The bulk of this unit is made of schists, quartzites, conglomerates and various types of carbonate deposits (Andresen and Bergh, 1985; Andresen, 1988). Lithological thickness and clast sizes variations in the conglomerates evidence for a fault controlled basin (Andresen, 1988) and deformation within the Balsfjord Group has been associated with late Silurian/early Devonian (Scandian event) orogenesis (Dallmeyer and Andresen, 1992). The Balsfjord Group forms the upper boundary of the Upper Allochton. Bergh and Andresen (1985) recorded three episodes of deformation, well-defined in this unit.

The uppermost unit observed in Troms, also composing the Uppermost Allochton is the *Tromsø Nappe Complex* (Andresen et al., 1985) and is composed of three non-fossiliferous lithotectonic units (Andresen et al., 1985; Dallmeyer and Andresen, 1992). A structural and metamorphic break is observed at the interface between Balsfjord Group and the Tromsø Nappe Complex (Andresen, 1988).

The TNC is divided into three parts. The Lower Tectonic Unit is made of gneisses, amphibolites, schists and metaigneous rocks. Overlying the Lower Tectonic Unit is the Skattøra Gneiss unit which is mostly composed of amphibolitic gneisses intruded by anorthositic dykes. The Tromsdalstind Complex is the uppermost unit observed in Troms and includes garnet-mica schist, quartzofeldspathic gneisses, calc-silicate gneisses, eclogite-bearing marbles, kyanite-garnet micas schist and biotite microcline gneiss (Dallmeyer and Andersen, 1992). Note that a more recent nappe terminology for this area is given by Zwaan et al. (1998). This paper proposes the following

succession, in ascendant order; the Lyngen Nappe, the Nakkedal Nappe associated with the Skattøra migmatite complexe and the Tromsø Nappe.

1.5 Previous work in the Nordmannvik Nappe

Litterature about the Nordmannvik Nappe is not extensive. If the area is mentioned in many papers treating about the Caledonian orogeny, the nappe is usually shorty described. I found very few papers describing thoroughly the lithological and structural aspects of the nappe. One of these documents is an Msc thesis from Elvevold (1988) (in Norwegian) and another one is a paper from Bergh and Andresen (1985) which has been the main source for the next paragraphs. In addition, a short but very informative paper from Lindstrøm and Andresen (1992) describes a high grade tectonic mega-lense from the Nordmannvik nappe and proposes an age dating for it.

Regarding dating works, a paper from Dallmeyer and Andersen (1992) has been used. This document summarizes previous works and present new data among which some measurements performed in the Nordmannvik Nappe (Table 1.2).

Table 1.2 Gathering of datation works carried out in Troms. After Dallmeyer and Andersen (1992).

Locality and material investigated	Authors	Datation method	Results
Foliated intrusive unit, Kåfjord Nappe	Dangla et al. (1978) Quarnardel et al. (1978)	Poorly-defined Rb-Sr isochron age	440-450 Ma
Eclogite within the Tromsø Nappe Complex.	Griffin and Brueckner (1985)	Sm-Nd mineral isochron age	598 +/- 107 Ma
Fine-grained biotite-microcline metagranite within the Lower structural units of the Tromsø Nappe Complex	Krogh et al. (1990)	Seven point Rb-Sr whole-rock isochron age	433 +/- 11 Ma
Three amphiboles concentrate from units of the Skattøra Gneiss and the Tromsdalstind Complex.	Krogh et al. (1990)	K-Ar ages	448-436 Ma
Syntectonic granite within upper portion of the Balsfjord Group.	Lindstrøm (1988)	Eight points Rb-Sr whole-rock isochron age	432 +/- 7 Ma
Pyroxene-bearing metaigneous rock within the Nordmannvik Nappe.	Lindstrøm (1988)	Rb-Sr whole-rock isochron age	492 +/- 5 Ma
Muscovite throughout southwest Senja	Cumbest et al., 1983; Clark et al., 1985; Cumbest and Dallmeyer, 1985; Dallmeyer, 1991.	^{40}Ar / ^{39}Ar plateau ages	380-390 Ma

Beside these data, Dallmeyer and Andersen (1992) analyzed twelve hornblendes and seven muscovite concentrates from sample collected within various Caledonian nappe complexes exposed in the Troms region. The samples locations are presented in Figure 1.6 and the ^{40} Ar / ^{39} Ar ages obtained are given in Table 1.3. Concerning the Nordmannvik nappe, two ages have been determined out of four samples taken in the area, both giving a calculated ^{40} Ar / ^{39} age of about 429 Ma.

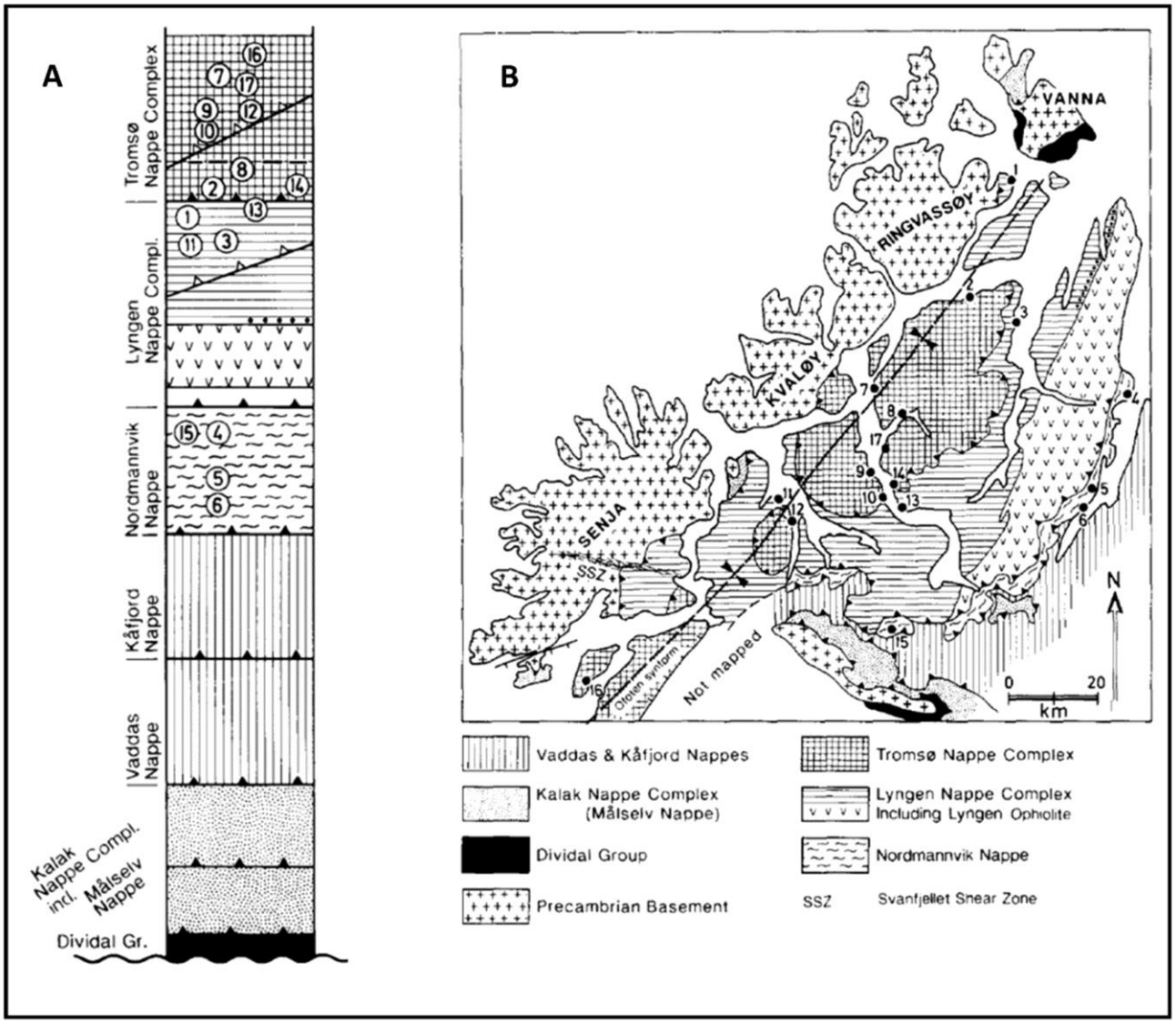

Figure 1.6 (A) Schematic cross section of the lithostratigraphic layout in Troms. Numbers indicate from which tectonic units each sample is originating from. (B) Map of the Troms County with numbers showing sample locations. Both figures are from Dallmeyer and al. (1992).

Table 1.3 ^{39} Ar/ ^{40} Ar isotope correlations from incremental-heating experiments on hornblende concentrates from Caledonian complexes. Modified after Dallmeyer and Andresen (1992)

Sample	% of Total ^{39} Ar	Calculated ^{40} Ar / ^{39} Ar age (Ma).
	Nordmanvik Nappe Complex	
5	92.42	425.8 +/- 2.1
15	98.06	425.8 +/- 1.0
	Lyngen Nappe Complex: Balsfjord Group	
11	56,63	431.8 +/- 1.5
1	85.01	no plateau defined
	Tromsø Nappe Complex: Lower Tectonic Unit	
2	90.47	no plateau defined
14	97.92	448.3 +/- 1.9
8	95.76	456.5 +/- 1.1
	Tromsø Nappe Complex: Tromsdalstind Complex	
10	65.07	485.8 +/- 1.7
12	74.32	no plateau defined
16	79.11	421.0 +/- 2.4
17	86.09	No plateau defined

1.6 DETAILED PETROLOGIC DESCRIPTIONS OF THE NORDMANNVIK NAPPE FROM THE LITERATURE

1.6.1 PRESENTATION

The Nordmannvik Nappe outcrops in several separate locations. Some of them consist in megalenses sandwidched between the underlying Kålfjord Nappe and the overlying Lyngen Nappe Complex whereas others are erosional klippen (Andresen et al., 1985). The nappe is several kilometers thick south of Aursfjord but is thinning eastwards, down to few hundred meters along the shore of Ytre Fiskelausvatn (Bergh et al., 1985). Both, the upper and lower boundary of the nappe are tectonic and mark a significant variation in metamorphic grade. The lower contact is defined by a jump in metamorphic grade from a greenschist / lower amphibolite facies (Kålfjord Nappe) to an upper amphibolite/granulite facies in the Nordmannvik Nappe whereas the upper

contact separates this high grade unit from the greenschist facies of the Lyngen Nappe Complex (Bergh and Andresen, 1985). Highly strained rocks along the contact zone allow determination of the nature of this upper contact. Movement along the contact post-dates the crystallization of the high grade assemblage but is synchronous with the first deformational episode in the Lyngen Nappe Complex. The study area has been divided into two distincts lithotectonic sequences. In the lower sequence, marbles calcsillicates, schists and kyanite-garnet-biotite gneisses dominate and outcrop closeby the mountain Orta. A marble horizon accounts for the base of this sequence. The upper sequence shows a rather similar lithology dominated by sillimanite-bearing kyanite-garnet-biotite gneisses displaying distinctive augen textures. Amphibolite is also present either as massive volumes or as bands in amphibole-biotite gneisses (Bergh and Andresen, 1985). Some gabbro and ultramafic rocks have also been locally observed (Andresen et al., 1985) and some sagvandite bodies are sometimes reported in these ultramafics (Schreyer et al., 1972; Andresen et al., 1985; Lindstrøm and Andresen, 1992). The sagvandite consists in massive carbonate-orthopyroxenites occurring in tectonic lenses within high-grade metamorphism zones and are thought to be metasomatically modified peridotitic ultramafic rocks which could be part of an ophiolitic sequence zones (Schreyer et al., 1972).

1.6.2 GARNET-MICA GNEISSES

Kyanite-garnet-two mica gneiss/schists account for the most widespread lithology. They occur as various types but remain petrographically similar throughout the whole unit. Typical lithologies are coarse-grained augen gneisses, banded gneisses (with alternating quartz-feldspar and biotite-rich layers) and strongly schistose banded micaceous gneisses. Quartz-feldspar lenses and thin layers occur frequently in the upper part of the nappe (Bergh and Andresen, 1985). The sillimanite observed in these mica gneisses appear post-kinematic and likely account for a drop in pressure (Andresen et al., 1985 and references therein).

1.6.3 GRANULITIC GNEISSES

Granulitic gneisses are described as lense-shaped body of felsic rock about 30-40 m thick, wrapped by feldspathic two-mica gneiss and occurring south of Aursfjord. The texture varies from coarse-grained granular to weakly foliated. These gneisses contain up to 50% K-feldspar with both perthitic and myrmekitic intergrowths in addition to kyanite, sillimanite, biotite, quartz and garnet. Secondary minerals comprise clinopyroxene, amphibole, white mica, epidote and chlorite (Bergh and Andresen, 1985).

1.6.4 AMPHIBOLITES

Amphibolites are commonly observed as very thin elongated bodies within the kyanite-garnet-two mica gneiss west of Store Mårtind, Gryta and Erikfjell (Bergh and Andresen, 1985). The massive amphibolite is usually made of hornblende and plagioclase (Bergh and Andresen, 1985) but may also contain a considerable amount of pyroxene (Lindstrøm and Andresen, 1992). The high content of quartz found in some amphibolites led Landmark (1973) to suggest that they may be of a sedimentary origin.

1.6.5 MARBLE AND CALC-SILLICATES

The *marble and calc-silicate rocks* most often display a distinct compositional layering which thickness range from 1 cm up to 2 m. Boudinaged layers of garnet-biotite gneiss and amphibolites are often observed within these marbles (Bergh and Andresen, 1985).

1.7 TECTONOMETAMORPHIC EVOLUTION OF THE NORDMANNVIK NAPPE BASED ON THE LITERATURE

At least two distinct tectonic episodes have been recognized in the Nordmannvik Nappe (Bergh and Andresen, 1985; Elvevold, 1988; Lindstrøm and Andresen, 1992). The deformational settings appear quite similar to those occurring in the underlying Kålfjord Nappe yet the mineral paragenesis is here defining a higher metamorphic grade (Bergh and Andresen, 1985).

An early deformational event D1 is observed and characterized by increasing P/T conditions which defined a prograde metamorphic event (Lindstrøm and Andresen, 1992). Isoclinal folding and mylonitic texture characterize this deformational episode, notably in the two-mica gneisses where the schistose mylonitic texture is clearly defined by parallel-oriented white mica, biotite and local kyanite (Bergh and Andresen, 1985; Lindstrøm and Andresen 1992). Early porphyroblasts (Feldspar, mica, garnet, and kyanite) have been deformed into elongated porphyroclasts oriented within the dominant foliation (Bergh and Andresen, 1985). According to Lindstrøm and Andresen (1992) and based on works carried out by Elvevold (1988), the peak metamorphic conditions are inferred to have been reached before the onset of mylonitization D1 as no evidences of granulite facies conditions have been encountered during the development of the mylonites. Bergh and Andresen (1985) on the other hand asserted that a granulite facies has been reached late in the main

deformational event (D1), northwest of Takvanet. The paragenesis orthoclase + garnet + quartz + kyanite + sillimanite + clinopyroxenes in gneisses accounts for the high metamorphic grade (Bergh and Andresen, 1985).

For Elvevold (1988) the peak metamorphism in the Takvanet area has been recorded in the porphyroclasts within the mylonitic gneiss. Geothermobarometric studies performed there have given P/T estimate of 9.2 +/- 1.0 Kbar and 715 +/-30 °C which demonstrate upper amphibolite facies conditions. In any cases, the dominant mylonitic fabric has been given as belonging to the medium-amphibolite facies (Bergh and Andresen, 1985; Lindstrøm and Andresen, 1992).

All authors then agreed on the idea that D1 was followed by a retrogression episode. A drop in pressure, evidenced by crystallization of sillimanite along garnet rims associated with several breakdown reactions accounts for it. This retrograde episode well observed in central Troms most likely post-dates the mylonitic layering and possibly occurred during the main nappe thrusting event of the orogeny (Bergh and Andresen, 1985).

A second deformation D2 event has been described by Bergh and Andresen (1985) as a minor folding phase affecting the mylonitic layering west of Fiskelausvatn. This event is of a minor extent and most of the considered folds are observed around the Mårfjell Antiform. Eventually, petrographic and structural indicators related to the Scandian orogeny and identified by Bergh and Andresen (1985) in Troms, are summarized in table 1.4.

Lindstrøm and Andresen (1992) carried out dating work in the Nordmannvik Nappe and obtained a Rb-Sr isochron in a local metadiorite outcrop of the area. According to the authors, the obtained age of 492 +/- 5 Ma can be interpreted either as the primary crystallization age of the rock or as the timing of the high-grade metamorphism recorded in the gneiss unit. Since the samples analyzed do not present any mylonitic texture, it is assumed that the obtained ages are not related to the mylonitization dominating the rock. Dating from two muscovite concentrates (prepared from mylonitic garnet-bearing schist) carried out by Dallmeyer and Andresen (1992) gave several calculated ^{40}Ar / ^{39}Ar ages of about 425-426 Ma (Table 1.3) and thus support the idea that mylonitization post-dates the primary crystallizations. Based on a personal communication from Krogh, Lindstrøm and Andresen (1992) suggested that a rift-origin from the metadiorite is probable, idea supported by the gabbroic composition of the samples. Correlation of this metadiorite age with other works performed in the surrounding nappes isn't straightforward. Nevertheless the

authors estimate that an age of 492 +/- 5 Ma supports the idea that the high-grade nappes located between the Vaddas and Lyngen Nappes (e.g Kålfjord and Nordmannvik Nappes) had a pre-Scandian history (Lindstrøm and Andresen, 1992). A truncation of the mylonitic foliation from the Nordmannvik Nappe by the thrust fault separating this unit from the Kåfjord/Vaddas Nappe has been taken as evidence for a pre-Scandian mylonitization of the Nordmannvik nappe, as it is accepted that the thrust fault is related to the main Scandian event (Lindstrøm and Andresen, 1992 and references therein).

1.8 SYNTHESE

Table 1.4, entirely based upon Bergh and Andresen (1985) aims to summarize the main structural and lithological aspect which affected the Nordmannvik Nappe during the Caledonian orogeny.

Table 1.4 Summary of the relationships between mineral growth, deformational episode and metamorphic grade in the Nordmannvik nappe. All data from Bergh and Andresen (1985).

Event	Early D1	D1	Late D1	D2
Mineral growth :				
- Quartz	yes	yes	yes	maybe
- Feldspar	yes	yes	yes	maybe
- Biotite	yes	yes	locally yes	maybe
- White mica	locally yes	yes	locally yes	yes
- Hornblende	locally yes	yes	yes	no
- Garnet	yes	locally yes	yes	no
- Epidote	locally yes	mainly yes	locally yes	yes
- Chlorite	no	no	locally yes	no
- Kyanite	locally yes	yes	mainly yes	maybe
- Silimanite	no	locally yes	locally yes	no
- Carbonate	locally yes	no	yes	no
- Titanite	no	no	mainly yes	no
- Pyroxen	no	no	yes	no
- Ilmenite	mainly yes	yes	no	no
- Turmaline	no	no	locally yes	no
Inferred mineralogical reactions and structural evolution	Helicitic metamorphic foliation defined by quartz, feldspar, mica and kyanite in the cores of garnet porphyroclasts.	Isoclinal folding associated with mylonitic layering, flattening and shearing. Elongation deformation of earlier formed porphyroblasts.	1. Growth of garnet, kyanite and hornblende under prograde metamorphism. 2. Significant drop in pressure evidenced by crystallization of sillimanite on garnet rims, breakdown of sillimanite into mica, chloritization of garnet, saussuritization of plagioclase and breakdown of kyanite into white mica.	Minor folds deforming the mylonitic layering. In the hinge zones of these folds the micas have recrystallized into polygons as have the epidote porphyroblasts.
Inferred metamorphic grade and P/T conditions when available.	Amphibolite facies conditions of approximately 535°C and 7 Kbar (inferred from garnet core inclusions studies).	Medium to high metamorphic grade.	1. At least Upper amphibolite facies has been reached. Granulite facies conditions (660°C and 10 Kbar) have been locally observed. 2. Transition from high to medium metamorphic grade.	Supposed to range between a low and medium metamorphic grade.

2 METHODS

2.1 MAPPING

During the field season, over 50 rock samples were taken along a 25 km long section of the E6 coastal road from Furuflaten to the road end in Koppangen. The main purpose of this large scale sampling was (1) to identify the dominant rock types and (2) measure foliation planes and lineations in order to determine the area structural trend. From this first step, important samples have been taken in the southern part of the fjord.

In a second time however, focus was done in the northern part of the nappe. In collaboration with Livia Nardini, some more detailed mapping was carried out in the peninsula located between Lyngseidet and Koppangen (Fig. 2.1). The N-S limit of the mapping area was set at the contact between the phyllites and the overlying Lyngne Nappe Complex, in the western part of the nappe. Nevertheless, and considering the difficult topography and the lack of valuable outcrops in the mainland, most of the work has been done along the costal road.

In order to construct the geological map, a systematic record of structural features and lithology has been done, with a special emphasis on the Scandian or earlier nature of the rocks. High grade lenses have been especially described. The geological map was carried out in collaboration with Livia Nardini by compiling and selecting the most accurate data from our combined datasets.

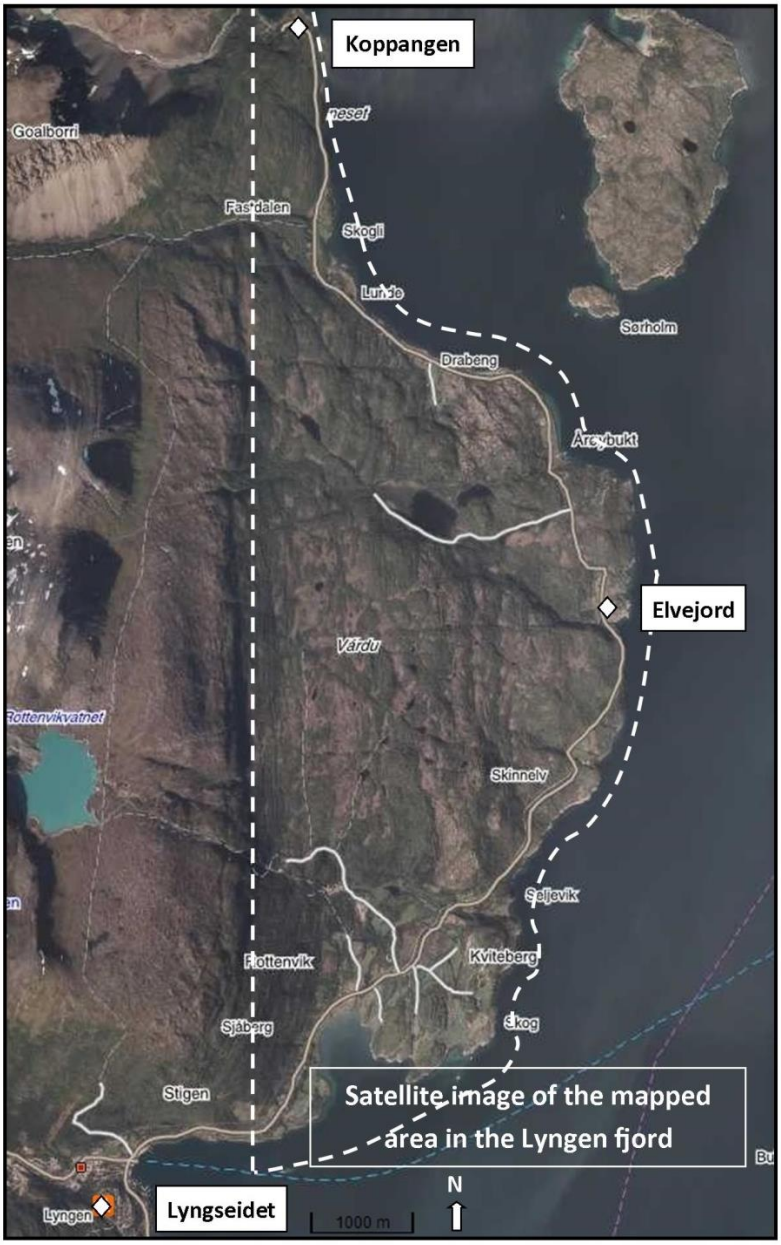

Figure 2.1 Northern peninsula in the Lyngen fjord. The dotted line delimits the mapping area assignated to this thesis. Landmarks mentionned in the text are indicated by white losanges. Satellite image is from http://kart.finn.no/.

2.2 POLARIZING MICROSCOPY

As the main analytic tool, a “Leica DM LSP2” polarization microscope has been used. Microphotogaphs were acquired with a microphotograph camera at the Norsk Polarinstitutt of Tromsø. Three sets of regular thin sections have been prepared depending upon the area they have been sampled (RB, U and K series). Thin sections were prepared cut normal to foliation and parallel to lineation when possible. Focus has been done on both the deformation microstructures and the petrology. The petrology has been studied with the help of textbooks from Mc Kenzie and Adams (1996), Twiss and Moores (2007), Vernon and Clarke (2008) and Bucher and Grapes (2011). Observations of deformation microstructure benefited greatly from the text book of Passchier and Trouw (2005).

3 RESULTS

3.1 GEOLOGICAL MAP AND STRUCTURES DESCRIPTION

3.1.1 GEOLOGICAL MAP

Based on investigations carried out in the northern peninsula, a geological map was constructed. Foliation planes and lineations are average measurements compiled from a common dataset obtained in collaboration with Livia Nardini.

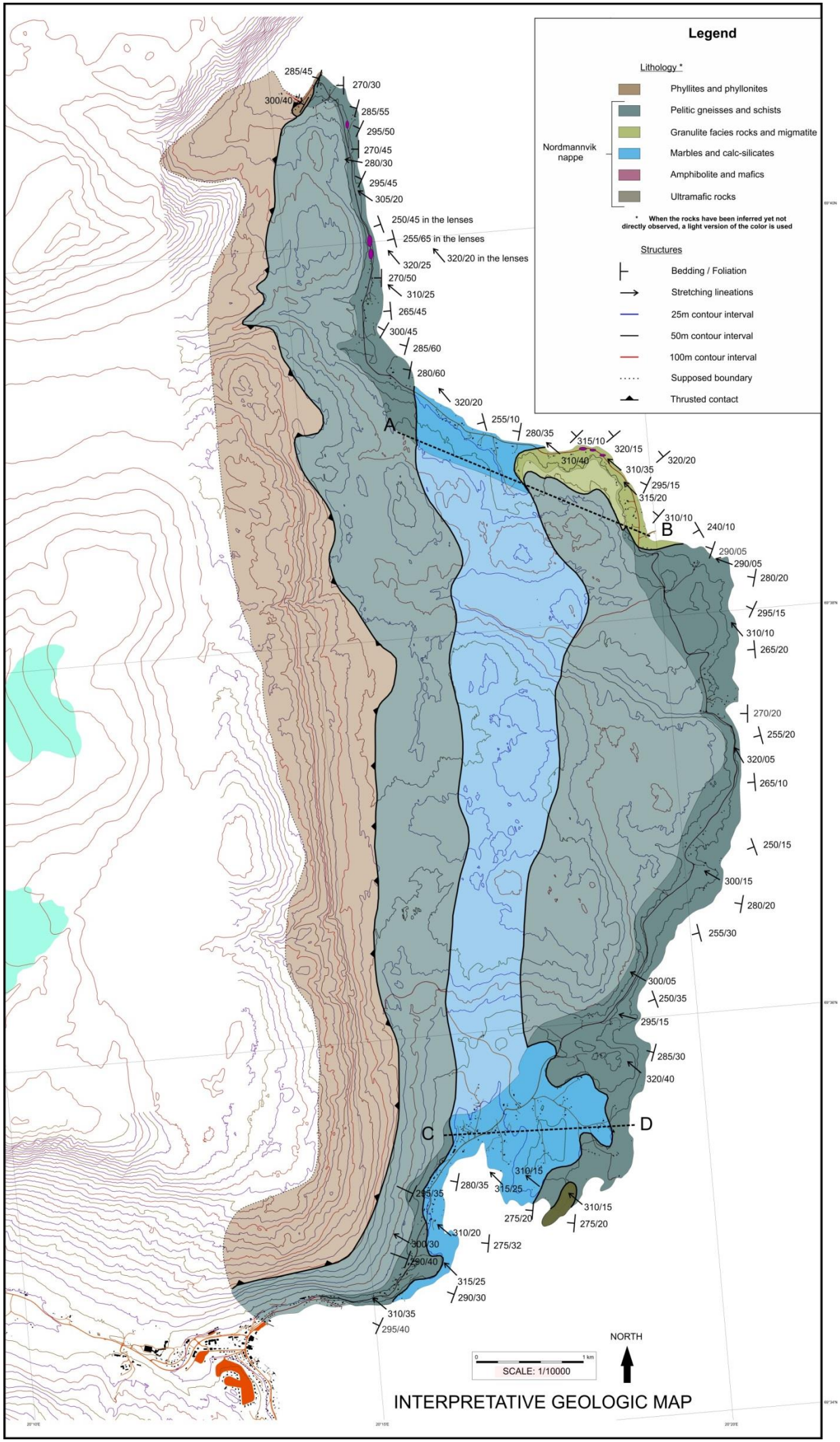
Legend
Lithology *
Nordmannvik nappe
Phyllites and phyllonites
Pelitic gneisses and schists
Granulite facies rocks and migmatite
Marbles and calc-silicates
Amphibolite and mafics
Ultramafic rocks
* When the rocks have been inferred yet not directly observed, a light version of the color is used
Structures
Bedding / Foliation
Stretching lineations
25m contour interval
50m contour interval
100m contour interval
Supposed boundary
Thrusted contact
285/45
270/30
300/40
285/55
295/50
270/45
280/30
295/45
305/20
250/45 in the lenses
255/65 in the lenses
320/25
320/20 in the lenses
270/50
310/25
265/45
300/45
285/60
280/60
320/20
255/10
280/35
315/10
320/15
310/40
320/20
310/35
295/15
315/20
310/10
240/10
290/05
290/05
280/20
295/15
310/10
265/20
270/20
255/20
320/05
265/10
250/15
300/15
280/20
255/30
300/05
250/35
295/15
285/30
320/40
310/15
280/35
315/25
310/15
275/20
275/20
310/20
275/32
300/30
290/40
315/25
290/30
310/35
295/40
A
B
C
D
NORTH
0
1 km
SCALE: 1/10000
INTERPRETATIVE GEOLOGIC MAP

Figure 3.1 Geological map of the area of study. Strongly colored area defines the rocks which have been directly mapped on the field. When lithology is inferred but not observed a light version of the corresponding color is used. Structural data are compiled from datasets made in collaboration with Livia Nardini working on the same project. From this study and Nardini (2013).

3.1.2 GEOLOGICAL PROFILES

Two geologic profiles have been constructed from the geological map and the location of these cross sections are indicated in Fig. 3.2. A first profile cuts in the northern part of the peninsula, through the high grade rocks, the metapelites and the carbonates. The second profile cuts across a megascale carbonate lens in the southern part of the peninsula. Both sections are oriented rather sub-parallel to the Caledonian fabric.

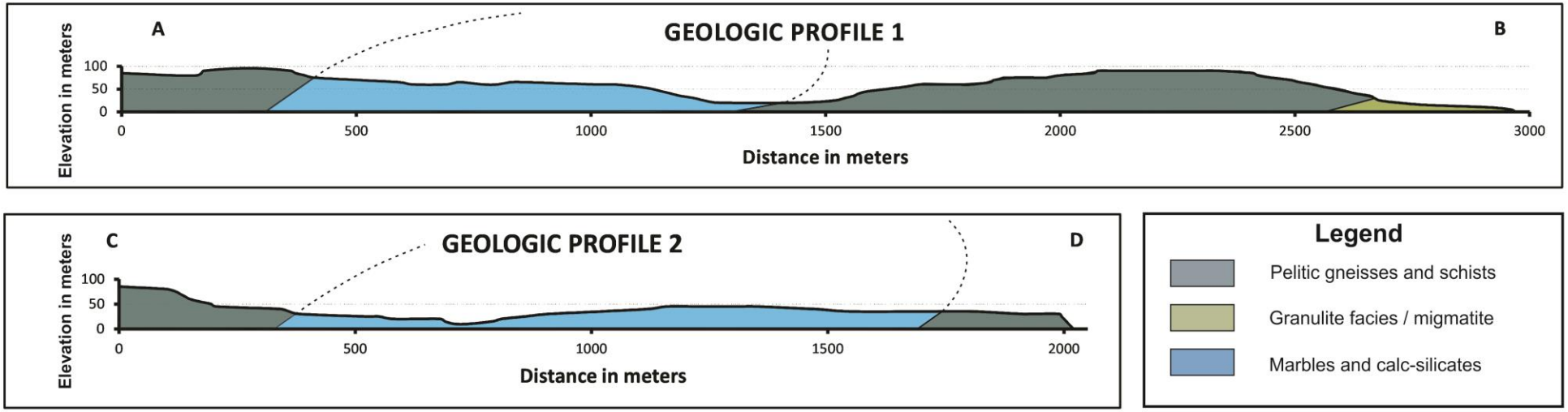

Figure 3.2 NW-SE geologic profiles cutting through the study area. Emplacement of these profiles is indicated on the geological map. Profiles are to scale and dip angles are conserved.

3.1.3 STEROGRAPHIC PROJECTIONS

Two types of measurements were carried out in the peninsula. Primary foliation is referred as S_1 and stretching lineations are defined as L_1. Only one generation of structures are reported wich relates to the Scandian event of the Caledonian orogeny. Foliation and stretching lineations were both plotted in stereonets, generated for metapelites, metamafics, carbonates and migmatite / high grade rocks as presented on the geological map. In addition a stereonet combining measurements in all rock types was generated. These stereonets are presented in Fig. 3.3A. Measurements used to generate these stereonets are those used in the geological map.

Because measurements were also taken in the entire nappe, a general steroplot is constructed with all data, including those from the mapped area. These stereoplots are generated for foliation planes and lineations, all lithologies combined (Fig. 3.3B).

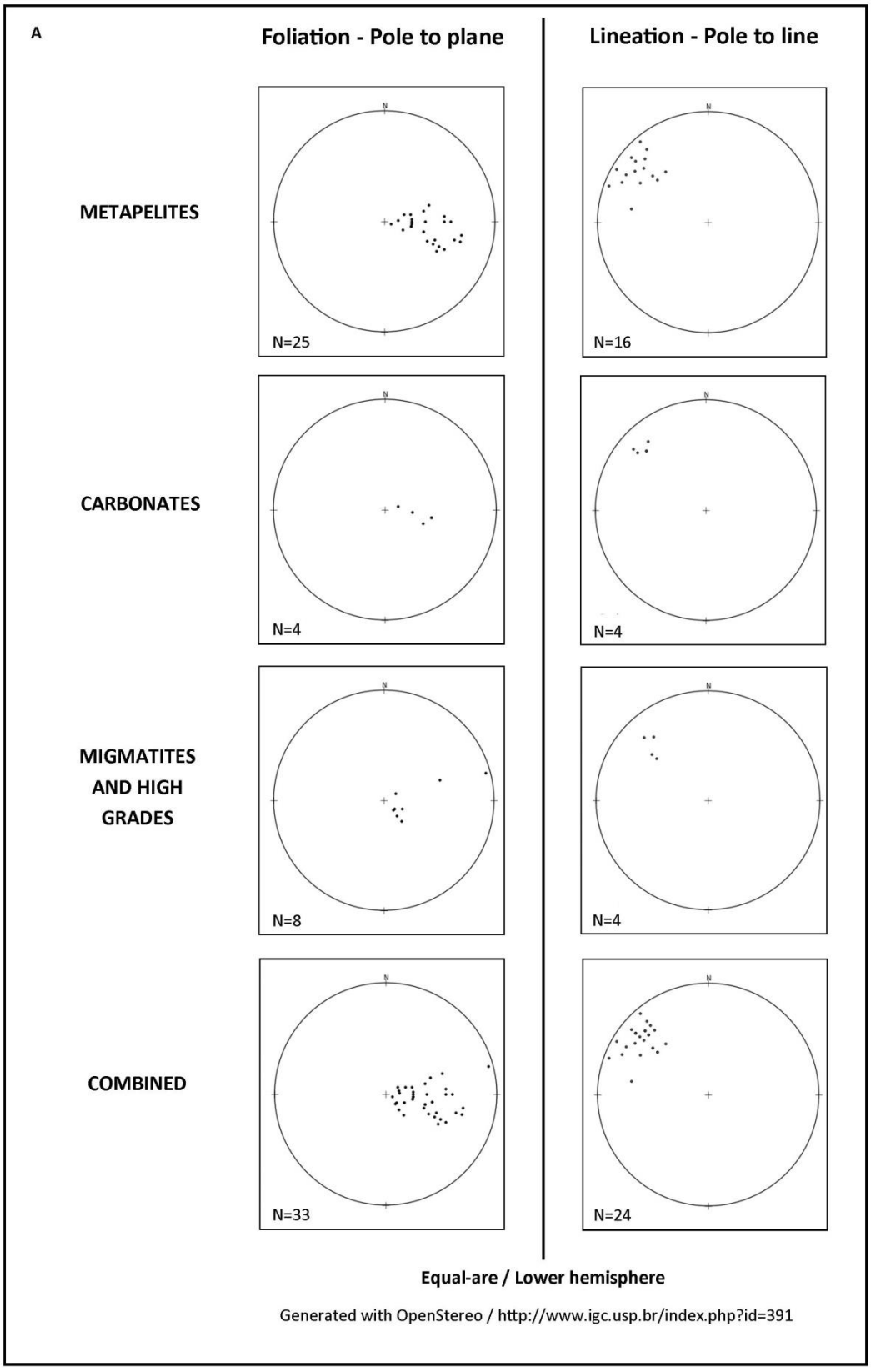
A
Foliation - Pole to plane
Lineation - Pole to line
METAPELITES
N=25
N=16
CARBONATES
N=4
N=4
MIGMATITES AND HIGH GRADES
N=8
N=4
COMBINED
N=33
N=24
Equal-are / Lower hemisphere
Generated with OpenStereo / http://www.igc.usp.br/index.php?id=391

.

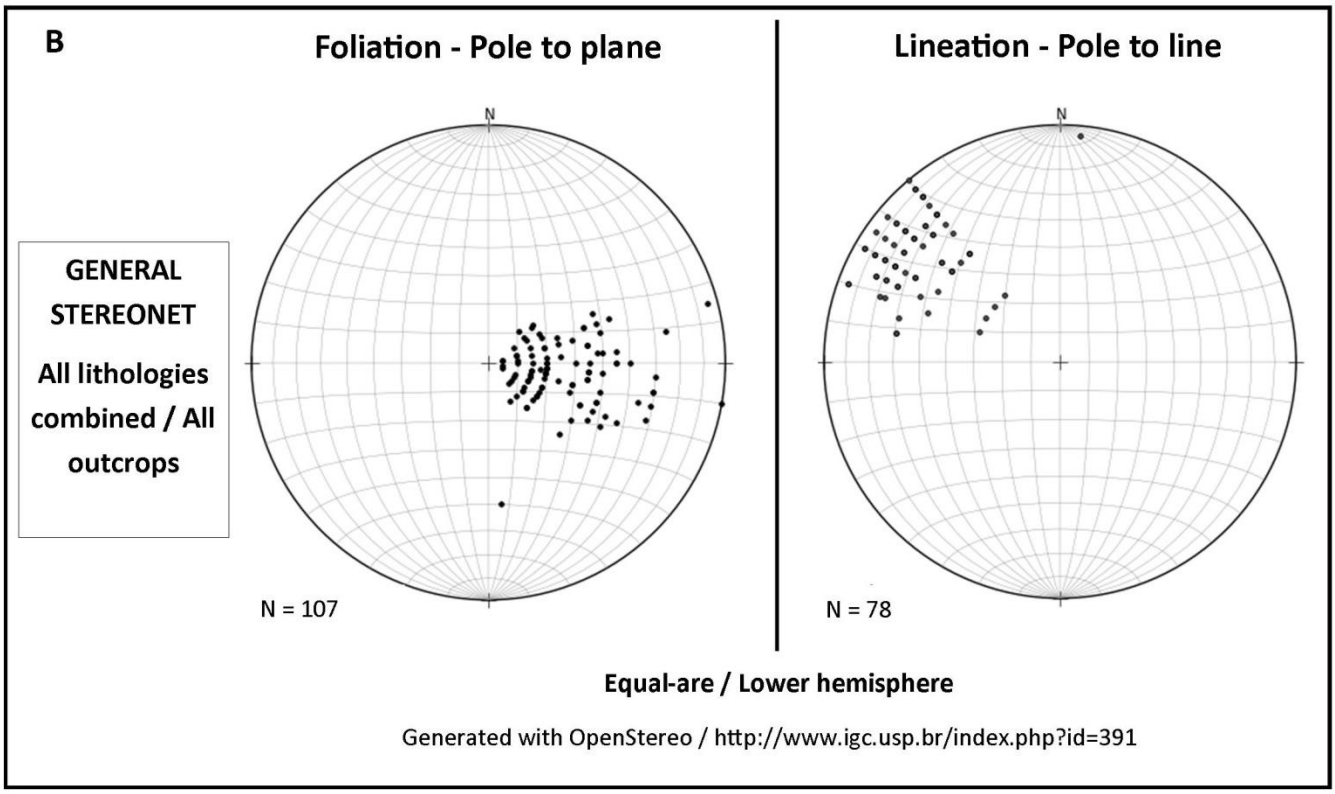

Figure 3.3 (A) Stereonets using a lower hemisphere projection for the different rock types observed in the mapped area. Data are those from the geological map. (B) Stereonets using a lower hemisphere projection for the different rock types observed in the entire area. Data combined measurements from the geological map and others from personal datasets.

3.2 NOMENCLATURE

Petrographic observations in the Nordmannvik have identified four different stages of "metamorphic evolution" and two metamorphic peaks which are defined by the highest grade assemblages M_0 and M_1 observed experimentally.

M_0 consists of pre-Scandian granulite facies assemblages which are weakly deformed when compared to the Scandian rocks. These pelitic and mafic assemblages are observed as elongated layers or lenses of high grade relic material. In metapelites, the metamorphic peak was reached in the sillimanite field.

M_1 is defined as the metamorphic peak assemblage reached during the principal deformation event of the Caledonian orogeny, most likely Scandian. Rocks in which M_1 was reported show an E dipping foliation (S_1) and are also affected by a late and superposable mylonitic fabric. This fabric, referred as S_2 precedes the metamorphic peak assemblage M_1 because M_1 minerals are not affected by the mylonitization. S_2 is associated to a retrograde path where late crystallizations of sillimanite are observed within the mylonitic fabric. M_1 has reached a minimum of an upper amphibolite facies in the kyanite field.

Beside these maxima, we define as "**pre-M_0"** the *weakly deformed* rocks belonging to a prograde metamorphic path leading to M_0 and "**post-M_0"** the *weakly deformed* rocks following a retrograde metamorphic path. Likewise, we define as "**pre-M_1**"the *deformed* samples belonging to a prograde metamorphic path leading to M_1 and "**post-M_1"** the *deformed and mylonitic* rocks which underwent a subsequent retrograde metamorphic episode.

In order to understand the temporal relationships between the metamorphic assemblages, the foliation and the mylonitic fabric, the figure 3.4 is presented. In this figure, D_1 refers to the entire Scandian event (composed of a prograde and a retrograde path) as generally described in the literature.

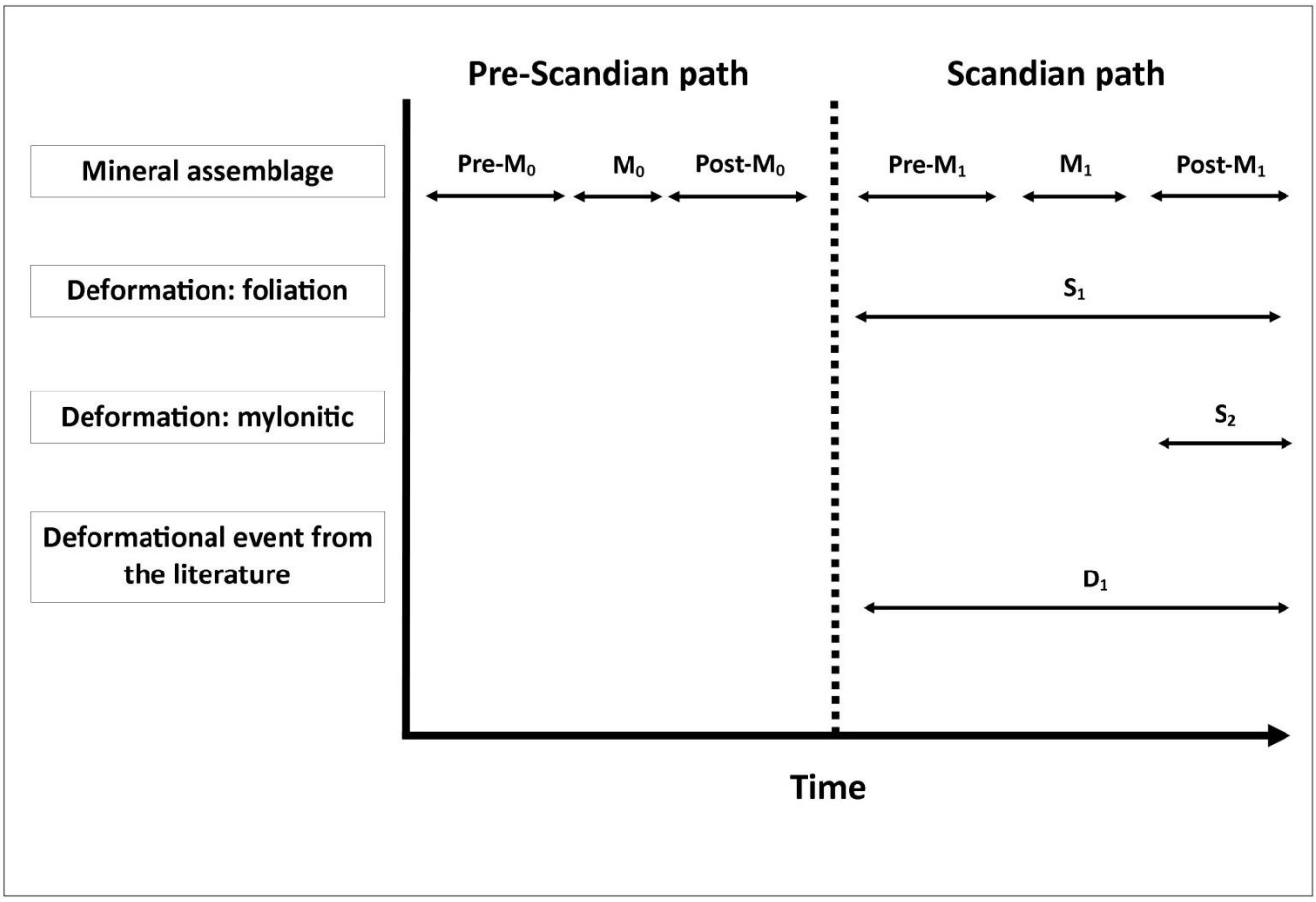

Figure 3.4 Nomenclature of the relationships between metamorphic assemblages and deformation features in the Nordmannvik nappe.

3.3 PETROGRAPHY

The Nordmannvik Nappe in the study area is dominated by metapelites. Other rock types include mafic, ultramafics and calc-sillicates rocks. A detail description of the different rock types is now given at both, the macro and the micro-scale.

3.3.1 GARNET-KYANITE-MICA GNEISSES AND SCHISTS

3.3.1.1 DISTRIBUTION AND APPEARANCE IN THE FIELD

MICA-GNEISSES

The dominant rock type found out in the investigated area is a blasto-mylonitic to ultramylonitic garnet-kyanite-mica gneiss (Fig. 3.5A and 3.5B), which occurs as a dark, layered and medium-grained massive rock. Typical mineralogy includes quartz, two micas, feldspars, garnet, kyanite, amphibole and epidote minerals. Minor constituents are calcite and rutile. Biotite and white micas are easily observable, these latter sometimes observed as wide flakes (up to 2 centimeters). Garnets are common and observed either as (1) medium sized grains scattered in the bulk rock, (2) large grained (1-3 cm) specimens in coarse grained layers (Fig. 3.5D) or (3) as aggregates concentrating in the restite (Fig. 3.5E). Calcite is seldomly observed in fractures and veins but the mineral is mostly identified in thin sections, where it occurs as pure small calcite crystals. Leucosome layers and lenses are present and are often garnet-free. Garnet-kyanite-mica gneisses are observed in two different settings; if most of them outcrop as a single rock type, interbedding of marble and gneisses are also encountered (see section 3.3.6). In such cases gneisses have been considered as part of the carbonate unit and referred as “calc-silicates”.

Garnet-kyanite-mica gneisses display an W dipping foliation, with an average dip of 20-30°. Melt spots, mafic and ultramafic lenses, K-feldspar porphyroclasts, and carbonates are commonly observed in inclusions lying sub-parallel to parallel with the main fabric (Fig. 3.5C). Such structures vary in size from few centimeters to few meters wide and are observed throughout the entire area. Boudins, pinch-and-swell and sigma clasts, ranging from few centimeters up to up few decimeters across are frequently observed (Fig. 3.5F). Sigma clasts are most often composed of K-feldspar porphyroclasts whereas boudin and pinch-and-swell structures are made of amphibolite and mafics, ultramafics, or high grade pelitic rocks.

MICA SCHISTS

Garnet-kyanite mica schists notably outcrop in the northern part of the peninsula, from Koppangen to Fastdalen, and have mainly been mapped along the E6 coastal road. These pelitic schists have a dark grey surface coated with a red oxide cover (Fig. 3.9A). The rock is fine grained and rather homogeneous. Porphyroclasts of garnets or felsic aggregates are present. The foliation which is defined by the parallel alignment of white mica and biotite outlines the porphyroclasts. Mineralogy is similar to that of gneisses with quartz, micas, feldspars, garnets, amphibole and epidote minerals as the dominant components. Kyanite, calcite and rutile are locally observed.

These pelitic schists behave in a similar manner as gneisses do. The same structures occur in the two rock types and both foliations and lineations are similar. Strain partioning is easily reported in pelitic schists. An increasing grade in ductile deformation is observed from East to West toward the contact with the overlying Lyngen Nappe Complex and is identified both macroscopically and under polarizing microscope.

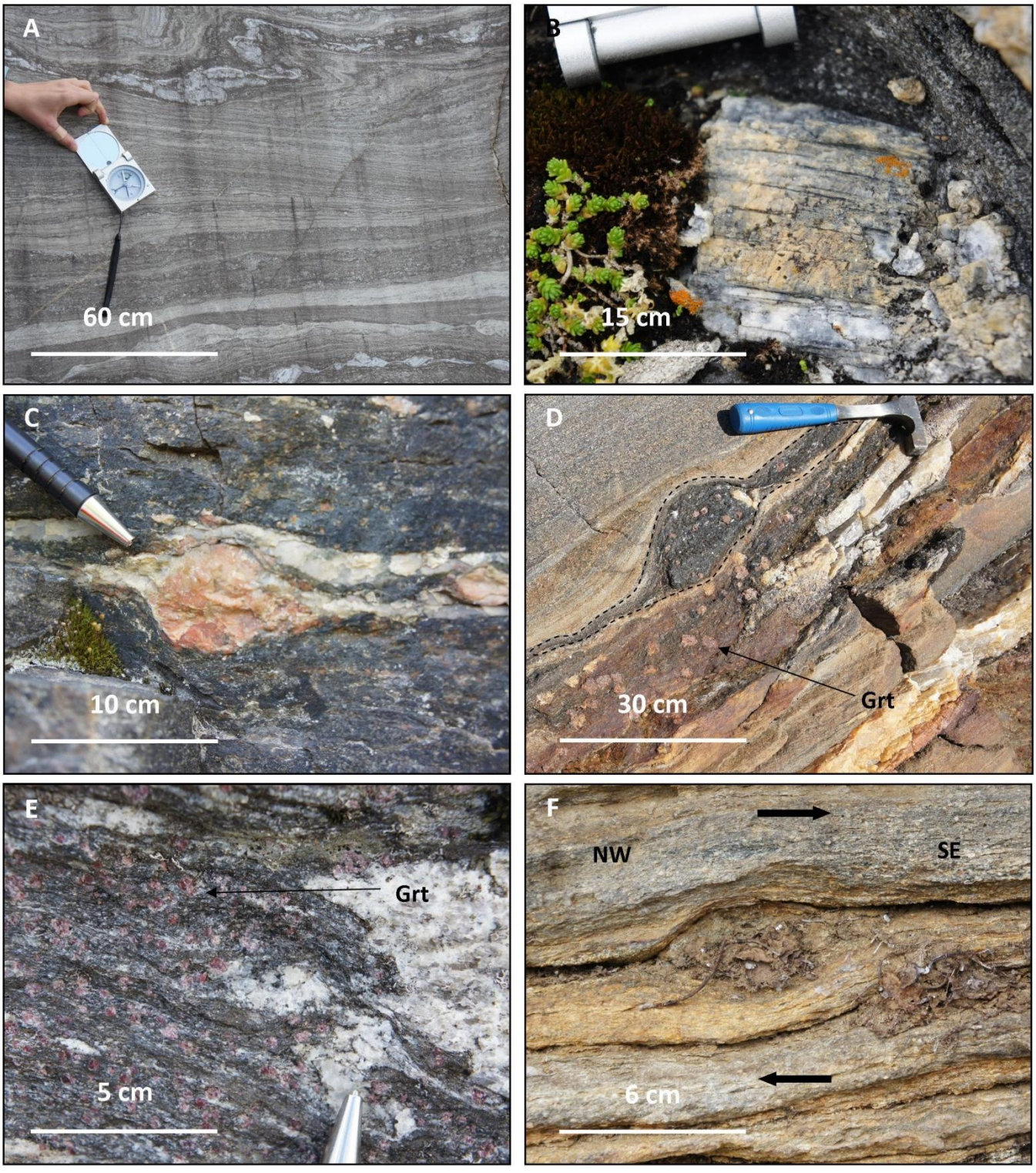

Figure 3.5 (A) Typical garnet-kyanite-mica gneiss texture. The outcrop is polished showing clear structures. Note the sheared leucosome layers. (B) Close-up on a coarse kyanite crystal. (C) K-feldspar porphyroclast in a garnet-kyanite-mica gneiss. (D) Coarse grained layer of garnet-kyanite-mica gneiss showing cm-wide garnets. Note the dark lens of high grade material (garnet-sillimanite gneiss) contoured by a dashed line.

(E) Restite in a garnet-kyanite-mica gneiss showing enrichment in small garnets. (F) Sigma clast in a garnet-kyanite-mica gneiss showing a dextral shearing related to a SE directed movement of the upper block.

3.3.1.2 Mineralogy and microstructure

Mineralogy

Garnet-kyanite mica gneisses and schists are treated together as they may be hardly distinguished from each other and share a similar pelitic composition. The following minerals are encountered:

***Quartz (30-70 %)*:** Occurs as ribbons or elongated aggregates. Individual subhedral grains vary in size between 0,05 and 1,5 mm. Grain size often increases in ribbons. Quartz is colorless, with no cleavage, no relief, it has a low birefringence and shows an undulose extinction. Quartz also occurs as inclusions and is locally suggested to be the result of late recrystallizations during retrograde metamorphism. Likewise, quartz annealing is often encountered and suggests late mineral re-equilibration.

Biotite (10-30%): Occurs in two dominant textural settings:

1 As pale brown subhedral and elongated large grains, up to few cms in strongly sheared samples (Fig. 3.6F).

2 As stretched crystals outlining porphyroclasts and accommodating the foliation (Fig. 3.6A)

Biotite shows straight extinction and has a single cleavage lined with its longest axis itself parallel to foliation. The extinction ranges within the 3rd to 4th order of birefringence. Zircon inclusions are commonly observed. Biotite may also include others phases such as quartz, garnet, plagioclase or hornblende. The mineral is locally partially recrystallized.

Muscovite (1-30%) has a high birefringence, a straight extinction and a single cleavage lined with its longest axis itself parallel to the foliation. The mineral is mostly found as a retrograde phase. Retrograde muscovite is observed either as lepidoblastic grains or as alteration mineral (sericite).

***Plagioclase (5-30 %)*:** Mineral with a low relief, and two cleavages at 90 degres. It possesses polysynthetic twins with an oblique extinction and a first order birefringence. Plagioclases occur in several settings:

1 As subhedral to anhedral large porphyroclasts locally zoned and showing well-formed deformation or growth twins (Fig. 3.6B).

2 As broken fragments, strongly altered with frequent twinning overlaps. Twins are dominantly growth twins.

In some strongly deformed samples, plagioclases have been barely found probably destroyed by the intense shearing which affected these samples.

***K-feldspar (0-5%)*:** Low relief mineral, mostly likely identified as orthoclase which is colorless with an undulose extinction and a first order birefringence. It occurs as rare and small subhedral grains.

***Garnet (5-20%)*:** Mineral colorless, anhedral to euhedral, showing 0.25 to 2 mm large grains. The mineral is isotropic, with no cleavage, a high relief and is locally zoned. Garnets are often cracked, and these cracks are often filled by late minerals such as chlorite and micas. Garnet often reacts with quartz and micas and may show oxides. In addition, the mineral includes quartz (Fig. 3.6A), biotite and is seldomly associated with amphibole and epidote minerals. Interestingly garnet growth is locally hampered when in contact with quartz. An explanation is that garnets do not have the possibility to find elements such as Fe or Mg required for their growth, in the silicates. Consequently, garnets cannot develop properly and show a truncated crystal shapes where in contact with quartz (Fig. 3.6B).

***Amphibole (0-15%)*:** Occurs as anhedral to subhedral <0,05 to 3 mm large grains. The mineral is mostly found as hornblende but can locally be observed as actinolite in the calcite-rich metapelites. The two varieties have an oblique extinction, a moderate relief and a low birefringence. Actinolite is pale brown whereas hornblende is more yellowish and show well developed fracture sets (Fig. 3.6F).

***Epidote (0-7%)*:** Mineral occurring as subhedral elongated crystals (<0,005 to 0,5 mm) or columnar aggregates. Epidote is colorless to light grey and shows a low birefringence. The mineral has a single cleavage and presents a straight extinction parallel to its length. The mineral is frequently observed in intergrowth with zoisite or plagioclase (Fig. 3.6C) or lying parallel with the biotite fabric.

***Zoisite* (0-5*%*):** Mineral occuring as small granular aggregates or stubby prisms (Fig. 3.6C). Zoisite is colorless, has a positive relief compared to quartz, a single cleavage and extinguishes parallel to its

crystal length. A blue interference color (low birefringence) is observed and typical of these minerals in our thin sections.

Kyanite (0-5%)**:** Mineral colorless with a moderate relief and a low birefringence. Grains are anhedral to subhedral and their size vary from 0,01 mm to 0.25 mm. Kyanite grains can include other phases, notably quartz (Fig. 3.6D).

Calcite (0-5%)**:** Mineral colorless with a low relief and a high birefringence. Extinction is symmetrical to the cleavage traces. Calcite is observed as anhedral to subhedral grains and shows a "dusty" aspect with local polysynthetic twins. The mineral is frequently associated with epidote minerals, zoisite and titanite (Fig. 3.6E.)

Tourmaline (0-3%): Mineral occurring as small anhedral blebs in the matrix. The mineral shows a dark green color under crossed polars, has a high relief and is locally observed associated with sillimanite needles.

Titanite (0-2%)**:** Mineral with a very high relief and an extreme birefringence. The grain may be rhomb-shaped to elongated ovoid, always showing a single cleavage and a pastel color. Titanite can include rutile and may itself be found as inclusion mineral. The mineral can be observed in relatively high proportion.

Chlorite (0-2%)**:** Occurs rarely as highly stretched crystals, in association with micas. The mineral is pale green, and displays an anomalous birefringence. Chlorite is observed lying with the biotite fabric and occurs in late retrograde stages. Strong variations (from brown to blue) in the interference color of the mineral indicate that compositional changes locally occured in the mineral.

Rutile (0-1%)**:** Mineral occurring as small anhedral blebs (< 0.05mm) in the matrix or in inclusions. Its dark yellow-orange color and very high relief are characteristic. Rutile is usually acessory but is locally found in relatively high proportions.

Zircon (<1%)**:** Occur as very small blebs including biotite. The mineral is colorless with a high relief and is easily identified by its dark halo, resulting from its radioactive decay.

Sillimanite (<1%): Mineral colorless with a low relief and a lower second order of birefringence. The aluminosilicate shows a parallel extinction and is observed as small needle aggregates.

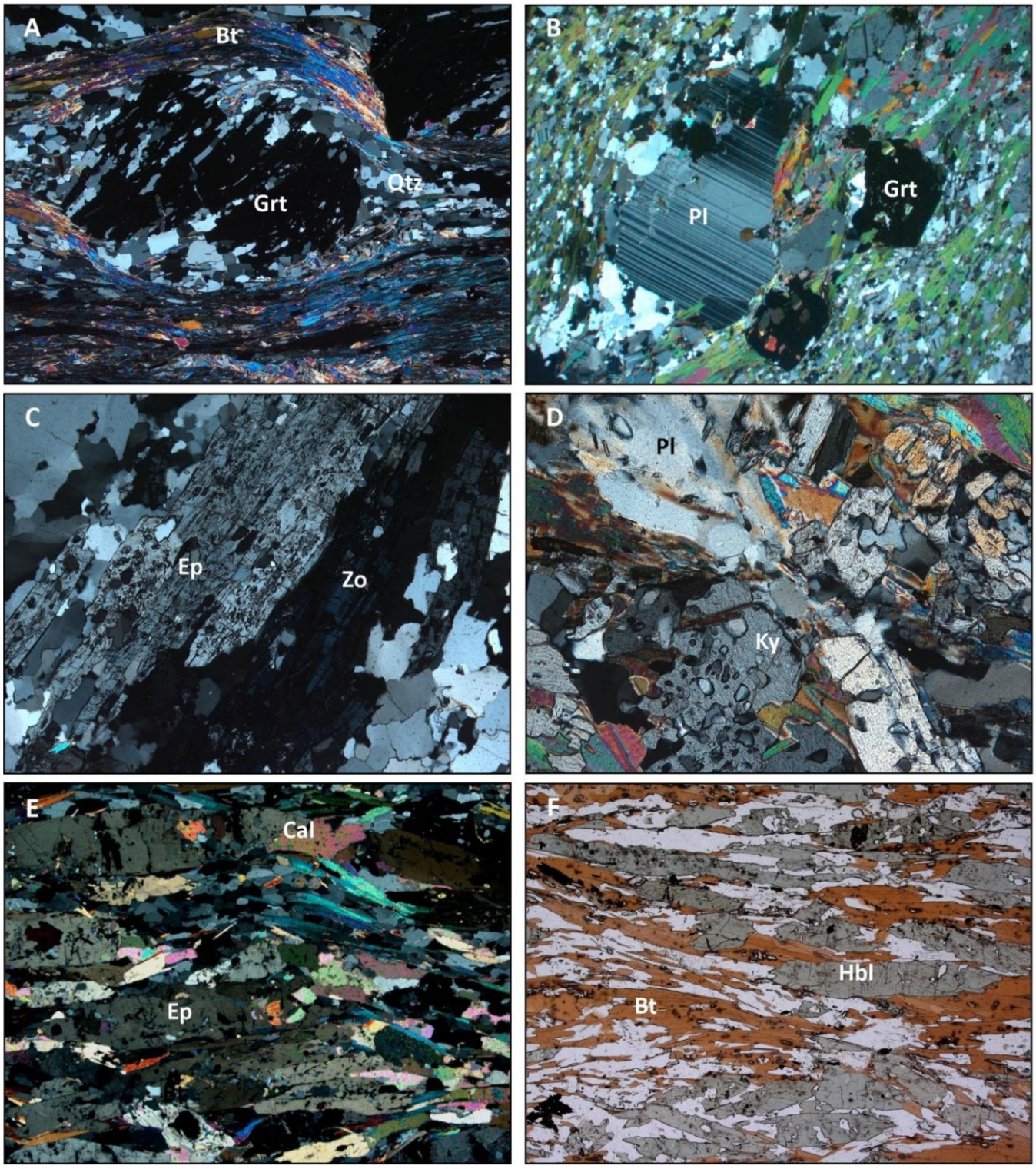

Figure 3.6 (A) Garnet porphyroclasts in a mylonitic garnet-kyanite-mica gneiss. Note the quarts inclusions and the biotite fishs contouring the porpyroclast. Crossed polars, base of image 12 mm. (B) Plagioclase porphyroclast in a garnet-kyanite-mica gneiss. Note the well-defined polysynthetic deformation twins. Crossed polars, base of image 12 mm. (C) Intergrowth of epidote and zoisite in a garnet-kyanite-kyanite schist. Crossed polars, base of image 12 mm. (D) Kyanite and altered plagioclase in a garnet-kyanite-mica gneiss. Crossed polars, base of image 1.5 mm. (E) Calcite and epidote in a garnet-kyanite schist. Crossed polars, base of image 6 mm. (F) Hornblende and biotite in a garnet-kyanite-mica schist. Natural light, base of image 6 mm.

MICROSTRUCTURES

In most cases, garnet-kyanite-mica gneisses show a strong mylonitic to ultramylonitic fabric (Fig. 3.7D) which overprinted the early aseemblages. In some samples however, this mylonitic fabric appears weak enough to observe some pre-mylonitic mineral such as kyanite and garnets (Fig. 3.6A and 3.6D). These garnets may show a strong zoning pattern of quartz inclusions (observed in sample RB 16E), which consist in small quartz grains restrictly observed in the garnets core (detailed in Fig. 3.7A). Kyanite, when observed, shows anhedral and skeletal crystals with abundant quartz inclusions (Fig. 3.6D) which appear similar to those scattered in the garnets core. The aluminosillicate is nevertheless rather undeformed and unaffected by the mylonitic fabric which wraps around the mineral.

Biotite is the dominant mica and is observed as poorly deformed to strongly sheared syn-mylonitic crystal. The mineral which show local mineral zoning (Fig. 3.7B) occurs in relatively high proportion unlike muscovite which is barely observed and strongly altered. K-feldspars are rare and seldomly observed but they occur in melt, filling intersticial spaces between coarse minerals such as garnets. Sillimanite occurs locally as small needles which crystallized in the mylonitic biotite fabric (Fig. 3.7C) and thus post-dates the pre-mylonitic kyanite. Sillimanite is nevers observed growing over the abundant biotite and most needle aggregates are stretched and lined with the mylonitic fabric. Therefore, sillimanite crystallization is most likely syn-mylonitic.

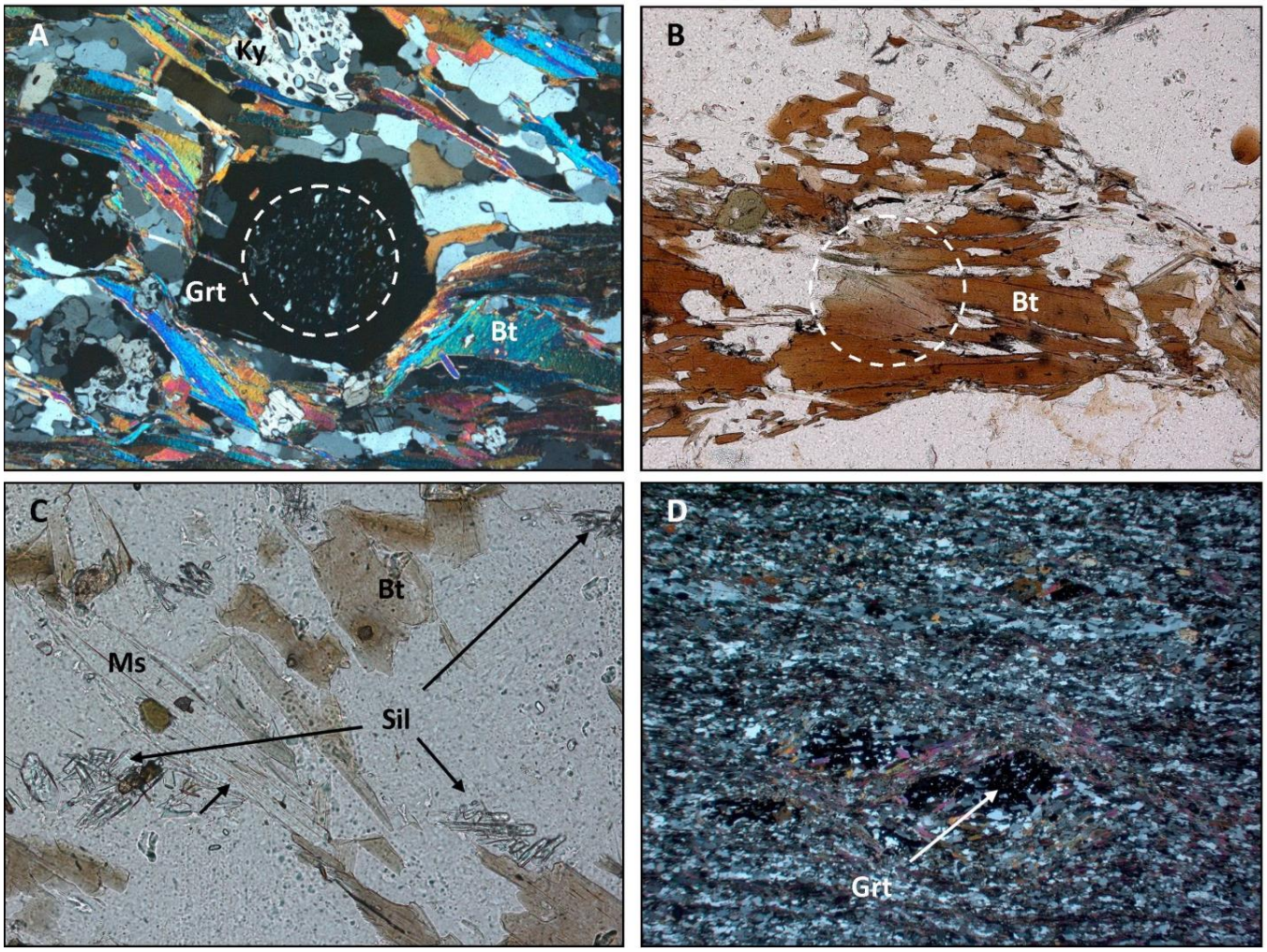

Figure 3.7 (A) High grade garnet-kyanite-mica gneiss focusing on a garnet crystal including quartz grains. The dashed white circle delimits the quartz inclusions. Crossed polars, base of image 3 mm. (B) High grade garnet-kyanite-mica gneiss focusing on biotite grains. The dashed white circle show mineral zonation evidenced by a color change in the biotite crystal. Natural light, base of image 1.5 mm. (C) Sillimanite needles in a high grade garnet-kyanite-mica gneiss. Natural light, base of image 0.75 mm. (D) Ultramylonitic fabric in a garnet-kyanite-mica gneiss. Note the importance of recrystallizations. Crossed polars, base of image 12 mm.

3.3.2 GARNET-SILLIMANITE GNEISSES

3.3.2.1 DISTRIBUTION AND APPEARANCE IN THE FIELD

Garnet-sillimanite gneisses occur as lens-shaped bodies wrapped in the mylonitic fabric of the garnet-kyanite-mica gneisses. These lenses are up to few meters across and show a massive and coarse-grained texture, or a more altered and crumbly aspect (Fig. 3.5D). K-feldspar is largely found, with about 20-30% as an average content, associated with quartz, K-feldspar porphyroclasts, and garnets.

The contact between these high grade rocks and the surrounding mylonitic metapelites is not always exposed. In these rocks, foliation is discordant when compared to that in the lower grade gneisses. According to the stereonets (Fig. 3.3A), this foliation has a lower average dip (about 10 degrees) than in garnet-kyanite-mica gneisses

3.3.3.2 Mineralogy and microtexture

Mineralogy

***Quartz (40-50 %)*:** Occurs as ribbons or thin packed aggregates. Individual subhedral grains vary in size between 0,05 and 1,5 mm and are subhedral to euhedral. Grain size often increases in ribbons. Quartz is colorless, with no cleavage, no relief, a low birefringence and an undulose extinction. Cupspate and sutured grain boundaries are commonly observed (Fig. 3.8B). Quartz melt is also reported, riming garnet porphyroclasts (Fig. 3.8F).

***K-feldspar (10-40%)*:** Colorless mineral with a low relief, an undulose extinction and a first order birefringence. The mineral occurs as coarse porphyroclasts or small anhedral grains reworked in the matrix. Specific K-feldspar varieties include (1) exsolution lamellae of perthitic albite occuring frequently in the porphyroclast (Fig. 3.8E), (2) microcline recognized by its characteristic cross-hatched twins and (3) sanidine, a high temperature polymorphe of orthoclase which has been identified very locally by its characteristic Carlsbad twin. K-feldspars porphyroclasts are often contoured by reaction rims (Fig. 3.8B).

***Biotite (1-5%)*:** Occurs as very stretched and recrystallized crystals. Zonations are evidenced by color variations which are commonly observed in single crystals. Biotite shows straight extinction and has a single cleavage lined with its longest axis itself parallel to foliation. The extinction ranges within the 3rd to 4th order of birefringence.

Muscovite (0-2%): Mineral with a straight extinction. The mineral has a single cleavage lined with its longest axis itself parallel to foliation. The birefringence is high (3rd order). The mineral is restrictly retrograde and is mostly found in coronas riming coarse garnets, or replacing sillimanite (Fig. 3.8F).

***Plagioclase (1-10 %)*:** Mineral with a low relief, and two cleavages at 90 degrees. It possesses polysynthetic twins, an oblique extinction and a first order birefringence. Plagioclases occur as (1)

broken and strongly altered grains with frequent overlaps of growth twins and (2) as myrmekite (vermicular mineral intergrowth) with quartz (Fig. 3.8D).

Garnet (5-30%)**:** Colorless mineral, anhedral to euhedral, with 0.25 to 2 mm large grains. The mineral is isotropic, with no cleavage and has a high relief. Garnets are often associated with quartz, micas and may show oxides. The mineral is seldomly observed with coronas-type reaction rims (Fig. 3.8B).

Sillimanite (0-3%)**:** Mineral colorless with a low relief and a lower second order of birefringence. The alluminosilicate shows a parallel extinction and is observed either as single needles or as fibrous aggregates riming garnet (Fig. 3.8G).

Tourmaline (0-3%): Mineral occurring as small anhedral blebs in inclusion or in the matrix (Fig. 3.8G and 3.8H). The mineral show a dark green color under crossed polars, has a high relief and is locally observed associated with sillimanite needles.

Rutile (0-3%): Mineral occurring as small anhedral blebs (< 0.05mm) in the matrix or in inclusions. Its dark yellow-orange color and very high relief are characteristic. Rutile can be found in relatively high proportions.

Calcite (0-3%)**:** Colorless mineral, uniaxial (-) with a low relief and a high birefringence. Extinction is symmetrical to the cleavage traces. Calcite is observed as disorganized grain aggregates and shows a "dusty" aspect.

Titanite (1<%)**:** Mineral with a very high relief and an extreme birefringence. The grain may be rhomb shaped to elongated ovoid, always showing a single cleavage and a pastel color. The mineral is only locally observed.

Zircon (<1%)**:** Occur as very small blebs including biotite. The mineral is colorless with a high relief and is easily identified by its dark halo, resulting from its radioactive decay

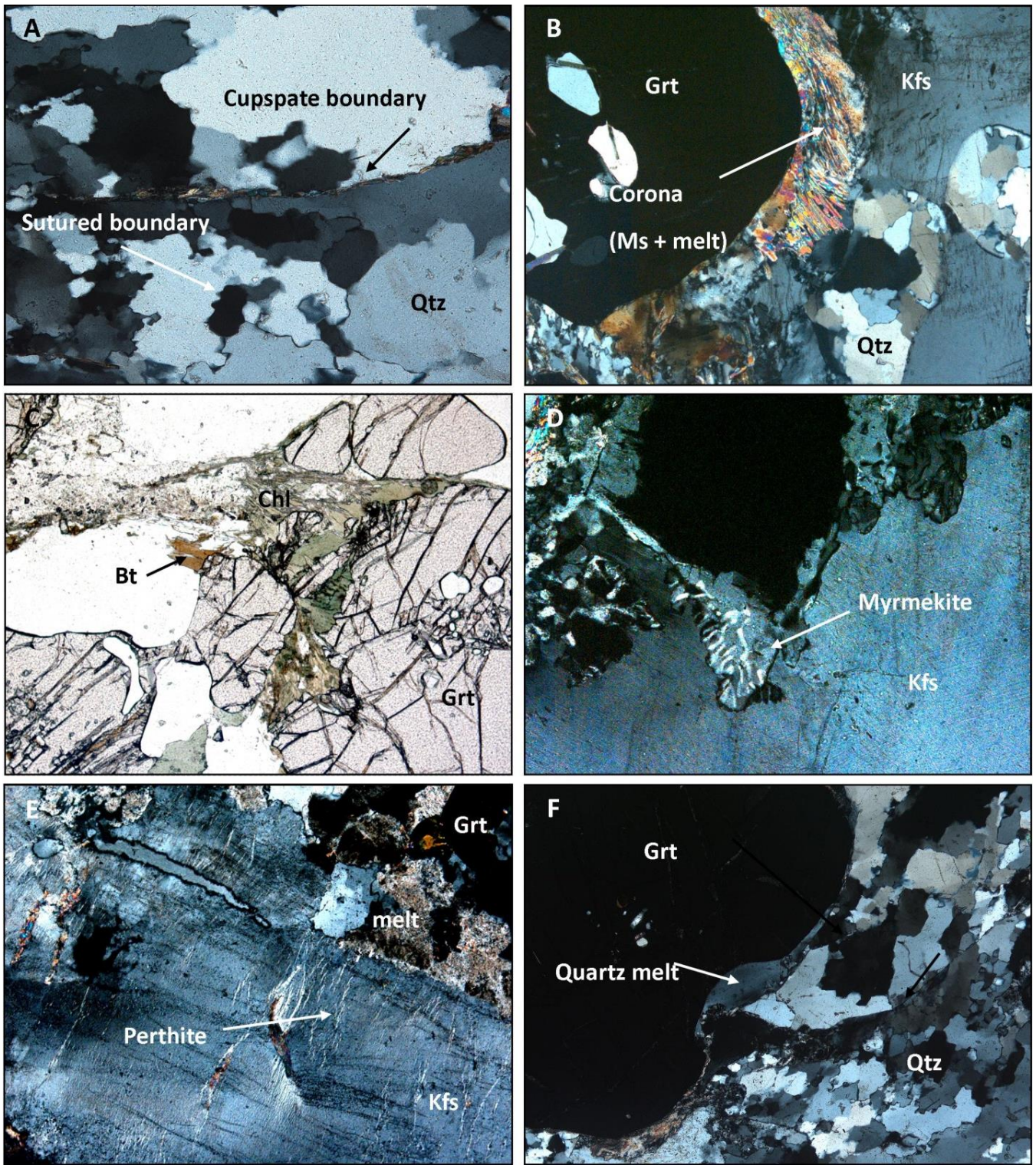
A
Cupspate boundary
Sutured boundary
Qtz
B
Grt
Kfs
Corona
(Ms + melt)
Qtz
C
Chl
Bt
Grt
D
Myrmekite
Kfs
E
Grt
melt
Perthite
Kfs
F
Grt
Quartz melt
Qtz

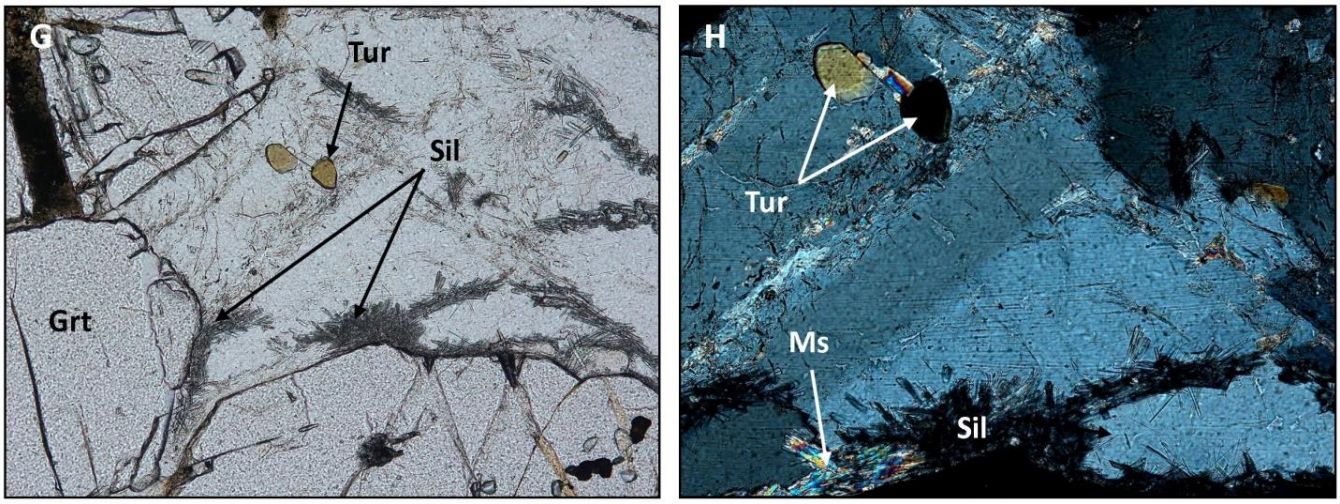

Figure 3.8 (A) Cupspate and sutured grain boundaries observed in a garnet-sillimanite gneiss. Crossed polars, base of image 1.5 mm. (B) Mvs + melt corona around a garnet porphyroclast in a garnet-sillimanite gneiss. Crossed polars, base of image 3 mm. (C) Chl-rich reaction rim contouring a garnet porphyroclast in a garnet-sillimanite gneiss. Natural light, base of image 3 mm. (D) Myrmekite intergrowth in a garnet-sillimanite gneiss. Crossed polars, base of image 1.5 mm. (E) Exsolution lamellae of perthite in a garnet-sillimanite gneiss. Crossed polars, base of image 3 mm. (F) Late quartz melt contouring a garnet porphyroclast in a garnet-sillimanite gneiss. Crossed polar, base of image 3 mm. (G) Sillimanite aggregates in a garnet-sillimanite gneiss. Natural light, base of image 1.5 mm. (H) Interaction between muscovite and sillimanite in a garnet-sillimanite gneiss. Crossed polars, base of image 0.75 mm.

MICROSTRUCTURES

Garnet-sillmanite gneisses are weakly deformed but they do not have recorded any mylonitic episode. The lack of pervasive fabric and the absence of widespread biotite associated with the abundance of sillimanite allow an easy differenciation of these rocks with the mylonitic garnet-kyanite-mica gneisses. K-feldspars vary in proportions depending upon the sample and they may be porphyroclastic (Fig. 3.8B) or hardly observed owing to an extensive melting. Garnets are rather euhedral and prophyroclastics (Fig. 3.8B and 3.8F). In one thin section, well-developed coronas (Fig. 3.8B and 3.8C) are observed around garnets and K-feldspar porphyroclasts (described in section 3.4). Sillimanite needles are widespread and form aggregates lying in the matrix or riming garnets (Fig. 3.8G). The alluminosilicate is locally replaced by late muscovite (Fig.3.8H) which is otherwise absent in the peak assemblage. Biotite is always observed yet in low proportions. Tourmaline and rutile occurs in similar proportion and settings.

3.3.3 AMPHIBOLITES AND METAMAFICS

3.3.3.1 DISTRIBUTION AND APPEARANCE IN THE FIELD

Amphibolites and other mafics are reported in the nappe. Amphibolites occur either as lenses or layers in the garnet-kyanite-mica gneisses and form massive bodies, with a homogeneous texture and a sharp contact with the surrounding rock (Fig. 3.9A). These rocks which show a color ranging from dark green to black are generally composed of hornblende, plagioclase, biotite and locally epidote. As lenses, amphibolite bodies commonly display a lens long axis lying co-planar with the Caledonian fabric. Interestingly, in such lenses, the foliation is clearly discordant with the Scandian fabric observed in the host rock (Fig. 3.9A) indicating that these lenses have undergone a pre-Scandian deformation episode. In some locations however, the rock must have been reworked giving the outcrop a messy aspect with a disorganized alignment of the structures. Melt was commonly identified in these rocks so that the term of "migmatitic amphibolite" can sometimes apply. This melt may occasionally show shear sense indicators as this melt is deformed within the massive host rock (Fig 3.9B).

In addition to these "pure"amphibolites, some more complex metamafics have been identified. These rocks which consist in amphibole and pyroxene-rich lenses seem to have variable compositions, and show some deformation yet with a chaotic aspect. Locally a strongly mylonitic and massive outcrop has been sampled in which a last type of mafic was identified. This "artifact" which does not belong to a lens structure, is described further as part of the Scandian metamorphic path.

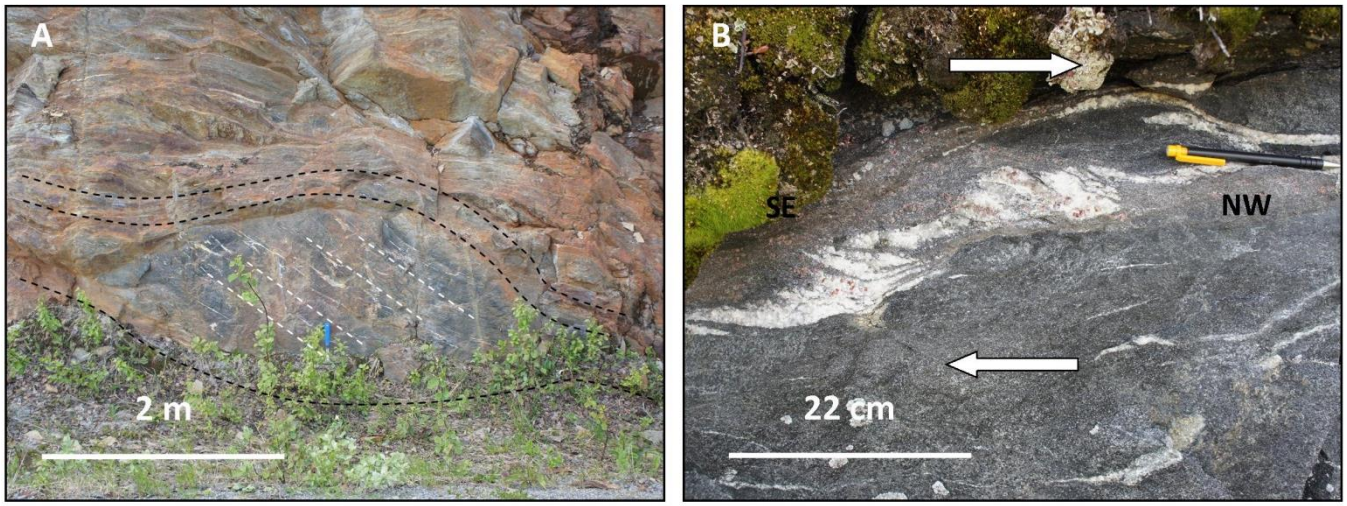

Figure 3.9 (A) Amphibolite lens in a garnet-kyanite-mica schist outcrop. Foliation in the lens and in the host rock is materialized by dotted lines. Note the discordant foliation in the lens. (B) Deformed melt pods in a massive amphibolite indicating a NW-directed dextral shearing.

3.3.3.2 Mineralogy and microstructure

In this section, metamafics only are described. Amphibolites did not show any interesting features and are therefore not reviewed here.

Mineralogy

***Quartz (10-30 %)*:** Occurs as ribbons or thin packed aggregates. Individual subhedral grains vary in size between 0,05 and 1 mm and are subhedral to euhedral. Grain size often increases in ribbons. Quartz is colorless, with no cleavage, no relief, has a low birefringence and an undulose extinction. Quartz also occurs as inclusion, in feldspar and garnets mostly.

K-feldspar (5-10%): Mineral with a low relief. The dominant alkalin feldspar is colorless with undulose extinction and a first order birefringence. The mineral occurs as small anhedral grain reworked in the matrix.

Biotite (5-20%): Occurs as very stretched and recrystallized skeletal crystals, which ressemble filaments braining around porphyroclasts and following the main fabric (Fig. 3.10A). Recrystallized biotite is evidenced with numerous and very fine subgrains (Fig 3.10B). Zonation is evidence by color variations which are commonly observed in single crystals (Fig. 3.10B). Biotite shows straight extinction and has a single cleavage lined with its longest axis itself parallel to foliation. The extinction ranges within the 3rd to 4th order of birefringence. Zircon inclusions are commonly observed. Biotite may also include others phases such as quartz, garnets, plagioclase or hornblende.

***Plagioclase (10-20%)*:** Mineral with a low relief, and two cleavages at 90 degres. It possesses polysynthetic twins, an oblique extinction and a first order birefringence. Plagioclases occur as broken fragments, strongly altered with frequent over-twinning of growth twins (Fig. 3.10C). Microcline is observed, well identified by its cross-hatched twin.

***Garnet (5-10%)*:** Colorless mineral, anhedral to euhedral, with 0.25 to 2 mm large grains. The mineral is isotropic, with no cleavage and has a high relief. Garnets are often cracked and may include quartz (Fig. 3.10C). The mineral is locally porphyroclastic and partially deformed (Fig. 3.10E).

***Hornblende (10-30%)*:** Occurs as very anhedral and sheared <0,05 to 3 mm pale green grains (Fig. 3.10A). The mineral shows an oblique extinction and has a high relief and a low birefringence. The characteristic diamond shaped cleavages are poorly defined but still observable. Zonations are locally reported and the mineral can be observed replacing clinopyroxenes (Fig. 3.10D).

***Clinopyroxenes (10-20%)*:** Colorless mineral with a moderate relief, a single cleavage and a low-birefringence. The mineral presents a straight extinction. Clinopyroxenes can be included, zoned and replaced by amphibole (Fig. 3.10D)

***Zoisite* (0-2*%)*:** Mineral occurring as small granular aggregates or stuby prisms. Zoisite is colorless, has a positive relief compared to quartz, a single cleavage and extinguishes parallel to its crystal length. A blue interference color (low birefringence) is observed and typical of these minerals in our thin sections. Locally, symplectites of zoisite and plagioclase are observed and evidence for diffusion controlled reactions (Fig. 3.10F and 3.11).

***Calcite (1-5%)*:** Colorless mineral with a low relief and a high birefringence. Extinction is symmetrical to the cleavage traces. Calcite is observed as individual grains and shows a “dusty” aspect.

***Titanite (1%)*:** Mineral with a very high relief and an extreme birefringence. Grains are deformed and altered, with a pastel color. The mineral is only observed locally.

***Rutile (0-1%)*:** Mineral occurring as small anhedral blebs in the matrix or in inclusions. Its dark yellow-orange color and very high relief are characteristic.

Tourmaline (0-1%): Mineral occurring as small anhedral blebs in the matrix. The mineral shows a dark green color under crossed polars and has a high relief

***Zircon (<1%)*:** Occur as very small blebs including biotite. The mineral is colorless with a high relief and is easily identified by its dark halo, resulting from its radioactive decay.

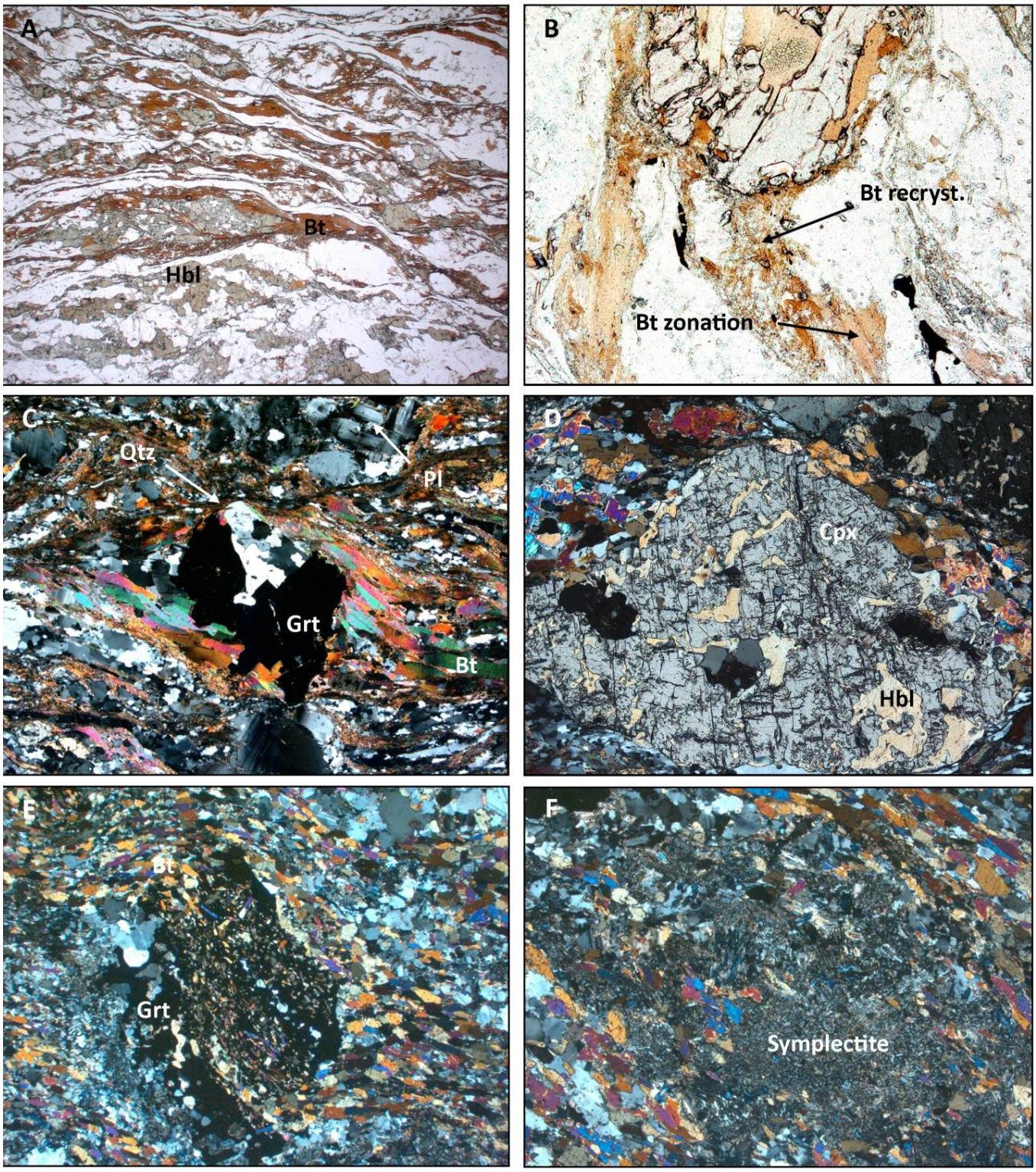

Figure 3.10 (A) Biotite fabric in a mylonitic mafic gneiss. Note the highly sheared hornblende crystals. Natural light, base of image 12 mm. (B) Close-up on biotite recrystallization and zonation in a mylonitic mafic gneiss. Natural light, base of

image 1.5 mm. (C) Anhedral garnet extensively replaced by quartz aggregates in a mylonitic mafic gneiss. Note the plagioclase fragments with strong twinning. Crossed polar, base of image 3 mm. (D) Clinopyroxene crystal replaced by hornblende in a mylonitic mafic gneiss. Crossed polars, base of image 3 mm. (E) Microphotograph of a pre-Scandian metamafic (sample RB 38). Note the late post-deformational garnet growing over the sheared matrix. Crossed polars, base of image 12 mm. (F) Microphotograph of a pre-Scandian metamafic (sample RB 38). Note the abundant symplectite structures. Crossed polars, base of image 6 mm.

MICROSTRUCTURE

Apart from sample RB 3 which is Scandian related, metamafic rocks are observed as highly retrogressed and partially deformed rocks which have undergone a strong reworking. Two thin sections (RB 38 and K 9) are described.

- RB 38 is a porphyric deformed metamafic rock characterised by the assemblage Qtz + Pl + Grt + Hbl + Ep which likely belongs to the epidote-amphibolite metamorphic facies. Garnets which are observed growing over the sheared matrix support a "post-deformation" mineral growth (Fig. 3.10E). In addition, the sample has revealed a retrograde mineral reaction evidenced by a clinopyroxene extensively replaced by a mélange of hornblende and epidote minerals (Fig. 3.11).
- K 9 is another retrogressed mafic sample distinguished from RB 38 by its lack of garnet and biotite. Apart from these minerals the mineralogy is similar. This sample does not contain any porphyroclasts and is assumed to originate from a different rock that for RB 38. Little can be said from this thin section as a strong reworking has overprinted most of the key features.

In both samples (RB 38 and K 9), a very developed mineral reaction is evidenced by large and widespread symplectites. These structures, characteristic of decompressional processes may cover up to a quarter of the whole thin section surface (Fig. 3.10F) and indicate that these rocks underwent a strong reworking. According to petrographical observations, symplectites involve feldspars, hornblende, epidote minerals, zoisite, calcite, and some calcic accessory minerals such as titanite.

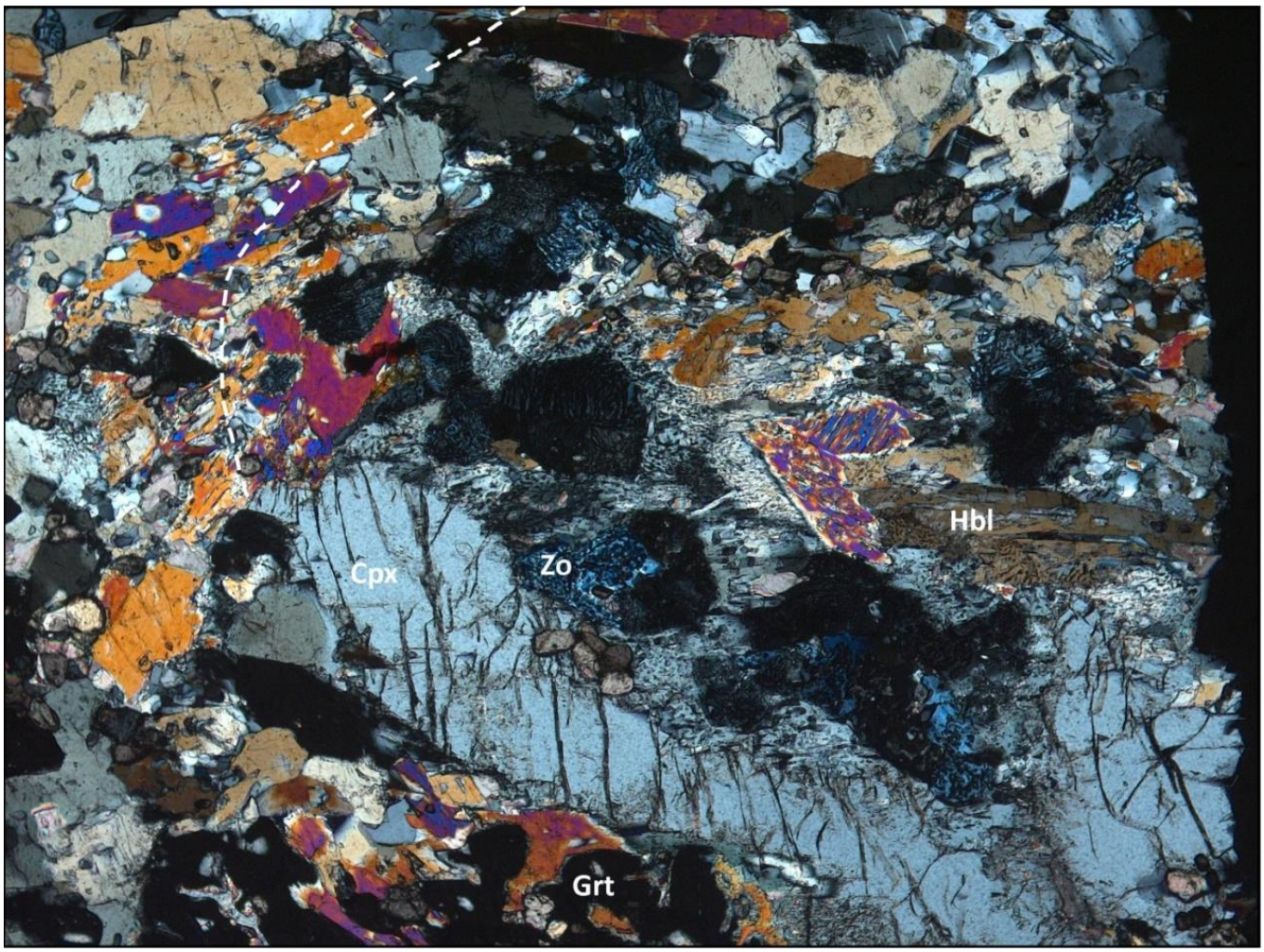

Figure 3.11 Microphotograph of a retrogressed pre-Scandian metamafic (sample RB 38). Focus on a mineral reaction of a wide clinopyroxene crystal being replaced by a mélange of hornblende, epidote minerals and melt. Zoisite is often observed in symplectite. The dashed white line suggests the clinopyroxene crystal boundaries. Crossed polars, base of image 12 mm.

3.3.4 PHYLLITES

3.3.4.1 DISTRIBUTION AND APPEARANCE IN THE FIELD

Phyllites outcrop as a linear unit sandwiched between the pelitic gneisses and schists of the Nordmannvik Nappe and the mafics of the Lyngen Nappe Complex. The unit is bounded by two thrust faults both dipping NW. These phyllites consist of heavily sheared rocks showing a crenulation cleavage, particularly well defined in the northernmost part of the area (Fig. 3.12A). The rock readily breaks as sheets along the cleavage planes and pyrite mineralizations are reported. Phyllites are

composed of quartz and micas, the latter yielding lustruous aspect to the foliation surfaces. Other phases include calcite, feldspars, garnets, and chlorite.

Phyllites fabric is parallel to that of the adjacent garnet micas gneiss/schists. This crenulation cleavage consists in a fold train lying subparallel to the Caledonian E-W foliation in a manner that the fold axes are almost perpendicular to the stretching lineations, and included in the foliation plane. Contact between the phyllites and the garnet-kyanite-mica gneisses is a thrust fault where the phyllites overthrust the higher grade rocks. Phyllites are dipping to the NW toward the Lyngen Nappe Complex with a dip angle of about 45 degres (Fig. 3.12B).

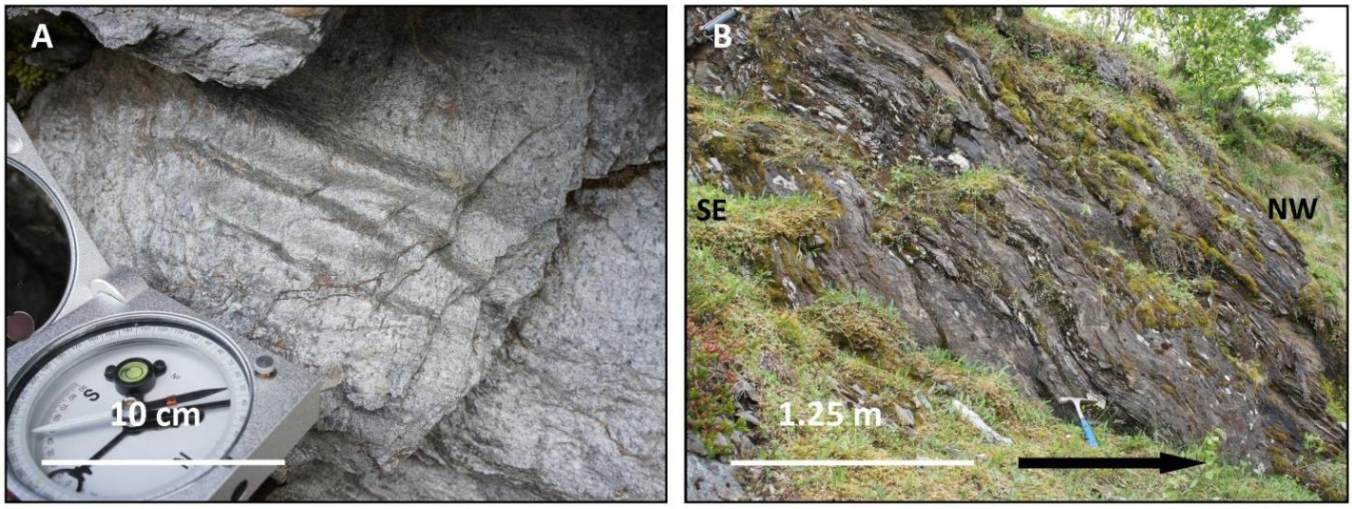

Figure 3.12 (A) Crenulation cleavage in phyllites. (B) Phyllite outcrop observed as a cross section oriented SE-NW.

3.3.4.2 Mineralogy and microtexture

Mineralogy

***Quartz (50-80 %)*:** Occurs as ribbons or thin packed aggregates. Individual grains vary in size between 0,05 and 1 mm and are subhedral to euhedral. Grain size often increases in ribbons yet they are rarely observed. Quartz is colorless, with no cleavage, no relief, has a low birefringence and an undulose extinction. The mineral is seldomly observed as inclusion in garnets.

***Biotite (20-30 %)*:** Occurs as highly stretched crystals braining around garnet porphyroclasts and accommodating the foliation. Biotite shows straight extinction. The mineral has a single cleavage lined with its longest axis itself parallel to foliation. The extinction ranges within the 3rd to 4th order of birefringence. Zircon inclusions are commonly observed.

Muscovite (20-30%) shows a straight extinction and has a single cleavage lined with its longest axis itself parallel to foliation. The birefringence is high (3rd order). The mineral occurs as "fish" and highly stretched crystals associated with biotite and chlorite.

***Garnet (0-10%)*:** Colorless mineral, subhedral to euhedral, with 0.25 to 2 mm large grains. The mineral is isotropic, with no cleavage and has a high relief. Garnets commonly include neoformed quartz grains.

***Chlorite (2-5%)*:** is seldomly observed as stretched crystals, in association with micas. The mineral is pale green, biaxial and displays anomalous birefringence colors.

***Calcite (5-15%)*:** Colorless mineral with a low relief and a high birefringence. Extinction is symmetrical to the cleavage traces. Calcite is observed as anhedral to subhedral grains and shows a "dusty" aspect.

***Tourmaline (0-3%)*:** Mineral occurring as small anhedral blebs in the matrix. The mineral show a dark green color under crossed polars and has a high relief.

Rutile (0-1%): Mineral occurring as small anhedral blebs (< 0.05mm) in the matrix or in inclusions. Its dark yellow-orange color and very high relief are characteristic. Rutile is usually accessory but is locally found in relatively high proportions.

MICROSTRUCTURE

Phyllites are fine grained and strongly sheared rocks mainly composed of quartz and micas (Fig. 3.13) yet subordinate minerals such as chlorite and calcite are also observed. In a lesser extent, accessory minerals notably comprise tourmaline and rutile. These minerals occur in identical settings as they do in other rock types of the Nordmannvik nappe, especially in garnet-kyanite-mica gneisses.

If the structural distinction between phyllites and gneisses / schists is rather easy at the macroscale, problems arise when it comes to thin section studies. Ultramylonitic gneisses may resemble phyllite

appearance owing to the uniform fabric and the strong grain size reduction. In order to classify a rock as phyllite, the following criterions have been considered:

- Phyllitic texture is very homogeneous, with almost no quartz ribbons, and a very regular grain size.
- Microfold, spaced foliation development and S-C structures are well-defined and easily observed.
- Micas are highly sheared and layered but dispersed and do not form competent and thick layers as they may do in mylonitic gneiss.

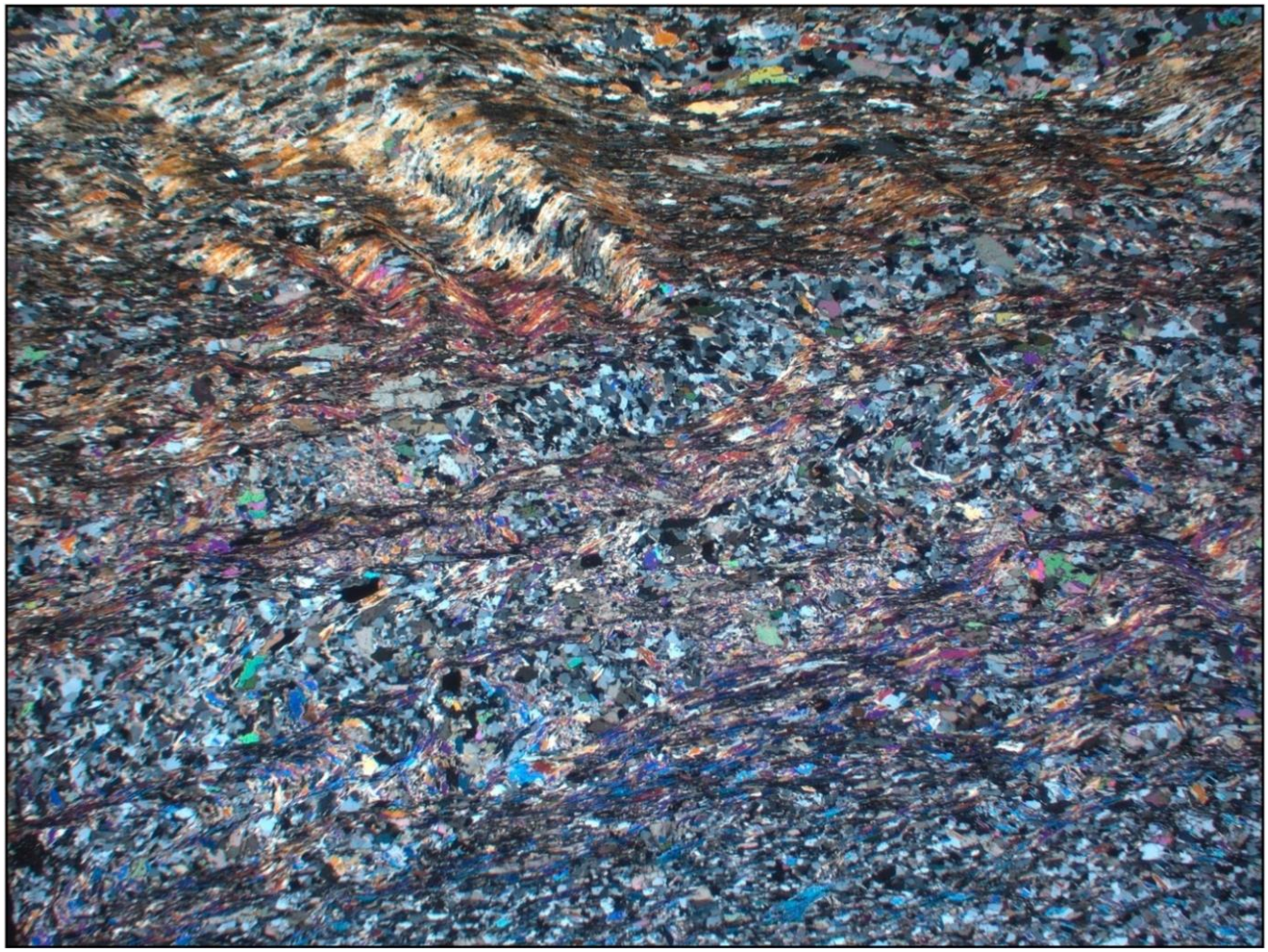

Figure 3.13 Microphotograph of a typical phyllitic texture. Note the micro-fold in the upper part of the picture as well as the spaced foliation in the lower part. Crossed polars, base of image 12 mm.

3.3.5 MIGMATITES

3.3.5.1 DISTRIBUTION AND APPEARANCE IN THE FIELD

Gneisses from the Nordmannvik have sometimes undergone partial melting. The resulting melt is mostly found as thin layers or elongated lenses of quartzo-feldspatic leucosome, lying sub-parallel to the dominant fabric (Fig. 14A). In one specific outcrop however, migmatite displays a chaotic aspect which contrasts with the fabric of the host rock. In such cases the contact between migmatites and "dry" metapelites is transitional and (Fig. 14B).

In addition, the term “migmatite” can also be applied to describe some amphibolites which have undergone an apparent anatexis, and are so called “migmatitic amphibolites” (Fig. 3.14D). Locally, high grade hand-sized relics of mafics intruded by sheared melt filaments are reported (Fig. 3.14C).

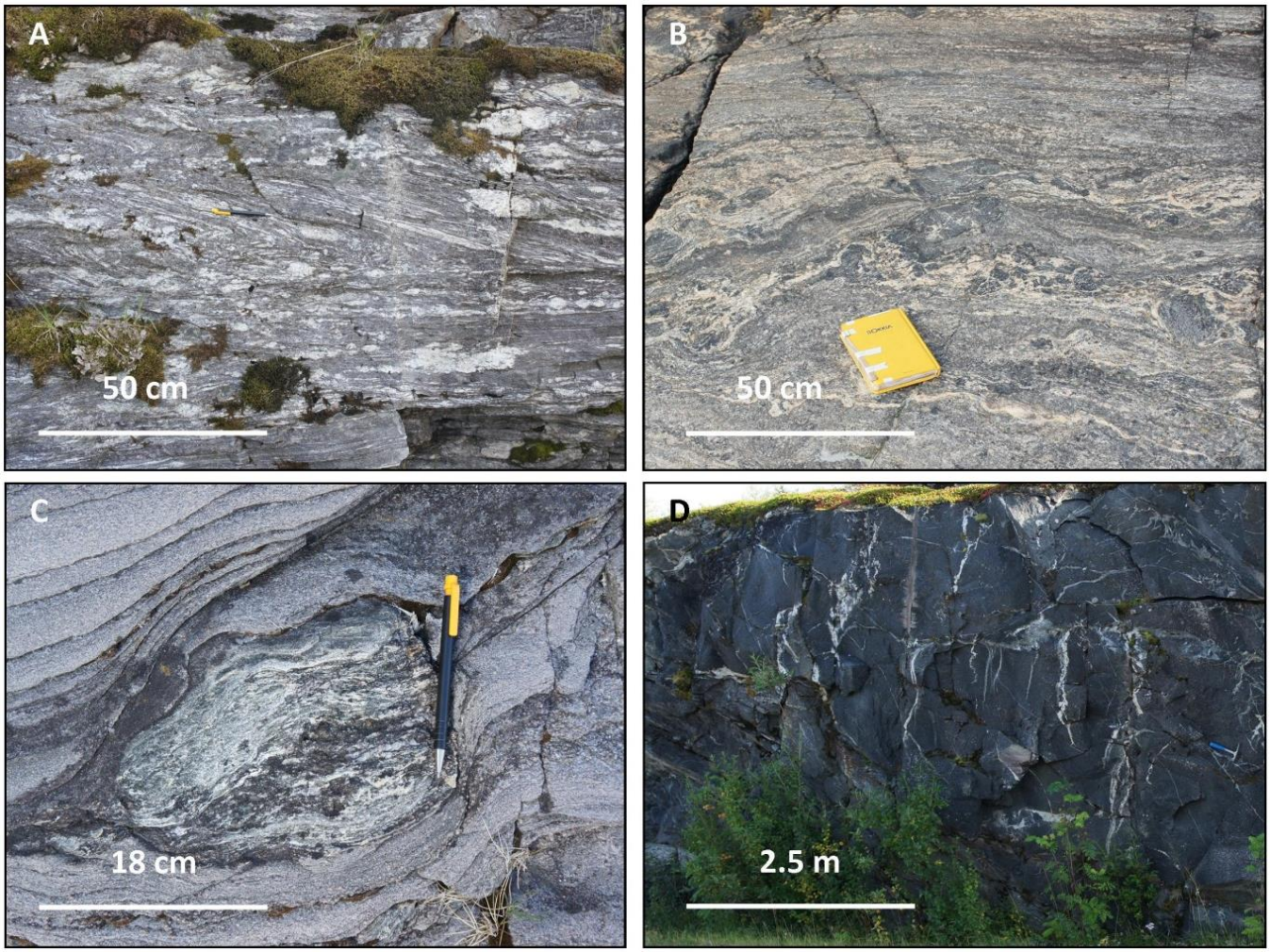

Figure 3.14 (A) Strongly migmatized garnet-kyanite-mica gneiss showing parallel to sub-parallel deformed melt layers. (B) Migmatite spot showing randomly shaped melt layers and mafic lenses. (C) High grade migmatized mafic lens showing an important proportion of melt. (D) Mega-lens of migmatitic amphibolite.

3.3.6 MARBLES AND CALC-SILLICATES

3.3.6.1 DISTRIBUTION AND APPEARANCE IN THE FIELD

Marbles and calc-silicates are observed rather frequently in the Nordmannvik Nappe. In the northern peninsula, south of Koppangen, marble occurs as N-S directed bands and lenses in the garnet-kyanite-mica gneisses (Fig. 3.15A). Calc-silicates (Fig. 3.15C) are less frequent and can be mistaken with pelitic

gneisses owing to the high proportion of pelitic material. Meta-conglomerates are locally reported. Marble and calc-silicates occurs as parallel layers displaying a foliation S_1 dipping to the W. Average dip is somewhat similar to that in the garnet-kyanite-mica gneisses (20-30°). Sigma clasts indicate a SE directed general movement of the upper block (Fig.3.15B).

3.3.7 ULTRAMAFIC LENSES AND SAGVANDITE

3.3.7.1 DISTRIBUTION AND APPEARANCE IN THE FIELD

Pyroxene-rich ultramafic rocks occur as lens-shaped, boudins or highly stretched bodies composed of pale green-grey prismatic crystals of pyroxene associated with some felsics minerals (feldspars, quartz), amphiboles and biotite (Fig. 3.15D). Boudins and lenses varying from a few centimeters to few meters have been reported. These structures are observed in association with pelitic gneisses, carbonates and amphibolites (Fig. 3.15E). In addition, mega-lenses of Carbonate-orthopyroxenite rock known as sagvandite (Schreyer et al., 1972; Elvevold, 1985; Bergh et al., 1989; Lindstrøm et al., 1992) are reported north of Lyngseidet (Fig. 3.15F). Their location is shown on the interpretative geological map. In comparison with amphibolite lenses, the ultramafic bodies are smaller.

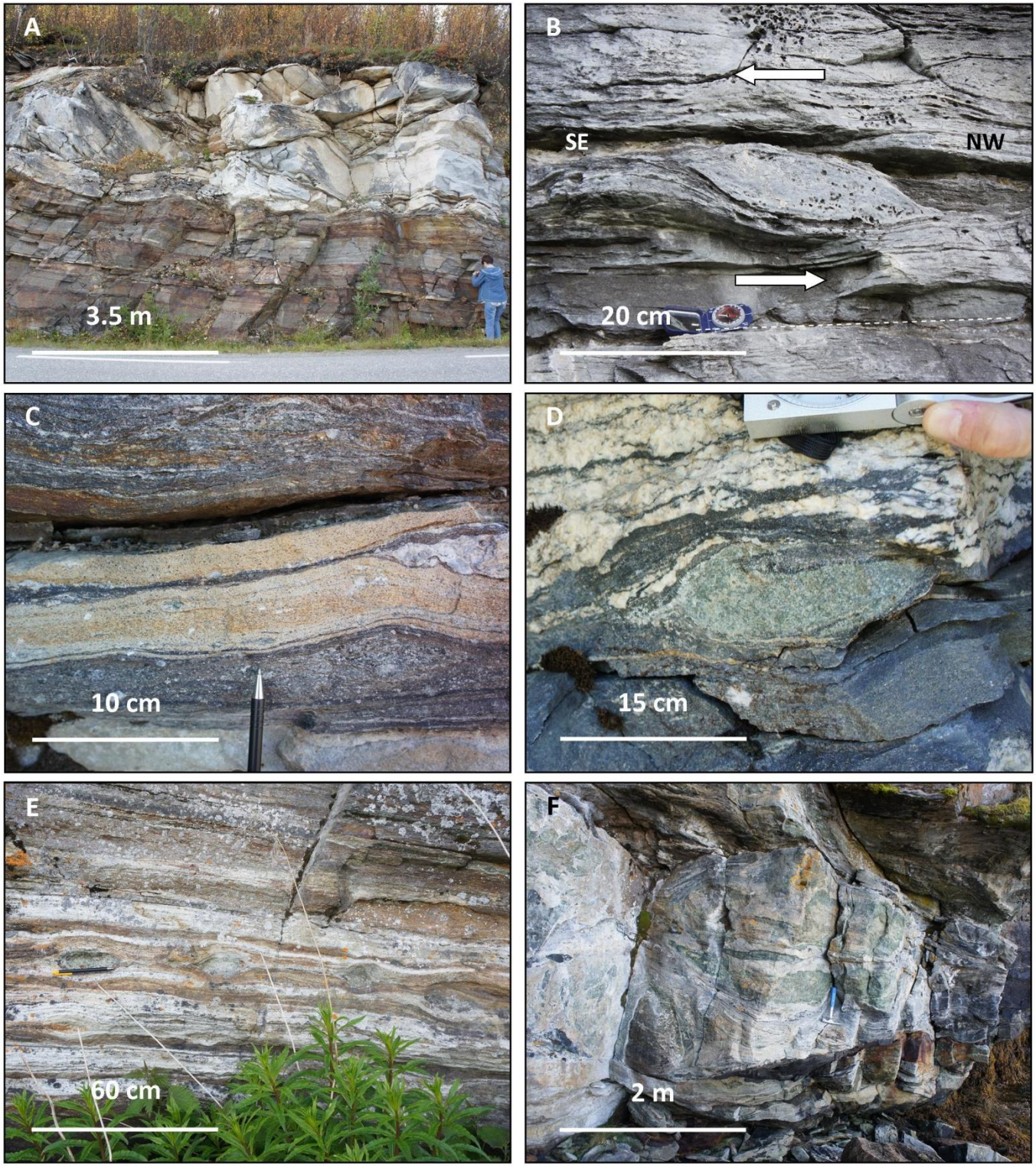

Figure 3.15 (A) Lithological contact between a pelitic schist outcrop and a mega-scale marble lens. (B) σ-shape marble clast in a marble body overlying the pelitic gneisses. A sinistral shearing is observed and the upper block move toward the SE. Contact with pelitic gneisses is observed at the base of the picture. (C) Close-up on a calc-silicate outcrop showing a dark garnet-kyanite-mica gneiss interbedded with a marble horizon (white layer).

(D) Close-up on a Cpx-rich ultramafic lens embedded in a calc-silicate outcrop. (E) Boudins of Cpx-rich ultramafic lenses in calc-sillicate outcrop. (F) Sagvandite outcrop with focus on a Cpx-lens.

3.4 METAMORPHISM

3.4.1 METAMORPHISM IN GARNET-KYANITE-MICA GNEISSES

3.4.1.1 METAMORPHIC PEAK (M_1) ASSEMBLAGE

Garnet-kyanite-mica gneisses are deformed rocks showing a biotite mylonitic foliation. The metamorphic peak assemblage is observed in some samples, notably because the mineral characteristics of the metamorphic peak facies (Grt, Ky and rare Kfs) are wrapped in the mylonitic fabric, and are therefore earlier. The assemblage Qtz + Grt + Ky + Pl + Bt ± Ms ± Kfs + melt + accessories describes the average rocks composition observed at the metamorphic peak but compositional variations are reported depending upon the sample. Locally, quartz ribbons and highly sutured quartz boundaries highlight the high temperatures the samples have reached.

Because of the low proportion of K-feldspar, the granulite facies assemblage Grt + Ky + Kfs + melt cannot be used as a robust characteristic assemblage of a granulite facies. Nevertheless, an upper amphibolite facies is certainly attained and the occurrence of melt indicates that the metapelites have crossed the 680°C isograde (Bucher and Grapes, 2011). The presence of kyanite, melt and rare K-feldspar as well as the low amount of early muscovite at the metamorphic peak strongly suggest that muscovite has decomposed along a Ky-type path through dehydratation reactions. These reactions discussed further (Chapter 4) involve the formation of K-feldspar which takes over on muscovite for the storage of alkali with increasing P/T conditions (Bucher and Grapes, 2011).

3.4.1.2 POST-M_1 ASSEMBLAGE

Two different sets of samples have shown a post-M_1 assemblage. The first one is composed of high grade rocks sharing a similar mineralogy to that of M_1 samples yet sillimanite is observed as very small recrystallized needle aggregates (Fig. 3.7C). The sillimanite is seldomly reported rimming garnets, or crystallizing within the biotite fabric. Biotite is mostly found as sheared crystals which define the mylonitic foliation. The mineral is sometimes zoned (Fig. 3.7B) indicating compositional variations.

A second set of metapelites is characterized by the lack of aluminosilicates, widespread muscovite, hornblende, some chlorite and common epidote mineral and zoisites. Calcite is also present in variable amount depending upon the sample. The association epidote minerals/zoisite + chlorite is taken as diagnostic of the epidote-amphibolite facies which is the lowest metamorphic assemblage encountered in the garnet-kyanite-mica gneisses.

In these samples, evidences for late retrograde reactions include (1) the discordance of late mineral phases such as chlorite, micas or garnet observed lying across the dominant fabric, (2) mineral recrystallizations in biotite and amphiboles and (3) mineral inclusions (quartz grains in garnets). Static recrystallizations are also observed in quartz, arguing for late re-equilibration processes. The mylonitization is retrograde because it affects retrograde assemblages, and wraps around undeformed mineral which belongs to the peak assemblage (M_1).

3.4.2 METAMORPHISM IN GARNET-SILLIMANITE GNEISSES

3.4.2.1 METAMORPHIC PEAK (M_0) ASSEMBLAGE

Metapelites reaching a granulite facies have all been observed at a peak (M_0) or late (post-M_0) metamorphic stage. The typical assemblage Qtz + Kfs + Grt + Sil + melt characterizes M_0. Evidences for a high grade regime include (1) numerous quartz ribbons with highly sutured boundaries (Fig. 3.8A), and (2) the presence of melt (Fig. 3.8E). Partial melting is supported by the widespread cuspate boundaries between quartz grains (Fig. 3.8A).

Granulite facies metapelites were always observed in lenses or elongater layers of relic material. One outcrop has shown to illustrate accurately these structures and is presented below in order to illustrate the differences between M_1 and M_0 assemblages. For this purpose, two samples (RB 16E and RB 16B) were especially valuable as they illustrate the difference between a mylonitic upper amphibolite (M_1) facies assemblage (RB 16E) and a lens of undeformed (M_0) granulite facies assemblage (RB 16B). Fig. 3.16 is a picture of the considered outcrop showing the outcrop location and the rock texture in which these samples have been taken. Both of them are pictured by a thin section microphotograph taken with the same settings for an easy comparison (same magnification with crossed polars).

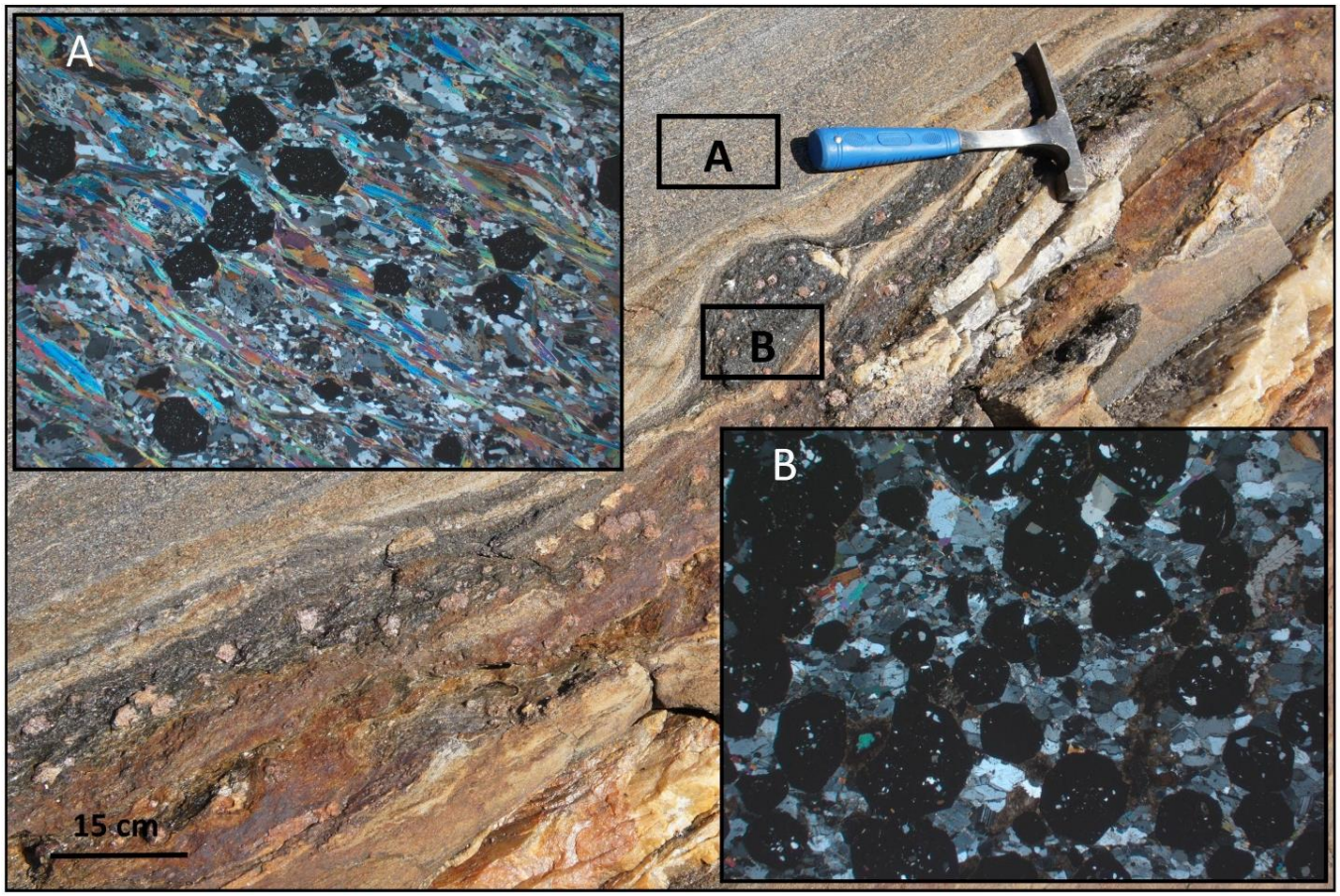

Figure 3.16 Photograph of a garnet-kyanite-gneiss outcrop intruded by granulitic facies metapelite lenses. Thin section microphotographs of part of the outcrop are shown: (A) Microphotograph showing a garnet-kyanite mica-gneiss. Note the euhedral garnets and their quartz inclusions as well as the mica fishs. Crossed polars, base of image 12mm. (B) Microphotograph showing a garnet-sillimanite gneiss, taken in a lens as shown on picture 3.16. Note the importance of the euhedral garnets porphyroclasts and the absence of muscovite. Crossed polars, base of image 12 mm.

- Fig 3.16A illustrates a high grade garnet-kyanite-mica gneiss which has reached M_1. Muscovite and biotite accommodate the late mylonitic foliation and contour garnets. These garnets are euhedral and show quartz inclusions which are restrictly observed in the garnets core. Kyanite is frequent and occurs as skeletal blebs. K-feldspar is rarely observed and muscovite is reported in low proportions. The deformed assemblage Grt + Pl + Ky + Bt + Mv ± Kfs characterizes this sample.

- Fig 3.16B shows a non-mylonitic garnet-sillimanite gneiss (assemblage M_0) notably characterized by the onset of K-feldspar and the quasi-absence of muscovite. K-feldspars are not large in numbers yet they are a major component of the melt widespread in the sample. Garnets are very abundant, porphyroclastic and present quartz inclusions. These inclusions do not show any pattern unlike in RB 16E. The undeformed assemblage Qtz + Kfs + Grt + Sil ± Bt + Melt characterizes this sample.

3.4.2.2 POST-M_0 ASSEMBLAGE

Some garnet-sillimanite gneisses which reached M_0 have shown evidences for a later retrograde episode. K-feldpars occur as perthite-rich porphyroclasts (Fig. 3.8D). Garnets are also porphyroclastic and rather euhedral. Both, K-feldpsars and garnet porphyroclasts are rimmed by two different late retrograde mineral assemblages which occur in similar settings. One rim type is composed of muscovite with some melt (Fig. 3.8B) and the other is made of chlorite (Fig. 3.8C). Other elements arguing in favor of retrograde processes include; (1) fine grained recrystallized quartz aggregates in K-feldspar and garnets porphyroclasts, (2) myrmekite growths (Fig. 3.8D) along the boundaries of K-feldspar porphyroclasts and (3) garnets which locally show a rim of quartz melt contouring their crystal boundaries (Fig. 3.8F). Note that rim structures and recrystallizations are compatible with a pressure drop.

In addition to these observations, a cooling episode is inferred from the abundant perthite intergrowths (Fig. 3.8E) supposed to form as the dominant orthoclase cools down. This cooling likely started at high temperature and is not necessary related to the rim structures previously mentionned.

3.4.3 METAMORPHISM IN SCANDIAN GRANULITE FACIES METAMAFICS

3.4.3.1 METAMORPHIC PEAK ASSEMBLAGE M_1

Mafic rocks have locally reached M_1 in the high-pressure granulite facies evidenced by the association Grt + Cpx + Qtz + Pl + Ru (described by Elvevold et al., 2003), in sample RB 3.This sample is strongly deformed and presents a blastomylonitic texture where biotite accommodates the mylonitic fabric (Fig 3.10A). Clinopyroxenes and garnets are rather euhedral. Because these minerals are characteristic of the metamorphic peak conditions and also wrapped in the mylonitic fabric, mylonitization post-dates

the metamorphic peak. Moreover, in the current fabric, minerals are not in contact as they should be in a granulitic rock. However, as a strong mylonitization has occurred, the original mineral layout is most likely not conserved.

3.4.3.2 Post-M_1 assemblages

In RB 3, evidences for post-M1 metamorphism are reported and two processes are identified. The first one relates to the extensive dynamic recrystallizations of biotite and hornblende in the mylonitic fabric. Late quartz inclusions, notably affecting the high grade garnets are also observed (Fig. 3.10C).

A second process involves early deformed clinopyroxenes which are progressively replaced by hornblende (Fig. 3.10D) according to a mineral reaction retrogressing the sample from the granulite to the amphibolite facies. Because hornblende appears stretched and recrystallized in a similar way as biotite does, the mylonitization is coeval with the retrogression of the high grade assemblage.

3.4.4 Metamorphism in pre-Scandian metamafics

In the Nordmannvik Nappe some metamafics are observed as highly retrogressed and partially deformed rocks. Owing to the strong reworking which affected these rocks, no metamorphic peak assemblage is identified. The abundance of symplectite structures highlight the intense mineral reactions which occurred in these mafics and suggest that decompression of the high grade assemblage occured. The abundance of epidote minerals and zoisite suggests a epidote-amphibolite facies and the local occurrence of clinopyroxenes may indicate that some samples reached a granulite facies. Nevertheless the chaotic structure and a clear lack of oriented structures do not allow robust observations.

3.4.5 Metamorphism in phyllites

Phyllites are highly recrystallized and sheared rocks which have not shown compositional variations. Because phyllites present structures oriented similarly to those from the garnet-kyanite-mica gneisses, we assume that both rock types evolved conjointly. Phyllites showed a low grade assemblage, likely formed during a retrograde metamorphic path, similarly to the gneisses and schists. The typical assemblage is devoid of alluminosilicates with rare amphibole and abundant quartz, micas, calcite and chlorite. Amphibole is sporadically observed and garnets develop in some thin sections. An upper greenschist facies is suggested.

3.4.6 Evidences for partial melting and fluid interaction

3.4.6.1 Partial melting

Partial melting, in the Nordmannvik Nappe is evidenced by the common occurrence of migmatite and leucosome volumes. In the first case, the rock itself is partially molten whereas leucosome volumes occur as intrusive dykes or chaotic pods composed of felsic minerals which segregated from the host rock during the partial melting. In this chapter we focus on these leucosome volumes, especially on their composition.

Thin section studies show a quartzo-feldspathic composition with rare biotite (Fig. 3.17A) and accessories. Zoisite can be encountered as well as scattered plagioclases and rare small garnets. Highly sutured quartz boundaries are common, indicating a high temperature episode (Fig. 3.17A). Melt shows similar evidences of a temperature drop as in the granulitic metapelite; late muscovite and biotite, as well as many perthite exsollution lamellae are commonly observed wrapped in a fine crystallized melt. Plagioclases are altered and replaced recrystallized melt or K-feldspars. Sillimanite needles are frequently observed (Fig. 3.17B) but require a high magnification to be identified. Biotite, strongly zoned is not always observed.

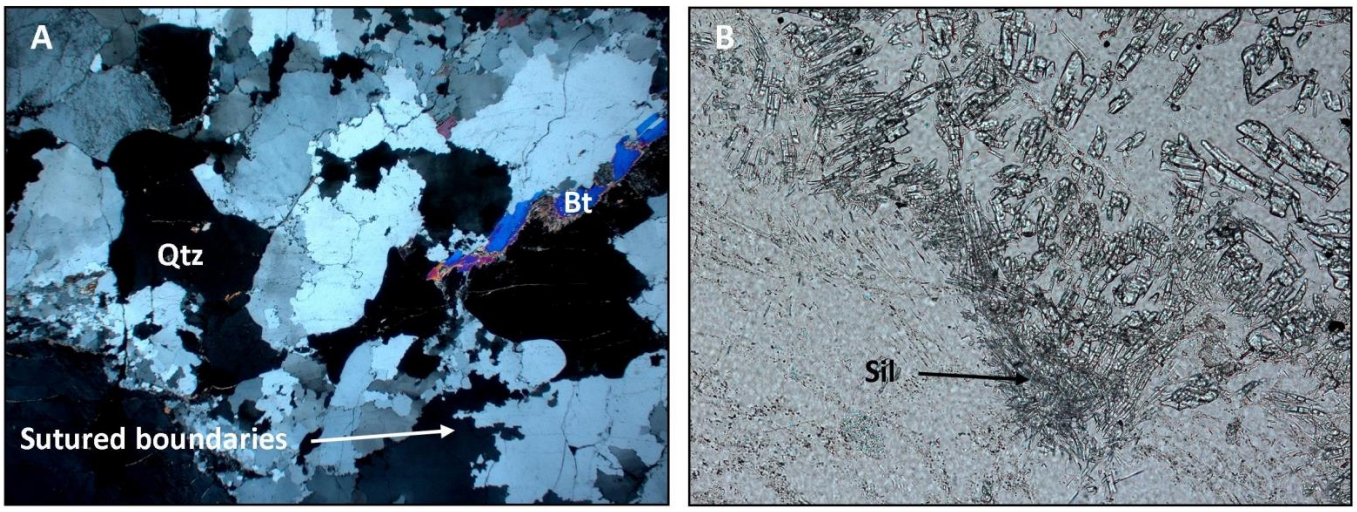

Figure 3.17 (A) Quartz and rare biotite in a leucosome volume. Note the sutured boundaries along quartz grains. Crossed polars, base of image 12 mm. (B) Sillimanite needles in a leucosome volume. Natural light, base of image 1.5 mm.

3.4.6.2 Fluid interaction

As the main catalyzer and reactant during partial melting, H_2O fluids have an important role in the whole rock chemistry. Based on the widespread occurrence of both calcite and calcic minerals (notably

titanite and zoisite) in metapelites and mafic rocks, it is believed that fluids are CO_2-rich. Zoisite, according to Poli and Schmidt (1998) can easily occur at mixed fluid (CO_2-H_2O) conditions. Likewise, titanite ($CaTiSiO_5$) requires a calcium-rich environment to form. Consistently, the abundant carbonate rocks which are observed in the area are thought to be a realistic source for the calcium observed in the system.

3.5 DEFORMATION MICROSTRUCTURES

3.5.1 SHEAR SENSE INDICATORS

3.5.1.1 DESCRIPTION OF SHEAR SENSE INDICATORS

In this section, deformation microstructures that have been encountered in the thin sections are reviewed. According to our observations, the following structures are observed.

Asymetric augen structures (described by Simpson and Schmid, 1983 and Bose and Marques, 2004) are large and flow-resistant grains, also named as porphyroclasts occurring within a more ductile and fine-grained matrix. They are typically feldspars, garnets or quartz grains wrapped by tails of weaker minerals (i.e. micas) or finer grained recrystallized material of the same mineral as the prophyroclast. This fine-grained material within the tails is usually the product of dynamic recrystallization but pressure solution may also be involved. These tails are used as shear sense indicators and are considered as reliable criteria. The dominant porphyroclast-tail geometry is described, as **σ**-clasts referring to the shape of the tail which develops around the porphyroclast. **σ**-clasts are unrotated clasts whose tail does not cross the shear plane (S_1), described as the reference plane (Fig. 3.18A and 3.18B). Such shapes are commonly observed in hornblende, quartz and garnets porphyroclasts.

According to Bose and Marques (2004), few majors factor control tail geometry among which the degree of adherence of the inclusion to the matrix and the rheological behavior of the mantle relative to the matrix. In case no tail is present around the prophyroclast, shearing sense may still be given if the porphyroclast has been rotated. In such case, the sense of shear is determined by the sense of rotation of the propyroclast. For a clockwise rotation, the shearing is dextral and vice versa.

Crenulation cleavage development (described by Passchier and Trouw, 2005) is observed in the phyllites and the ultramylonitic rocks (Fig. 3.18C). These structures observed in a strongly deformed stage are thought to be formed by solution transfer and rotation. They are composed of a spaced foliation which is observed where micas are lined along the dominant fabric (S_1) and form the cleavage domain whereas quartz-rich assemblages delimited by the cleavage domains are defined as microlithons (Fig. 3.18C). Passchier and Trouw (2005) proposed a step-by-step possible development of crenulation cleavages (Fig. 4.4). Evolution of crenulation cleavages involves shear but does not indicate shear sens.

Microfolds are observed in phyllosilicate (Fig. 3.18D) as fold trains which axial planes cut the foliation at about right angle. According to Passchier and Trouw (2005), owing to solution transfer and oriented crystallization or recrystallization of new grains, the fold limbs in many cases will develop a spaced foliation after the fold has reached certain amplitude.

S-C fabrics (described by Berthe et al., (1978) and Simpson and Schmid, (1983)) are commonly observed in the phyllites (Fig. 3.18E), and occasionally in the garnet-kyanite-mica-schists. They are composed of two sets of planar anisotropies named “C” and “S” surfaces. The C surfaces (for “cisaillement” or shearing) are rather regularly spaced slip surfaces which sens of shear matches the overall shear zone. These C-surfaces are thin layers of recrystallized, polymineralic aggregates showing a reduced grain size (Simpson and Schmid, 1983). S-surfaces (for “schistosite” or foliation) are defined by the mineral-shaped orientation of the old grains between the C-surfaces. Initially S surfaces are at 45 degres to the C-surfaces but flatten as deformation increases. Note that in ultramylonites, where extreme shearing occurs, S-C surfaces may be parallel so that S and C surfaces can no longer be distinguished (Berthe et al., 1979). This angular relationship between both types of surfaces defines the sense of shear.

Mica fishs (also referred as “displaced broken grains”) are elongate lozange or lens-shaped single mica crystals either tilted back against the sense of shear or sub-parallel to the C-surfaces (Passchier and Trouw, 2005; Lister and Snoke, 1984; Fig. 3.18F). Trails of small micas fragments commonly extend into the matrix from the tips of isolated mica fish (Passchier and Trouw, 2005).

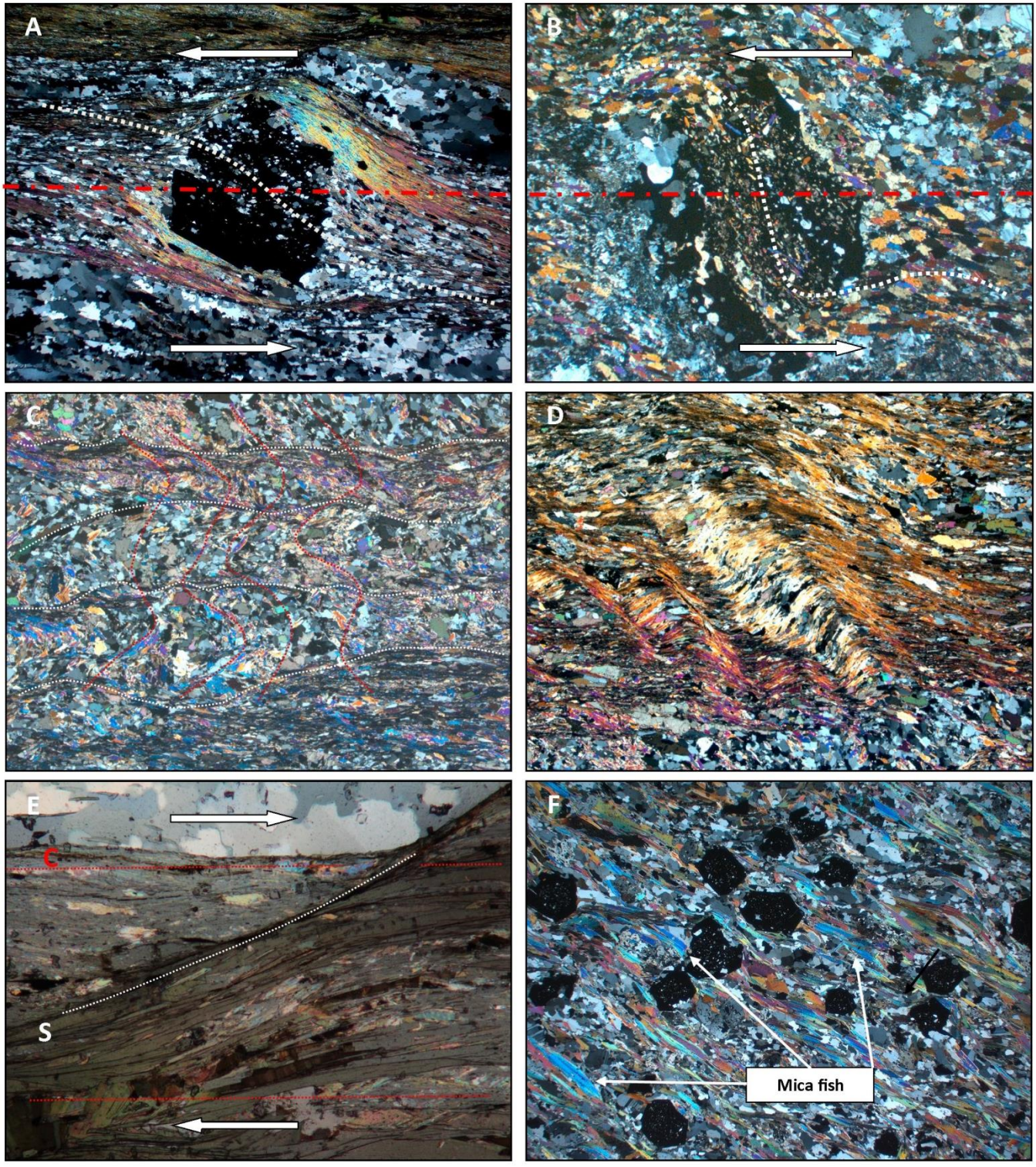

Figure 3.18 (A) Garnet sigma clast in a mylonite. The red dotted line indicates the reference plane, and the white dotted line outlines the sheared fabric. The upper block moves toward the SE. Crossed polars, base of image 12 mm. (B) Garnet delta clast in a metamafic. The red dotted line indicates the reference plane, and the white dotted line outlines the sheared fabric. The upper block moves toward the SE. Crossed polars, base of image 12mm.

(C) Crenulation cleavage showing a spaced crenulation in a phyllite. The white dotted line indicates the cleavage domains and the red dotted line shows the folded microlithons. Crossed polars, base of image 6 mm. (D) Microfold in a phyllite. Note the strong amplitude of the fold limb. Crossed polars, base of image 6 mm. (E) S-C fabric in a mica schist. The upper block moves toward the SE. Natural light, base of image 1.5 mm. (F) Mica fishs in a mylonitic gneiss. Crossed polars, base of image 12 mm.

3.5.1.2 OBSERVATIONS IN THIN SECTIONS

In this paragraph, shear indicators (described in section 3.5.1) are reported in table 3.1 for 11 metasedimentary and 3 metamafic samples.

Table 3.1 Shear indicators sorted par type, for 14 thin sections from the Nordmannvik nappe.

Thin section reference	σ clasts	Micas fish	Microfolds	S-C fabrics	Crenulation cleavage	Structures orientation	Movement of the upper block
Metapelites and Calc-silicate							
RB 25			X	X	X	N 310	-
RB 26	X	X	X	X	X	N 312	to the SE
RB 27	X	X	X	X	X	N 305	to the SE
RB 28	X	X				N320	to the SE
RB 16E	X	X				N290	-
RB 39B	X	X				N 310	-
K1			X	X	X	N 308	-
K2	X	X	X	X	X	N 280	to the SE
K4	X	X	X	X	X	N 320	to the SE
K5		X				N 290	to the SE
K8	X	X				N 286	to the NW
Metamafics							
RB 3	X					N 310	-
K9	X					-	-
RB 38	X					-	-

From table 3.1, three groups are defined on the basis of which shear indicators are observed. The following comments are made:

- A first group gathers RB 26, RB 27, K2 and K4. These samples have shown all the different microstructures and are described as strongly mylonitic to ultramylonitic samples. Grain size reduction is important but micas fish and σ – clasts, yet small are still observed.
- A second group gathers RB 25 and K1. These samples are characterized by an extrem grain size reduction and a total recrystallization of the matrix which did not display mica fishs or any clasts. Contrastingly, these samples showed very developed S-C fabrics, microfolds and crenulation cleavage development. These samples are phyllitic and account for the most sheared and recrystallized ones.
- A last group gathers all the remaining samples (RB 28, RB 16E, RB 39B, K5, K8, RB 3, K 9 and RB 38). All of them are characterized by a light-to medium mylonitic fabric, restrictly showing σ– clasts and/or micas fish. This group also includes the mafic samples which, apart from RB 3, have shown a very weak deformation.

Eventually, all garnet-kyanite-mica gneisses have shown a mylonitic fabric (S_2). This fabric is sub-parallel to the mineral foliation (S_1) and is accommodated by sheared biotite. The development of spaced foliations and microfolds only indicated shearing without shear senses and mica fishs were sometimes difficult to intepretate. However, the remaining structures most often indicated a SE directed movement of the upper block (seldomly NW directed) when shear sens could be inferred.

3.5.2 QUARTZ DEFORMATION

3.5.2.1 INTRODUCTION

As a rock undergoes increasing P/T metamorphic conditions, minerals are subjected to an increasing flow stress and the internal strain energy which also increases needs a counterpart to prevent the crystal lattice from breaking down. In order to reduce this flow stress, physical processes occur, among which dynamic recrystallization, which is reviewed here.

3.5.3.2 DEFORMATION IN QUARTZ

Quartz easily deforms by dynamic recrystallization which is a key mechanism for understanding deformation processes and the most important deformation mechanism in quartz. Three sub-processes commonly occur depending upon temperature conditions and strain rate. They originate from two physical mechanisms which are namely the migration of existing grain boundaries and the formation of new grain boundaries (Stipp et al., 2002). Two classification systems have been proposed. The first one, from Hirth and Tullis proposed a classification based on experimental results and defined three deformation regimes which are described in Hirth and Tullis (1992).

Stipp et al. (2002) proposed another classification based on observation from natural conditions. This system focuses on quartz dynamic recrystallization mechanisms and divides them in three sub-processes, namely bulging, subgrain rotation and grain boundary migration recrystallization. The authors defined quartz microstructures depending upon the quartz dynamic recrystallization mechanisms taken into consideration whereas the three regime of Hirth and Tullis groups specific dislocation creep structures with recrystallization processes in “regimes” according to their coexistence in specific experimental and geological settings. Both approaches are thus different but share noticeable similarities. The classification of Stipp et al. (2002) is now presented.

Bulging recrystallization (BLG) is a low temperature mechanism. Bulging is the formation of small recrystallized grains along the boundaries of original quartz grains during dynamic recrystallization (Fig. 19.A). It relates to low temperature conditions and the domain has been divided into two sub-domains based on observed structures and quartz behavior.

BLG 1 which occurs at the lowest temperatures is characterized by very small recrystallized grains. Fractures are still observable in the porphyroclasts and newly formed grains are found along segments of the grain boundaries.

BLG 2 occurs at higher temperature and is evidenced by an increase in the recrystallized grain proportion which no longer locates at a localized site along the grain boundary. Instead, the recrystallized grains are observed surrounding the entire porphyroclast leading to the onset of core and mantle structures in the upper level of this domain. Note that fracturing is absent in the porphyroclasts which are more elongated and commonly show deformation lamellae.

Subgrain rotation recrystallization (SGR) accounts for medium temperature conditions and is characterized by a re-orientation of the grain boundaries under a rotational component. The rotated recrystallized grains commonly show a strong CPO observable with the U-stage method. Core mantle structures may still be observed in the lower part of the SGR domain. Quartz ribbons are common (Fig. 3.19B) and tend to be completely consumed in the upper part of the SGR domain where the onset of grain boundary migration is suggested by the appearance of high amplitude lobate grain boundaries.

Grain boundary migration recrystallization (GBM) is observed within high temperature conditions. This domain is characterized by highly amoeboid grain shapes (Fig. 3.19C). Two subdomains are described, once again individualy characterized by specific features.

Within ***GBM 1*** sub-domain, grain sizes and shapes are variable but contour of individual grains are still observable and grain boundary pinning commonly occurs.

GBM 2 evidences for even higher temperature where quartz grains are larger displaying even more amoeboid shapes and grain boundaries which are not always detectable (Fig. 3.19D). Grain boundary pinning is weak and for the highest temperature conditions, chessboard patterns are observed. The transition from GBM 1 to GBM 2 is suggested to be related to the transition between quartz α / β.

Both *Hirth and Tullis* and *Stipp et al.* models can be correlated even though the first one only covers a small fraction of natural recrystallization microstructures (Stipp et al. 2010; 2001). The model of Stipp et al. (2002) is here preferred because it covers a higher temperature range and allows more accurate observations.

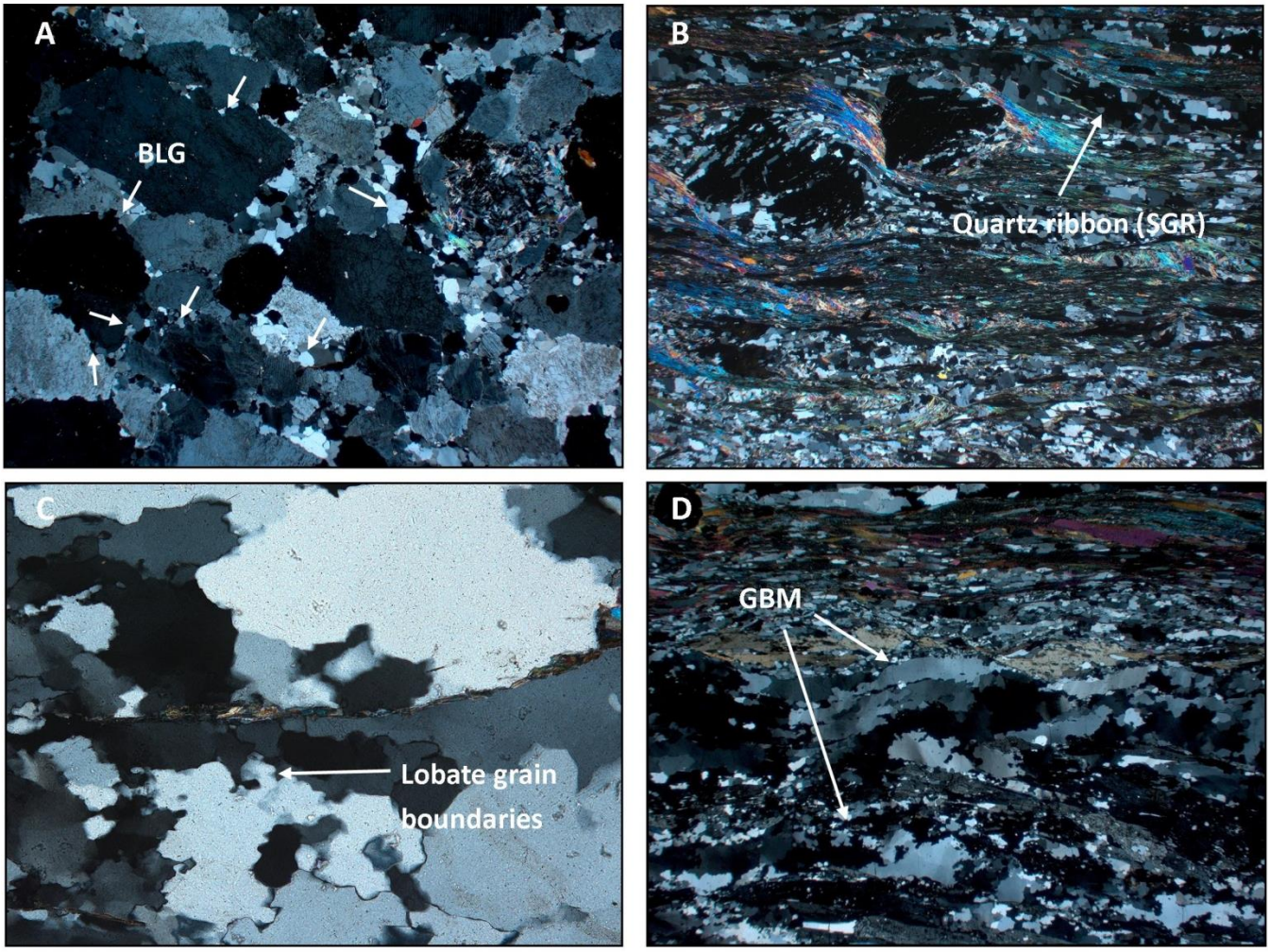

Figure 3.19 (A) Bulging in a quartz aggregate. Crossed polars, base of image 12 mm. (B) Subgrain rotation in a garnet-kyanite-mica gneiss. Note the quartz ribbons. Crossed polars, base of image 12 mm. (C) Close-up on lobate grain boundaries illustrating GBM mechanisms. Crossed polars, base of image 1.5 mm. (D) Grain boundary migration in a garnet-kyanite-mica gneiss. Crossed polars, base of image 12 mm.

3.5.2.3 EXPERIMENTAL RESULTS

Fifteen thin sections have been investigated and the results are reported in table 3.2.

Table 3.2 Deformation mechanisms reported in thin section from the Nordmannvik Nappe. (X): Some or no-recrystallizations. (XX): Important recrystallizations. (XXX): Dominant recrystallizations.

Thin section reference	BLG 1	BLG 2	SGR	GBM 1	GBM 2
RB 25	X	X	XXX	X	X
RB 26	X	XX	XXX	X	X
RB 27	X	XX	XXX	X	X
RB 28	X	X	XXX	XX	X
RB 16E	X	X	X	XXX	X
RB 16B	X	X	X	XXX	X
RB 33	X	X	X	X	XXX
RB 39B	X	X	XX	XXX	X
K1	X	X	XX	XXX	X
K2	X	X	XXX	XX	X
K4	X	X	XXX	X	X
K5	X	X	XX	XXX	X
K8	X	X	XX	XXX	X
RB 3	X	XXX	XX	X	X
K 9	X	X	XXX	XX	X
RB 38	X	X	XX	XXX	X
U 1	X	X	X	XXX	X
K 7	X	X	X	X	XXX

From table 3.2 three groups of sample are proposed based on the dominant quartz deformation mechanism which affected them.

The main group is characterized by a dominance of SGR and GBM domains and by the systematic coexistence of both mechanisms. Samples belonging to this group are mylonitic garnet-kyanite-mica gneisses and metamafics belonging to the middle amphibolite facies (or higher).

A second group gathers few samples characterized by the dominance of GBM 2. In such rocks, the large and very amoeboid quartz grains indicate a high to very high temperature deformation. Leucosome samples and granulite facies garnet-sillimanite gneisses have shown such quartz deformation mechanism.

The last group, defined by a dominance of bulging is only evidenced in RB 3, a metamafic wich reached the high pressure granulitic facies.

3.6 STRAIN PARTITIONING

Rocks in the Nordmannvik nappe are often mylonitic. However, mylonitisation intensity is variable and deformation gradients are observed at different scales. Outcrops often show strain partionning, well evidenced by small shear zones or chaotic deformed pods with a width of few centimeters. These small features occur rather randomly and no spatial pattern is observed for them.

In a larger view however, deformation intensity seems to increase toward the contact with the LNC. Few samples, taken on an E–W segment have shown an increase in mylonitisation rate to the W. These observations go along with an overall grain-coarsening to the E, illustrated notably by the occurrence of coarse grained granulitic rocks on the western part of the peninsula, whereas phyllites bordering the contact with the LNC show an intense grain size reduction.

4 DISCUSSION

4.1 OUTLINE

In the Nordmannvik nappe, the metamorphic evolution was investigated by optical microscopy. Thin section study allowed defining two distincts metamorphic events based on petrographical and microstructural evidences. The principal event is believed to be Scandian because the metamorphic peak assemblage $_{M1}$ showed the same characteristics and structures orientations as it has been described in the literature. In addition, an older event was identified, in some undeformed high grade relics. Due to the lack of datings, this event is simply referred as “pre-Scandian”. In the present chapter, experimental results are discussed and a tectono-metamorphic evolution of the area is proposed.

4.1 REACTION HISTORY

4.1.1 PRE-SCANDIAN ASSEMBLAGE (M_0)

4.1.1.1 PROGRADE PATH

IN METAPELITES

Evidences for a pre-Scandian metamorphic episode have been reported. Metapelitic rocks defined as garnet-sillimanite gneisses and characterized by the assemblage Qtz + Kfs + Grt + Sil ± Bt + melt were observed at high-temperature conditions as indicated by (1) myrmekite structures, (2) melt and (3) high temperature grain boundary migration affecting the quartz boundaries. Considering a lack of muscovite, rare biotites and the occurrence of melt it is very likely that mica breakdown reactions have been a major actor (if not the only ones) of the prograde metamorphic evolution in these rocks.

Sillimanite is important because its occurrence is considered as a characteristic feature of these pre-Scandian metapelites. The second distinctive element is the lack of mylonitic fabric even though a weak mineral foliation is observed.

4.1.1.1 RETROGRADE PATH

IN METAPELITES

High-grade metapelites from the Nordmannvik nappe evidenced a retrograde metamorphic episode. Two samples (RB 16B and RB 33) showed valuable informations but the entire metamorphic path is undetermined. Nevertheless, a cooling episode, supported by abundant perthite intergrowths, is evidenced. Perthite formed as the temperature decreases because a miscibility gap then, appeared between contrasting alkali feldspar compositions. Consequently, sodic elements segregated and formed albite lamellae cutting in the host orthoclase grain. This process started at high temperature which is supported by the several evidences of HT metamorphic conditions previously mentioned.

In addition, late metamorphic processes were reported and evidenced in post-M_0 assemblages by (1) late quartz recrystallizations, (2) quartz melt rims and (3) reaction rims and coronas composed of low grade minerals (chlorite and muscovite). These coronas are well-developed and compatible with a pressure / temperature drop, most likely driven by the exhumation of the high grade assemblages. Note that non-mylonitic *post-M_0* assemblages are most likely distinct from mylonitic *post-M1* assemblages based on the different textures observed in both of them. Nevertheless, there is a small probability that pre-Scandian assemblages could have been reworked during the Scandian episode. In such cases, the post-M_1 mylonitization would have not affected the pre-Scandian lenses (which preserved the pre-Scandian structures) when some mineralogical changes related to the Scandian path would be observed in these lenses.

IN METAMAFICS.

Mafic rocks in the Nordmannvik nappe have been locally sampled in lenses. Apart from RB 3 which displayed a Scandian fabric, metamafics have shown complex and unraveled mineral assemblages. Strong reaction textures affected the samples and retrograde processes are evidenced by mineral reactions and widespread symplectites, which also support exhumation processes. The presence of amphibole and widespread zoisite may suggest that ultimately, the samples reached an epidote-amphibolite facies. Deformation is locally outlined by shear indicators and a weak foliation. Orientation of this fabric is not precisely measured but it is definitely discordand as regard with the Scandian foliation.

Two thin sections (RB 38 and K9) have been described. If they shared similar aspect together, with notably the same reaction textures, it is uncertain if they originated from the same protolith as the

mineralogy was sensibly different. In the end, the metamorphic history is little documented in pre-Scandian mafics which are therefore inappropriate for determining any P/T path.

CONCLUSION

In conclusion, pre-Scandian rocks are identified in granulite facies lenses of pelitic rock and in a lesser extent, mafic material. These rocks characterized by the absence of a strong pervasive foliation, the lack of a mylonitic fabric and the occurence of HT metamorphism indicators in the sillimanite field are not well-constrained. Nevertheless, evidences for a P/T drop in these samples suggest that these rocks have undergone an early metamorphic cycle prior to the nappe stacking of the Scandian event. During this cycle, the prograde path may have been bounded to micas dehydratation reactions considering the importance of melt, garnet and K-feldspar as well as the absence of muscovite in the M_0 peak assemblages. A subsequent cooling episode may have started at high-temperature as indicated by the abundant perthite lamellae and an exhumation process may have taken place, supported by rim structures in the garnet-sillimanite gneisses. Pre-Scandian metamafics are poorly informative but they also support exumation processes due to the abundant symplectite observed in them.

4.1.2 SCANDIAN ASSEMBLAGE (M_1)

4.1.2.1 PROGRADE PATH

IN METAPELITES

Garnet-kyanite-mica gneisses account for the dominant rock type observed in the Nordmannvik nappe. These rocks were observed at upper amphibolite facies conditions (M_1) or in a retrograde and lower grade metamorphic stage. In our samples, the assemblage Grt + Kfs + Ky + melt defined the metamorphic peak and terminated the prograde path. Observations support that micas breakdown was the main prograde process. Melt is observed as well as alkali feldspars yet in low proportion. White micas are barely observed and strongly altered suggesting that muscovite breakdown reactions went to completion. Biotite which was later mylonitized did not show evidences for dehydratation reactions. Nevertheless and considering the system settings, it is very likely that these reaction proceeded and it is proposed that two generations of biotite occurred; the first one decomposed before the metamorphic peak M_1 whereas the second generation was formed coevally with the

emplacement of the retrograde mylonitic fabric D_2 after M_1 was reached. During this prograde path melt was probably partially removed from the system owing to the increasing confining pressure.

In the literature, an increase of the confining pressure due to the E-W continental collision and subsequent subduction of Baltica beneath Laurentia is suggested to be the leading process for the prograde Scandian path (see section 1.7). Evolution of the nappe followed a Ky-path (also referred as Barrovian or MP/MT) and geothermobarometric studies have given P/T estimate of 9.2 ± 1.0 Kbar and 715 ± 30 °C for the metamorphic peak (Elvevold, 1988; Lindstrøm et al., 1992).

In order to interpretate our experimental results, a reference paper is used from Gilotti and Elvevold (2002) who have been studying high grade metapelites in Payer Land (Greenland) where geological settings appear strikingly similar with those from the Nordmannvik Nappe. In both area, mylonitic pelitic and semi-pelitic high grade gneisses intruded by mafic and ultramafic lenses are observed and relate to the Caledonian continental collision. The authors described upper amphibolite facies rocks locally reaching a granulite facies in a kyanite field, which have been subsequently retrogressed during the exhumation of the subducted plate. In the same paper, three reactions are proposed to describe the metamorphic history of the pelitic gneisses in Payer Land. As it comes that these reactions accurately describe our observations, they are listed in table 4.1.

Table 4.1 Reaction history in metapelites of Payer Land (Greenland) from Gilotti and Elvevold (2002).

Reference	Reaction
R1	Mv + Qtz + Pl = Ky + Kfs + melt
R2	Bt + Ky + Pl +Qtz = Grt + Kfs + melt
R3	Grt + Kfs +H_2O = Bt + Sil + Pl

Reaction R1 is a fluid-absent melting reaction forming Kyanite and K-feldspar and reaction R2 comes as a second stage dehydratation melting reaction. The first reaction explains the disappearance of muscovite whereas the second one is proposed to explain the low proportion of non-sheared and altered biotite grains. The combination of both reactions forms K-feldspar, melt, kyanite and garnet which compose the peak assemblage M_1. R1 and R2 are believed to occur between the onset on the

metamorphism and the metamorphic peak assemblage M_1. These dehydratation reactions are similarly described by Le Breton and Thompson (1988), Spear et al. (1999) and Indares and Dunning, (2001).

Considering the paper from Gilotti and Elvevold (2002), the metamorphic peak M_1 can be estimated based on a synthetic P/T diagram proposed by the authors. This diagram partly relies on Le Breton and Thompson (1988) as well as Hodges and Crowley (1985) for barometry works.

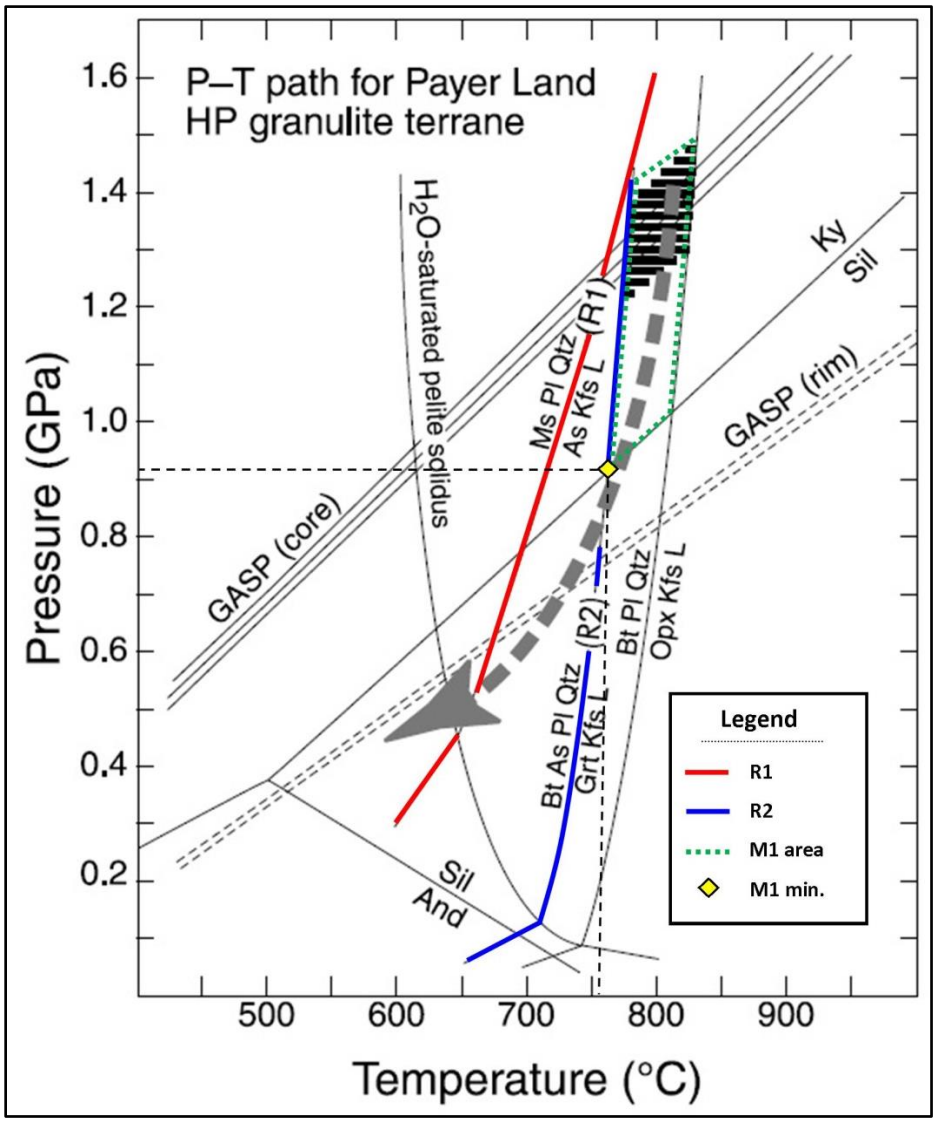

Figure 4.1 Melting reaction and estimated P/T path for the Payer Land metapelitic paragneisses. Dehydratation melting reactions and H_2O-saturated pelite solidus are from Le Breton and Thompson (1988). GASP (Garnet-Kyanite-Quartz-Feldspar) barometry on core and rim compositions are after Hodges and Crowley (1995). Dehydratation reaction R1 and R2 are highlighted. P/T area for M1 occurrence is delimited (green dotted area) and the minimum metamorphic peak possibly defined is indicated by a yellow losange. The grey arrow describes the retrograde path in Payer Land. The dark

shaded area indicates the metamorphic peak area for the rocks from Payer Land. Modified after Gilotti and Elvevold (2002).

Figure 4.1 aims to delimit the area where the metamorphic peak is expected to occur. This area, outlined by a green dotted line is constructed from the previously mentioned dehydratation reactions (R1 and R2). Considering that samples have shown the assemblage Grt + Kfs + Ky + Melt with low primary micas but no Opx, M_1 is inferred to range between 750-800 °C and 0.9-1.4 GPa. M_1 minimum is therefore plotted at about 750°C / 0.9 GPa.

In addition, and because thin sections have shown both kyanite and garnet, it is suggested that our samples have shown a metamorphic assemblage which "just passed" the R2 reaction. Consequently, M_1 is probably close to the R2 line in the P/T diagram.

IN METAMAFIC

In the Nordmannvik nappe, mylonitic metamafic gneisses were reported in RB 3 and are identified by the assemblage Grt + Cpx + Amp + Qtz + Pl + Ru. In that sample, garnets, clinopyroxenes and plagioclases are unaffected by the mylonic fabric. Therefore, the assemblage Grt + Cpx + Pl + Qtz is taken as the metamorphic peak assemblage and is typical of a high-pressure granulite facies (Elvevold and al. (2003). However, such an assemblage may occur in the amphibolite facies and is not necessarily diagnostic of granulite facies conditions (Bucher and Grapes, 2011). P/T conditions of the metamorphic peak M_1 are estimated in figure 4.2.

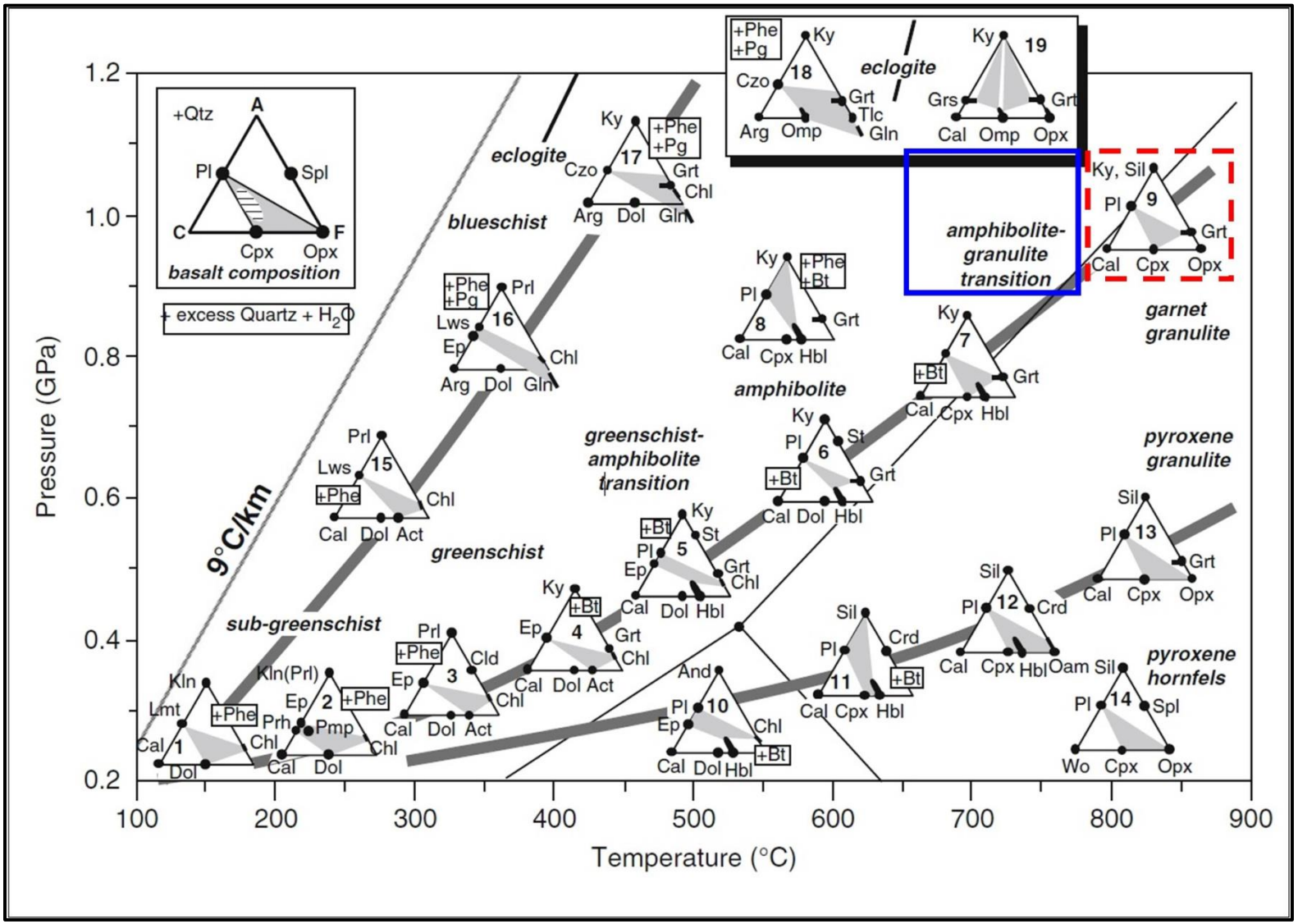

Figure 4.2 Metamorphism of mafic rocks (metabasalts) represented by ACF diagrams. The red dotted frame indicates the mineral AFM diagram which fit the mineral composition of RB 3 (Grt – Cpx – Pl). The blue frame indicates the probable area where M_1 should occur considering a similar mineralogy in the kyanite field. Modified after Bucher and Grapes (2011).

Figure 4.2 is constructed based on the fact that M_1 is characterized by the assemblage Grt + Cpx + Pl (+Qtz) in the high pressure granulite or upper amphibolite facies, and that M_1 occurs in the kyanite field in metapelites. Because it is unlikely that mafic rocks have undergone a different metamorphism than the dominant garnet-kyanite-mica gneisses, metamafics most likely occured in P/T conditions where kyanite is stable. As such, the red dotted frame in the sillimanite field, which indicates an AFM diagram matching M_1 composition, is not suitable. Instead a blue frame is drawn in order to estimate the P/T conditions of M_1 in the kyanite field. In my opinion, this assumption remains very approximative and should not be used to conclude. Nevertheless, this blue frame would indicates P/T conditions of 0.9-1 GPa and 725-750 °C which are consistent with the experimental results obtained in the garnet-kyanite-mica gneisses.

In these metamafics the metamorphic peak M_1 was reached before the mylonitization occurs, in the same way as in the garnet-kyanite-mica gneisses. This mylonitic fabric, which shows the same trend as in the metapelites is another argument supporting that these rocks have undergone the same Scandian event as the metapelites. Petrological observations clearly demonstrate that mylonitization occurred during a retrograde path like in the garnet-kyanite-mica gneisses.

4.2.2.2 Retrograde path

In metapelites

In the metapelites, the main argument for a retrograde path is given by a set of middle–low amphibolite facies samples and by some reaction textures affecting the peak assemblage in the upper amphibolite facies samples. This retrograde path is somehow related to the onset of a E-W mylonitic episode yet an absolut timing of its emplacement is not determined.

During the retrogression, Grt and Kfs proportions decrease while biotite (very abundant) is produced coevally with the strong mylonitic shearing. The result is a biotite fabric composed of highly stretched and lined biotite grains which locally show altered crystal from former breakdown processes. Sillimanite, which was not observed before the metamorphic peak, occurs as small needle aggregates crystallizing coevally with the biotite mylonitic fabric. Kyanite is still observed, but in lower proportion than in the early stages (Nardini, 2013). Consequently, kyanite is believed to have been replaced by sillimanite due to a pressure drop.

Because the mylonitization post-dates the metamorphic peak, the mylonitic middle-low amphibolite facies samples are retrograde and late. This assumption is furthermore supported by (1) the abundant mineral recrystallizations in biotite and hornblende (2) the static recrystallization in quartz and (3) the late growth of low-grade minerals (muscovite and chlorite) across the mylonitic fabric.

In the Nordmannvik nappe, an exhumation process is inferred from the literature (Bergh and al., 1985; Elvevold, 1988) and it has been generally accepted that this retrogression is characterized by crystallization of sillimanite along garnet rims associated with breakdown reactions.

In Payer Land (Greenland), Gilotti and Elvevold (2002) stated that retrogression of the high grade assemblages was accompanied by crystallization of sillimanite and biotite with foliation which anastomosed between lenses of leucocratic material and wraps around garnet porphyroblasts. The authors proposed a reaction (R3 in Table 4.1) which accurately describes our observation in the Nordmannvik nappe and is chosen as valid for this work. Thus, garnet-kyanite-mica gneisses of the Nordmannvik nappe are likely to have evolved in a similar way as the metapelites from Payer land in Greenland (see figure 4.1).

IN METAMAFICS

In metamafics, retrogression is also reported, but only one thin section (RB 3) is considered. However, a strong mineral reaction is observed in there where early deformed clinopyroxenes are progressively replaced by hornblende. As the reaction proceeded, the neo-formed hornblende infilled the clinopyroxene grains but it also formed new single grains. Barink (1984) published a paper in which he investigated pyroxene replacement in a metagabbro. The author described the replacement of pyroxene by hornblende, assumed to be isochemically balanced with replacement of plagioclase by garnet. As a conclusive metamorphic reaction he obtained the following equation:

R4 H_2O + Pl + Cpx ± Fe-Ti oxides → Grt + Hbl + Qtz

The authors also noticed that this reaction is actually the reverse of one of the De Waard reactions (De Waard, 1965; Jen and Kretz, 1981) which are thought characteristic for the progressive amphibolite-granulite facies transition. Unfortunatly around 30 % of quartz is observed in RB 3 prohibiting the use of the term metagabbro. The abundance of quartz however does not necessarily have an impact of the

proposed reaction, and the other settings of this equation remain relevant with our observations. Fe-Ti oxydes can be evidenced by rutile, well-observed in RB 3.

In the end, RB 3 is suggested to have reached a high pressure granulite facies before a subsequent retrogression of the peak assemblage, probably due to the same exhumation mechanism which affected the garnet-kyanite-mica gneisses.

CONCLUSION

In short, observation related to the Scandian evolution of the Nordmannvik leads to similar conclusions than those from previous works. These observations, also ressemble those made by Gilotti and Elvevold (2002) for rocks from Payer Land in Greenland. From our experiments, Scandian metamorphism is believed to describe an orogenic P/T loop with a prograde loading followed by a decompression episode. The prograde segment following a Ky-path was dominated by the dehydratation of micas with production of melt, and it reached a peak assemblage, estimated at a minimum of 750°C / 0.9 Gpa in garnet-kyanite-mica gneisses belonging to an upper amphibolite facies. During the retrogression, a strong mylonitic shearing occurred, notably characterized by the syn-kynematic crystallization of sillimanite at the expense of kyanite. Bergh and Andresen (1985) suggested that sillimanite crystallized after the mylonitic episode but our experimental results do not support this assumption. In figure 4.1 the replacement of kyanite by sillimanite is illustrated by the grey arrow, proposed as a approximate retrograde path for the Scandian event.

In mafic rocks, the metamorphic peak is most likely identified in the high pressure granulite facies and the P/T path followed by the samples is supposed similar to the described by the metapelites. Because metapelites and metamafics occurred in a restricted area, it is likely that both rock types evolved simultaneously. Estimation of the metamorphic peak conditions in the metamafics are consistant with those determined in the metapelites.

4.2 PARTIAL MELTING

In the Nordmannvik nappe, partial melting relates to the dehydratation of the metapelites and has been recorded in M_1 and M_0 assemblages. In both cases, the water initially bounded to the mica molecular structure is released as free water when P/T conditions increase during the prograde path. The subsequent hydratation of the system tends to lower the minimum temperature at which pelites start to melt. The fate of this melt varies as it may either stay in situ and forms magmatic rocks or be removed from the host rock and crystallizes as individual leucosome pods or layers. Two thin sections (U1 and K7) have shown a quartzo-feldspatic composition with local remnant of some dark minerals and garnets.

4.3 ROLE OF ACCESORIES

Samples from the Nordmannvik nappe have commonly shown high proportion of zoisite, epidote mineral, titanite, rutile and tourmaline.

4.3.1 ZOISITE AND EPIDOTE MINERALS

Zoisite and epidote minerals were extensively found in the low-middle grade and retrograde metapelites. Often associated with calcic minerals they were observed in plagioclase and amphibole-rich samples. According to Enami (2004), epidote minerals and zoisite can occur as an epidote-amphibolite or amphibolite facies overprint during exhumation processes to crustal depth < 35 km. During this stage titanite (± ilmenite) replaces rutile and epidote + amphibole replaces garnets. In general, our experimental results fit Enami's descriptions and support the exhumation of the high grade assemblage during the Scandian event.

4.3.2 RUTILE, TITANITE AND TOURMALINE

Rutile and tourmaline formed an interesting association as they were reported in all rock types, including the pre-Scandian lenses. The origin of these accessory minerals is discussed.

Rutile, according to Meinhold (2010) can be observed in high grade and ultrahigh-grade metamorphic rocks (granulite or eclogites) where it forms mainly single crystals in the matrix. Figure 4.3A, presents a P/T phase diagram showing experimentally determined formation of rutile, titanite and ilmenite for a

mid-ocean ridge basalt-H_2O system (after Liou et al., 1998). From figure 4.2A and Meinhold (2010) two conclusions are proposed for our samples:

1 Rutile is most likely not of a metamorphic origin because its stability field as a metamorphic mineral starts in the granulite facies, for pressures exceeding 12 Kbar. Such high pressures have not been reported in our samples (unless maybe in the high pressure metamafics). In addition, rutile was reported in epidote-amphibolite facies metapelites, phyllites low-middle grade marbles, as well as in the pre-Scandian lenses suggesting that rutile may simply have been a component of the sedimentary cover of the Nordmannvik nappe.

2 Titanite, which is observed along the retrograde Scandian path in middle-low grade samples, is potentially metamorphic because this path has crossed the stability field of titanite described in figure 4.3A.

Tourmaline has a wide stability field (Brunnsmann and al., 2000 and figure 4.2B) so determining if the mineral is metamorphic or not would require composition analyses. Nevertheless and considering that tourmaline was always observed associated with rutile in all rock types, it is suggested that both mineral originate from the same rocks. Because both of these minerals where observed in higher proportion within sedimentary derived rocks (metapelites and calc-sillicates) than in the mafic rocks, rutile and tourmaline probably share a same sedimentary origin.

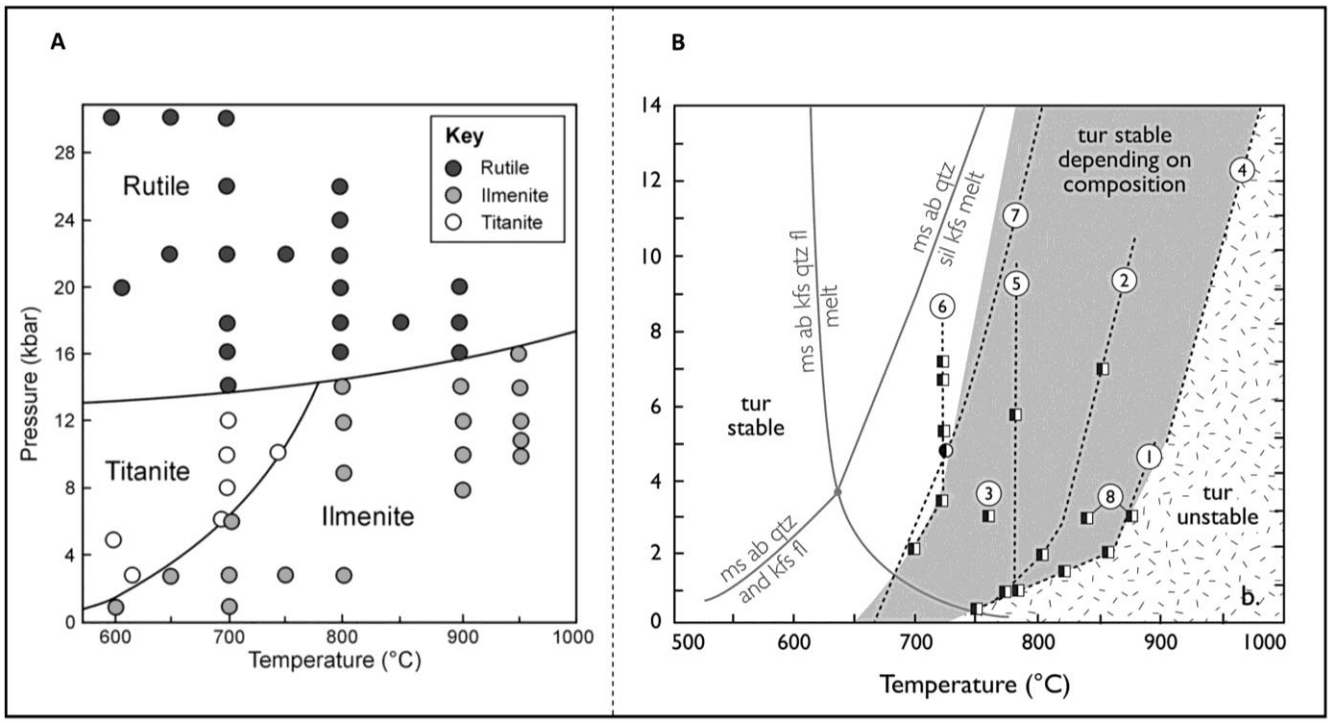

Figure 4.3 (A) Experimentally determined formation of rutile, titanite and ilmenite for a mid-ocean ridge basalt-H_2O system (after Liou et al., 1998). The *P-T* field phase boundaries were not reversed and hence should be considered as synthesis boundaries, although they are topologically consistent with natural occurences of Ti-phases. Liou et al. (1998) furthermore pointed out that these Ti-rich phases are not related to one another by simple polymorphic transitions, and thus two or even three of them may coexist under certain physicochemical conditions, but this was not investigated experimentally. From Meinhold (2010). (B) Compilation of P–T stability estimates for tourmaline of varying compositions, with high-P stability. Circles represent constraints from natural samples, squares are experimental data, and dashed lines, the extrapolations presented by the original authors. The curves for H2O-saturated melting reactions, and the quartz–coesite and graphite–diamond phase transitions are shown for reference. Data are for: 1) dravite: Robbins & Yoder (1962), 2) magnesio-foitite: Werding & Schreyer (1984), 3) schorl: Holtz & Johannes (1991), 4) dravite: Krosse (1995), 5) Na-free Mg system: von Goerne et al. (1999), 6) Na-bearing Mg system: von Goerne et al. (1999), 7) natural tourmalines: Kawakami (2004), 8) natural tourmaline: Spicer et al. (2004), 9) dravite: Ota et al. (2008). Modified after Van Hinsberg et al. (2001).

4.4 Deformation in the Nordmannvik Nappe.

4.4.1 Deformation at the large scale

Deformation in the Nordmannvik Nappe is outlined by the mineral foliation (S_1), the lineations (L_1) and a late mylonitic fabric. Stereoplots in Fig. 3.3 illustrate the orientation of S_1 and L_1.

Foliation planes are all showing a similar trend whatever the rock type considered. They are dipping to the W with a dip angle between 10 and 50°. Migmatite and granulite rocks present a low angle foliation plane when metapelites and carbonates may vary. Pole to lineations, are observed in a cluster which appears similar regardless to the rock type they are found in. These lineations indicate a NW-SE motion which matches the orientation of continental collision involved in the Scandian event of the Caledonian orogeny. Shear sense indicators support a SE directed transport of the nappe.

4.4.2 Deformation microstructures

At the microscale, deformation has shown to be strongly dependant of the mylonitic fabric. S_1 was always reported in association with the mylonitic fabric. Based on the results presented in section 3.5.2, it is suggested that:

1 Ultramylonitc samples and phyllites which are found close to the upper contact of the Nordannnvik nappe are the most sheared and recrystallized samples. These rocks recrystallized during the retrograde mylonitization D_2.
2 Strongly to moderately mylonitic rocks are believed to have formed late in the Scandian history and it is suggested that these rocks are formed during various stages of the retrograde path. Because some moderately mylonitic rocks may show a similar metamorphic grade as the ultramylonitic samples, strain partitioning is inferred in the Nordmannvik nappe.
3 Moderatly to weakly mylonitic rocks are represented by samples in which the metamorphic peak assemblage is still observed. Grain size is small though deformed clasts and mica fishs are still observed. These samples which belong to the upper amphibolite facies or higher probably crystallized when the mylonitization started during the retrograde path.

Moreover, and based on figure 4.4, the development of crenulation cleavage in phyllites and ultramylonitic gneisses suggests that deformation was high at rather low temperature. Yet the figure is very schematic, it supports the idea that phyllites are highly strained rocks which crystallized at rather low temperature.

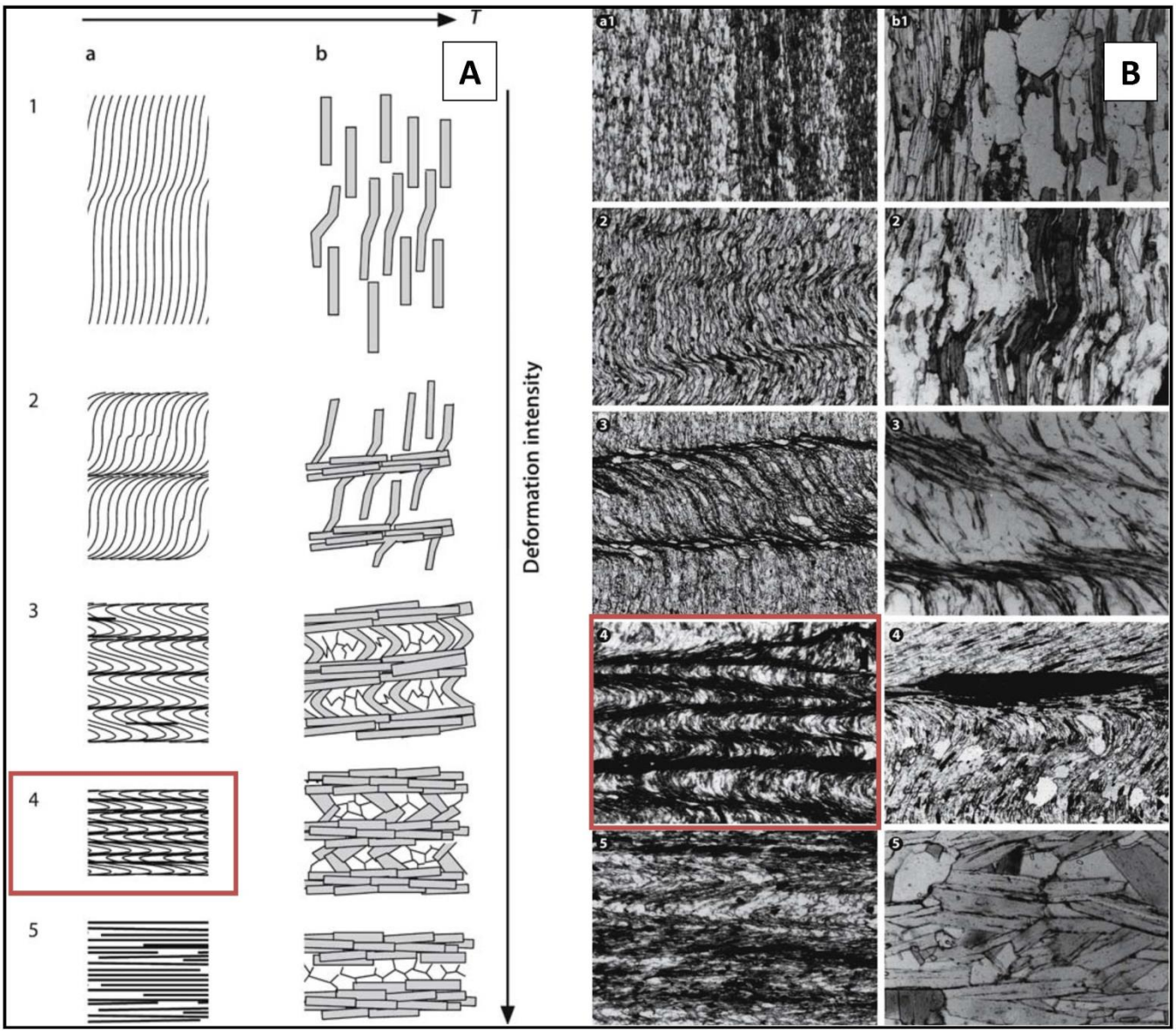

Figure 4.4 (A) Illustration of the inferred range of stages in crenulation cleavage development with increasing deformation (vertical axis) and temperature (Horizontal axis). The (a)-marked column describes the evolution of crenulation cleavages deformed by solution transfer and rotation and low-medium temperatures. The (b)-marked column describes the evolution of crenulation cleavages deformed by grain growth and recrystallization at higher temperatures. The red frame illustrates the development stage reached in our samples. (B) Microphotographs of

crenulation cleavages taken at different stages which match the illustrations in Fig. 4.4 (A). The red frame illustrates the development stage reached in our samples. Crossed polars, width of view a1 2 mm ; a2 2 mm ; a3 2.5 mm ; a4 2 mm ; a5 2 mm ; b1 1 mm ; b2 2 mm ; b3 2 mm ; b4 1 mm ; b5 1 mm. Modified after Passchier and Trouw (2005).

4.4.3 QUARTZ DEFORMATION

In the investigated area, quartz deformation has been identified in nearly all the samples. Quartz recrystallizations affected Scandian and pre-Scandian rocks and correlation between quartz deformation mechanisms and the mineral paragenesis give consistent results summarized by the following remarks:

1. Upper amphibolite facies rocks, observed close to the metamorphic peak of the Scandian event, are dominated by subgrain rotation and grain boundary migration processes (GBM 1).
2. High temperature metapelites from the pre-Scandian path as well as melt samples resulting from the Scandian path were characterized by a dominant GBM mechanism sometimes reaching a GBM 2 domain with highly sutured grain boundaries and local chessboard patterns.
3. A deformed metamafic sample belonging to the high pressure granulite facies has shown abundant bulging (sample RB 3). Bulging is characteristic of high strain rate (Fig. 4.4B).

Based on Figure 4.5A, samples dominated by SGR or GBM 1 may have recorded a temperature of about 500-550 °C. Those dominated by BLG recrystallized between 300 and 400 °C and the samples evidencing GBM 1 or GBM 2 above 530 °C. These estimations are large but the lack of data concerning an average recrystallized grain size does not allow an optimal use of Fig. 4.5A.

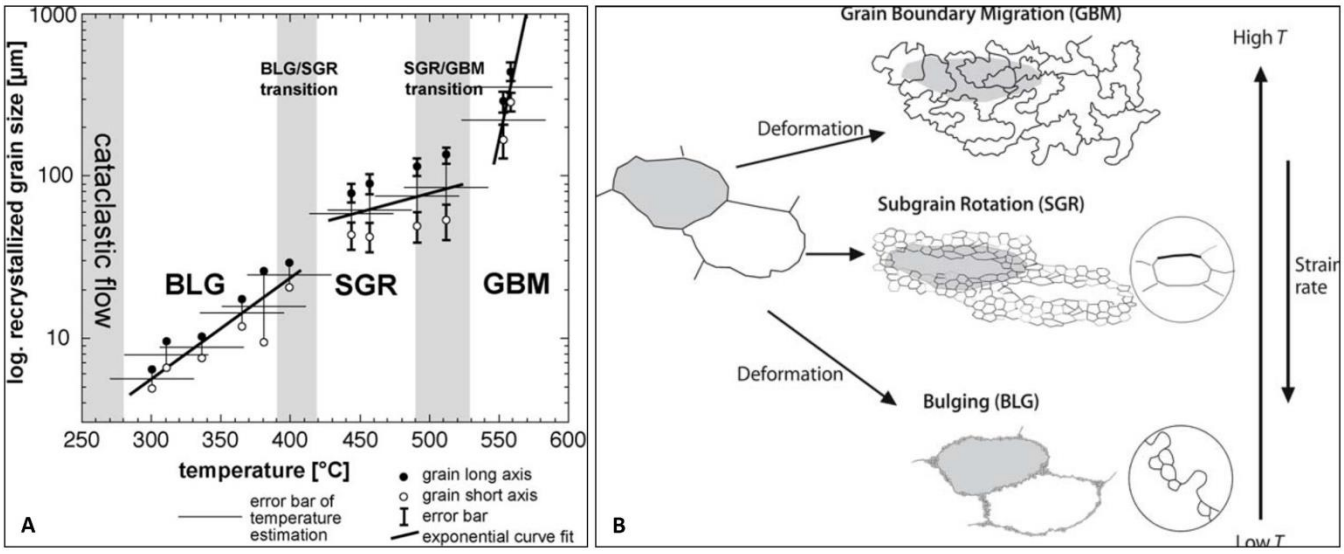

Figure 4.5 (A) Diagram of recrystallized grain size versus temperature: curve fit is based on the geometric mean of long and short axis. From Stipp et al. (2002). (B) The three main types of dynamic recrystallization in a polycrystal. The substance of one of two large grains that recrystallize is indicated by shading, before and during recrystallization. From Passchier and Trouw (2005).

4.5 About phyllites

Phyllites, according to the geological map are comprised between the Nordmannvik nappe and the overlying Lyngen Nappe Complex. In fact, it is not clearly determined whether these phyllites derived from the high grade metapelites of the Nordmannvik nappe of whether they are metasediments from the LNC. Litterature is not extensive on the topic and assumption only can be made from petrographic evidences reported in our thin sections.

At first, petrography of the phyllites is similar to that of metapelitic gneiss with abundant quartz and micas, some garnets and secondary minerals such as calcite, chlorite, tourmaline and rutile. The distinction between phyllites and metapelites from the Nordmannvik nappe is not always obvious notably when the association rutile + tourmaline occur in the same settings in both rock types. The strong mineralogical similarities between these rocks suggest a common protolith.

Structural features also argue for a “Nordmannvik nappe origin” of the phyllites. Indicators of strong shearing were massively reported, these structures being similar to those observed in the adjacent metapelites from the Nordmannvik nappe.

Nevertheless and despite these similarities, sulphides were observed in the phyllites only. A lack of data is also to be mentioned and it is possible that phyllites derived from sedimentary rocks of the LNC. In the end, a Nordmannvik nappe origin is suggested with caution as a lack of relevant data prevent from concluding. In the present state, further investigations appear necessary.

4.6 Garnet-sillimanite gneisses and their implication in the current tectonostratigraphy in Troms

The discovery of pre-Scandian assemblages (M_0) in high grade lenses within the Nordmannvik nappe has several implications on the stratigraphy in Troms. In the current view, many authors agree on the fact that the Nordmannvik nappe belongs to the Upper allochton (Corfu et al., 2007; Janak et al., 2012), which is basically composed of rocks derived from the ancient Iapetus Ocean (see section 1.4.2). In such case then, the occurrence of the garnet-sillimanite gneisses as pre-Scandian rocks (which therefore precede the nappe stacking episode of the Caledonian orogeny) is not compatible with the inferred oceanic composition of the rocks from the Upper allochton.

In this section, an alternative stratigraphy is proposed (Fig. 4.6). Because the high grade relics from the Nordmannvik have a similar composition to that of rocks from the lower units (namely the Kåfjord and the Vaddas nappe as well as the Kalak Nappe Complex), the Nordmannvik nappe is believed to be part of the same allochton as these lower units (the detailed petrographic description of each units is to be found in section 1.4.2). Consequently, the Nordmannvik nappe with the Kålfjord, the Vaddas nappe and the KNC are proposed to be part of the Middle Allochton, believed to represent the pre-collisional continental margin of Baltica (Gee et al. 2008).

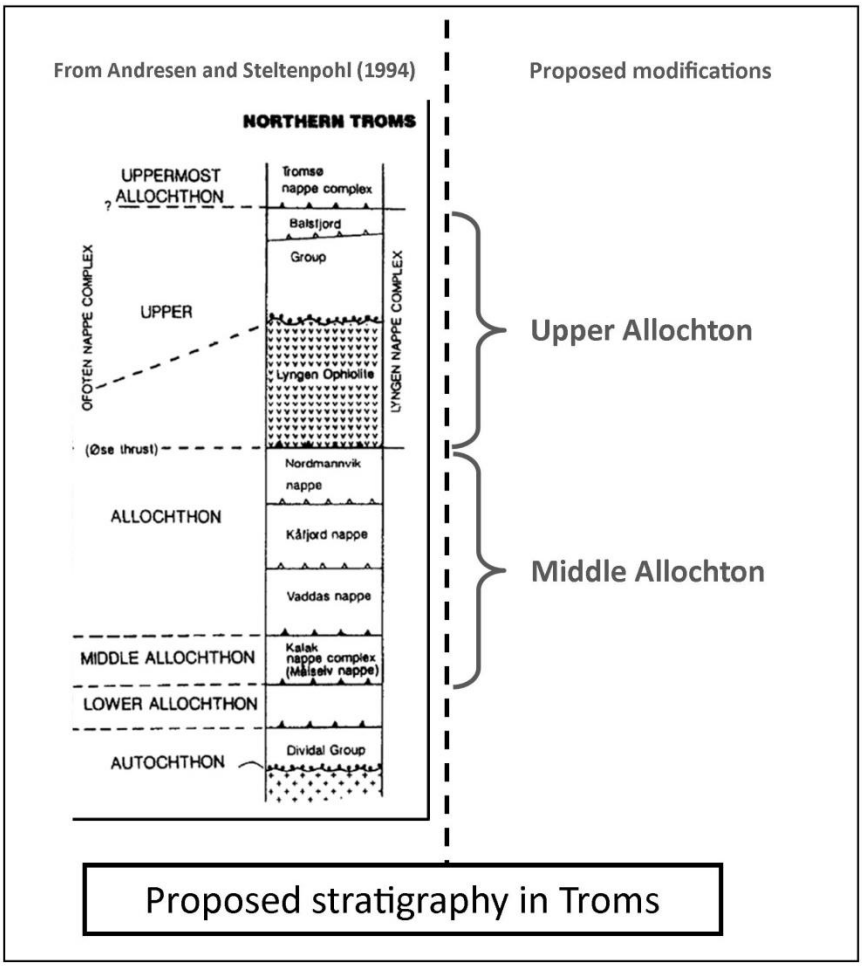

Figure 4.6 Proposed stratigraphy in Troms. Comparison between the model from Andresen and Steltenpohl (1994) and the one presented in this thesis. Modified after Andresen and Steltenpohl (1994).

4.7 TECTONOMETAMORPHIC EVOLUTION

The present contribution relies on our experimental results, combined with data from the literature. Two metamorphic events are identified, both of them composed of a prograde and a retrograde evolution. A major difference with data from the literature concerns the identification of a pre-Scandian metamorphic event, recorded in high grade lenses from the nappe. If such event has already been suggested in the literature (see section 1.6), a pre-Scandian event affecting the Nordmannvik nappe is here documented in pelitic and mafic rocks. A Taconian related origin of this pre-Scandian event seems to be a logical option but this remains purely speculative. A tectono-metamorphic evolution is proposed:

- **Pre-Scandian event:** A metamorphic event reaching a granulite facies in the sillimanite field notably characterized by a lack of mylonitic deformation and the occurrence of sillimanite as the only aluminosilicate is identified. A metamorphic peak assemblage (M_0) is reported, characterized by the assemblage Qtz + Kfs + Grt + Sil ± Bt + Melt. Prograde path was likely driven by mica breakdown reactions as partial melting and K-feldspars were reported at the expense of muscovite. In a second stage, a retrograde episode related to a decompression of the high grade assemblage probably affected the pre-Scandian rocks. Abundant perthite and rim structures in metapelites as well as widespread symplectite overprinting some clinopyroxenes in metamafics argue for a post-M1 P/T drop. In the literature, this event was not mentioned but Lindstrøm and al. (1992) proposed an age of 492 ± 5 Ma for a metadiorite lens, supporting at least, a pre-Scandian metamorphic history for the mafic lenses.
- **Scandian event:** A Scandian event has taken place in the Nordmannvik nappe. Dated around 425-426 Ma by Dallmeyer and Andresen (1992), this collisional episode associated to subduction of Baltica beneath Laurentia is characterized by a Ky-type prograde path followed by a decompression of the high grade assemblage. The prograde segment is built on two consecutive dehydratation reactions (R1 and R2 from table 4.1) which progressively removed micas to form the inferred granulitic peak assemblage Grt + Kfs + Ky + melt. M_1, which was reported with a low Kfs content is estimated at a minimum of about 0.9 GPa / 750°C in the

upper amphibolite facies, which appears marginally different than the 0.92 ± 0.1 GPa / 715 ± 30°C given by geothermobarometric studies from Elvevold (1988). In metamafics, the metamorphic peak was locally identified in the high pressure granulite facies at P/T conditions estimated similar to those determined in the garnet-kyanite-mica gneisses.

Subsequently to the metamorphic peak, a pressure drop is recorded acting coevally with the emplacement of a strong mylonitic fabric. This retrogression, likely bounded to the exhumation of the subducted slab is evidenced by the recrystallization of middle-low grade minerals such as epidote/zoisite, muscovite and chlorite (in metapelites) and by the extensive replacement of clinopyroxenes by amphiboles according to the reaction R4 (table 4.1) in metamafics. The mylonitic fabric is composed of recrystallized biotite and additional sillimanite formed by reaction R3 from table 4.1. An exhumation path has been estimated by Gilotti and Elvevold (2002) in Payer Land (Greenland) and it is proposed that metapelites from the Nordmannvik nappe followed a similar one. In our samples, petrographic observations showed that some samples have been retrogressed down to the epidote-amphibolite facies.

5 CONCLUSION

Based on the different observations performed in the Nordmannvik nappe, the following conclusions are made.

- In the Nordmannvik nappe, evidences of a pre-Scandian metamorphic event are reported in high grade lenses of mafic and pelitic rocks.
- Two different types of pelitic gneisses are identified; Scandian and mylonitic garnet-kyanite-mica gneisses dominate whereas garnet-sillimanite gneisses are observed in the pre-Scandian lenses.
- Due to the pelitic composition of the pre-Scandian garnet-sillimanite gneiss, the Nordmannvik nappe cannot belong to the Upper Allocton which is composed of rocks from the oceanic floor. Based on petrographic similarities, the Nordmannvik nappe as well as the Kålfjord nappe, the Vaddas nappe and the Kalak Nappe Complex are most likely part of the upper Middle Allochton.
- In garnet-kyanite-mica gneisses, Scandian prograde metamorphism followed a kyanite-path wich reached a metamorphic peak M_1 set at a minimum of 750°C / 0.9 GPa in the upper amphibolite facies. These results are consistent with geothermobarometric studies from Elvevold (1988).
- During the Scandian path, petrographic evidences for a retrograde episode are reported, witnessing exhumation processes. This retrogression occured in conjonction with a strong retrograde mylonitization and recrystallization of sillimanite (at the expense of kyanite) within the mylonitic fabric of the garnet-kyanite-mica gneisses.
- In the lenses of garnet-sillimanite gneisses, a granulite facies was reached. The metamorphic peak assemblage M_0 was most likely retrogressed during exhumation processes, as abundant low grade rim structures are reported around minerals composing this metamorphic peak assemblage M_0.
- Mafic rocks are mostly found in pre-Scandian lenses which showed a complex and unraveled history, yet exhumation processes are suggested by abundant symplectite structures. In addition, Scandian and mylonitic metamafics are locally encountered, probably reaching M_1 in

the high pressure granulite facies and following a similar metamorphic path that in the garnet-kyanite-mica gneisses.

- In the Nordmannvik nappe, dehydratation of micas was most likely the dominant prograde metamorphic process. Importance of partial melting is outlined by the importance of migmatites as well as leucosome lenses and layers scattered in the nappe.
- The association rutile + tourmaline was found in all pre-Scandian and Scandian rock types which might suggest a common protolith for the different lithologies composing the Nordmannvik nappe.
- Phyllites are suggested (yet with caution) to have derived from the Nordmannvik nappe, based on the similar mineralogy (notably the association tourmaline + rutile) and the identical deformation structures that they share with the garnet-kyanite-mica gneisses.
- Structural features (Foliation planes, lineations and shear sense indicators) are compatible with a SE directed transport of the Nordannvik nappe, relating to the subduction of Baltica underneath Laurentia.
- In the nappe, temperature ranges of quartz dynamic recrystallizations are not accurately constrained but the given approximations do not conflict with P/T conditions inferred from petrographic studies.
- The occurrence of similar microtextures and mineral reactions between rocks from the Nordmannvik nappe and those from Payer Land in Greenland might suggest a shared tectonometamorphic evolution for both areas.

6 REFERENCES

1. **Andersen, T. B. (1998).** "Extensional tectonics in the Caledonides of southern Norway, an overview." Tectonophysics 285(3): 333-351.

2. **Andréasson, P.-G., et al. (1998).** "Dawn of Phanerozoic orogeny in the North Atlantic tract; evidence from the Seve-Kalak Superterrane, Scandinavian Caledonides." GFF 120(2): 159-172.

3. **Andréasson, P. (1994).** "The Baltoscandian margin in Neoproterozoic-early Palaeozoic times. Some constraints on terrane derivation and accretion in the Arctic Scandinavian Caledonides." Tectonophysics 231(1): 1-32.

4. **Andresen, A. (1988).** "Caledonian terranes of northern Norway and their characteristics." Trabajos de geología 17(17): 103-119.

5. **Andresen, A. and M. G. Steltenpohl (1994).** "Evidence for ophiolite obduction, terrane accretion and polyorogenic evolution of the north Scandinavian Caledonides." Tectonophysics 231(1): 59-70.

6. **Andresen, L. a. (1992).** "Evidence of Early Caledonian high-grade metamorphism within exotic terranes of the Troms Caledonides?" Nor. Geol. Tidsskr 72: pp. 375–379.

7. **Austrheim, H. and W. L. Griffin (1985).** "Shear deformation and eclogite formation within granulite-facies anorthosites of the Bergen Arcs, western Norway." Chemical Geology 50(1): 267-281.

8. **Barink, H. (1984).** "Replacement of pyroxene by hornblende, isochemically balanced with replacement of plagioclase by garnet, in a metagabbro of upper-amphibolite grade." Lithos 17: 247-258.

9. **Bergh, S. G., et al. (1985).** "Tectonometamorphic evolution of the allochthonous Caledonian rocks between Malangen and Balsfjord, Troms, North Norway." Norges Geologiske Undersøkelse.

10. **Berman, R. G. (1988).** "Internally-consistent thermodynamic data for minerals in the system Na2O-K2O-CaO-MgO-FeO-Fe2O3-Al2O3-SiO2-TiO2-H2O-CO2." Journal of Petrology 29(2): 445-522.

11. **Berthé, D., et al. (1979).** "Orthogneiss, mylonite and non coaxial deformation of granites: the example of the South Armorican Shear Zone." Journal of structural geology 1(1): 31-42.

12. **Binns, R. E. (1989).** "Regional correlations in NE Troms-W Finnmark: the demise of the "Finnmarkian" orogeny." The Caledonide Geology of Scandinavia: London, Graham and Trotman: 27-45.

13. **Bjørlykke, A. and S. Olaussen (1981).** "Sibirian Sediments, Volcanics and Mineral Deposits in the Sagelvvatn Area, Troms, North Norway." Universitetsforlaget.

14. **Bose, S. and F. O. Marques (2004).** "Controls on the geometry of tails around rigid circular inclusions: insights from analogue modelling in simple shear." Journal of structural geology 26(12): 2145-2156.

15. **Boullier, A.-M. and J.-M. Quenardel (1981).** "The Caledonides of northern Norway: relation between preferred orientation of quartz lattice, strain and translation of the nappes." Geological Society, London, Special Publications 9(1): 185-195.

16. **Brunsmann, A., et al. (2000).** "Zoisite-and clinozoisite-segregations in metabasites (Tauern Window, Austria) as evidence for high-pressure fluid-rock interaction." Journal of Metamorphic Geology 18(1): 1-22.

17. **Bucher, K. and R. H. Grapes (2011).** "Petrogenesis of metamorphic rocks." Springerverlag Berlin Heidelberg.

18. **Clark, A., et al. (1985).** "Basement/cover relations along the eastern margin of the Western Gneiss Terrane, Senja, Troms, Norway". Geological Society of America, Abstracts with Programs.

19. **Corfu, F., et al. (2007).** "Peri-Gondwanan elements in the Caledonian nappes of Finnmark, northern Norway: implications for the paleogeographic framework of the Scandinavian Caledonides." American Journal of Science 307(2): 434-458.

20. **Cumbest, R.J., Dallmeyer, R.D., Solomon, C., and Andresen, A. (1983).** "Age and origin of ductile fabrics in the western gneiss terrane of the Norwegian Caledonides (Troms)." Geol. Soc. Am., Abstr. Programs, 15 (6): 552.

21. **Cumbest, R. and R. Dallmeyer (1985).** "Polyphase Caledonian tectonothermal evolution of the Western Gneiss Terrane, Senja, Troms, Norway." Geol Soc Am Abs Prog 17: 14.

22. **Dallmeyer, R.D., (1991).** "$^{40}Ar/^{39}Ar$ mineral ages from the Western Gneiss Terrane, Troms, Norway: evidence of a variable Caledonian record: Terranes in The Arctic Caledonides." Terra Nova Abstr., 3 (4): 12.

23. **Dallmeyer, R. and A. Andresen (1992).** "Polyphase tectonothermal evolution of exotic caledonian nappes in Troms, Norway: Evidence from $^{40}Ar^{39}Ar$ mineral ages." Lithos 29(1): 19-42.

24. **De Waard, D. (1965).** "The occurrence of garnet in the granulite-facies terrane of the Adirondack Highlands." Journal of Petrology 6(1): 165-191.

25. **Eide, E. and J.-M. Lardeaux (2002).** "A relict blueschist in meta-ophiolite from the central Norwegian Caledonides—discovery and consequences." Lithos 60(1): 1-19.

26. **Elvevold, S. (1988).** "Petrologiske undersøkelser av kaledonske bergarter i takvatnområdet, Troms." MsC Thesis. Institutt for Biologi or Geologi. University of Tromsø.

27. **Elvevold, S. and J. A. Gilotti (2000).** "Pressure–temperature evolution of retrogressed kyanite eclogites, Weinschenk Island, North–East Greenland Caledonides." Lithos 53(2): 127-147.

28. **Elvevold, S., et al. (2003).** "Metamorphic history of high-pressure granulites in Payer Land, Greenland Caledonides." Journal of Metamorphic Geology 21(1): 49-63.

29. **Enami, M., et al. (2004).** "Epidote minerals in high P/T metamorphic terranes: subduction zone and high-to ultrahigh-pressure metamorphism." Reviews in Mineralogy and Geochemistry 56(1): 347-398.

30. **Fossen, H. (1992).** "The role of extensional tectonics in the Caledonides of south Norway." Journal of structural geology 14(8): 1033-1046.

31. **Gee, D. (1975).** "A tectonic model for the central part of the Scandinavian Caledonides." American Journal of Science 275: 468-515.

32. **Gee, D. G. (1978).** "Nappe displacement in the Scandinavian Caledonides." Tectonophysics 47(3): 393-419.

33. **Gee, D. G., et al. (2008).** "From the early Paleozoic platforms of Baltica and Laurentia to the Caledonide orogen of Scandinavia and Greenland." Episodes 31(1): 44.

34. **Gilotti, J. A. and S. Elvevold (2002).** "Extensional exhumation of a high-pressure granulite terrane in Payer Land, Greenland Caledonides: structural, petrologic, and geochronologic evidence from metapelites." Canadian Journal of Earth Sciences 39(8): 1169-1187.

35. **Gilotti, J. A. and W. C. McClelland (2007).** "Characteristics of, and a tectonic model for, ultrahigh-pressure metamorphism in the overriding plate of the Caledonian orogen." International Geology Review 49(9): 777-797.

36. **Gilotti, J. A., et al. (2004).** "Devonian to Carboniferous collision in the Greenland Caledonides: U-Pb zircon and Sm-Nd ages of high-pressure and ultrahigh-pressure metamorphism." Contributions to Mineralogy and Petrology 148(2): 216-235.

37. **Gilotti, J. A. and E. J. K. Ravna (2002).** "First evidence for ultrahigh-pressure metamorphism in the North-East Greenland Caledonides." Geology 30(6): 551-554.

38. **Griffin, W. L. and H. K. Brueckner (1985).** "REE, Rb Sr and Sm Nd studies of Norwegian eclogites." Chemical Geology: Isotope Geoscience section 52(2): 249-271.

39. **Hirth, G. and J. Tullis (1992).** "Dislocation creep regimes in quartz aggregates." Journal of structural geology 14(2): 145-159.

40. **Hodges, K. and P. Crowley (1985).** "Error estimation and empirical geothermobarometry for pelitic systems." American Mineralogist 70(7-8): 702-709.

41. **Holtz, F. and W. Johannes (1991).** "Effect of tourmaline on melt fraction and composition of first melts in quartzofeldspathic gneiss." European Journal of Mineralogy 3(3): 527-536.

42. **Huang, W.-L. and P. J. Wyllie (1975).** "Melting Reactions in the System to 35 Kilobars, Dry and with Excess Water." The Journal of Geology: 737-748.

43. **Janák, M., et al. (2012).** "UHP metamorphism recorded by kyanite-bearing eclogite in the Seve Nappe Complex of northern Jämtland, Swedish Caledonides." Gondwana Research.

44. **Jen, L. and R. Kretz (1981).** "Mineral chemistry of some mafic granulites from the Adirondack region." The Canadian Mineralogist 19(3): 479-491.

45. **Kawakami, T. (2004**). "Tourmaline and boron as indicators of the presence, segregation and extraction of melt in pelitic migmatites: examples from the Ryoke metamorphic belt, SW Japan." Transactions of the Royal Society of Edinburgh: Earth Sciences 95(1-2): 111-123.

46. **Kearey, P. (2001).** "The new Penguin dictionary of geology." Penguin Global.

47. **Krogh, E., et al. (1990).** "Eclogites and polyphase P–T cycling in the Caledonian Uppermost Allochthon in Troms, northern Norway." Journal of Metamorphic Geology 8(3): 289-309.

48. **Krosse, S. (1995).** Hochdrucksynthese, stabilität und eigenschaften der borsilikate dravit und kornerupin sowie darstellung und stabilitätsverhalten eines neuen Mg-Al-borates.

49. **Landmark, K. (1973).** "Beskrivelse til de geologiske kart Tromsø og Målslev." Universitetet i Tromsø. Tromsø Museum.

50. **Le Breton, N. and A. B. Thompson (1988).** "Fluid-absent (dehydration) melting of biotite in metapelites in the early stages of crustal anatexis." Contributions to Mineralogy and Petrology 99(2): 226-237.

51. **Lindahl, I., et al. (2005).** "The geology of the Vaddas area, Troms: a key to our understanding of the Upper Allochthon in the Caledonides of northern Norway." NORGES GEOLOGISKE UNDERSOKELSE 445: 5.

52. **Lindstrom, M., (1988)**. “Geochemical studies of intrusive rocks in Ofoten.” Thesis, Univ. Tromso

53. **Lindstrøm, M. and A. Andresen (1992).** "Early Caledonian high-grade metamorphism within exotic terranes of the Troms Caledonides?" Norsk geologisk tidsskrift 72(4): 375-379.

54. **Lister, G. and A. Snoke (1984).** "SC mylonites." Journal of structural geology 6(6): 617-638.

55. **MacKenzie, W. S., et al. (1996).** "Atlas d'initiation à la pétrographie: avec 180 photos en couleurs de roches et minéraux en lames minces. " Masson.

56. **McClay, K. R., et al. (1987).** “The mapping of geological structures.” Open University Press.

57. **McClelland, W. C., et al. (2006).** "U-Pb SHRIMP geochronology and trace-element geochemistry of coesite-bearing zircons, North-East Greenland Caledonides." SPECIAL PAPERS-GEOLOGICAL SOCIETY OF AMERICA 403: 23.

58. **Meinhold, G. (2010).** "Rutile and its applications in earth sciences." Earth-Science Reviews 102(1): 1-28.

59. **Minsaas, O. and B. Sturt (1985).** "The Ordovician-Silurian clastics sequence overlying the Lyngen Gabbro Complex, and its environmental significance." The Caledonide Orogen:-Scandinavia and related areas 1: 569-577.

60. **Nardini, L. (2013)** “Metamorphic evolution and relationship between deformation and metamorphism in the Nordmannvik nappe in lyngenfjord area, north of lyngseidet". MsC Thesis. Institutt for Biologi or Geologi. University of Tromsø.

61. **Ota, T., et al. (2008).** "Tourmaline breakdown in a pelitic system: implications for boron cycling through subduction zones." Contributions to Mineralogy and Petrology 155(1): 19-32.

62. **Padget, P. (1955).** “The geology of the Caledonides of the Birtavarre region, Troms, Northern Norway.” I kommisjon hos Aschehoug.

63. **Passchier, C. W. and R. A. Trouw (2005).** “Microtectonics.” Springer Verlag.

64. **Pattison, D. R. and R. J. Tracy (1991).** "Phase equilibria and thermobarometry of metapelites." Reviews in Mineralogy and Geochemistry 26(1): 105-206.

65. **Quenardel, J. M. (1978).** "Geologie de la rive orientale du Lyngen Fjord (Caledonides de Norvege du Nord)"**.** Comptes rendus du Congrès national des sociétés savantes: Section des sciences, Bibliothèque nationale, Université Paris Sud, Orsay.

66. **Ramberg, H. and H. Sjöström (1973).** "Experimental geodynamical models relating to continental drift and orogenesis." Tectonophysics 19(2): 105-132.

67. **Robbins, C. and H. Yoder Jr (1962).** "Stability relations of dravite, a tourmaline." Carnegie Inst Wash Yearb 61: 106-107.

68. **Roberts, D. (1983).** "Devonian tectonic deformation in the Norwegian Caledonides and its regional perspectives." Bull. Nor. Geol. Unders 380: 85-96.

69. **Roberts, D. (2003).** "The Scandinavian Caledonides: event chronology, palaeogeographic settings and likely modern analogues." Tectonophysics 365(1): 283-299.

70. **Schreyer, W., et al. (1972).** "Carbonate-orthopyroxenites (sagvandites) from Troms, northern Norway." Lithos 5(4): 345-364.

71. **Simpson, C. and S. M. Schmid (1983).** "An evaluation of criteria to deduce the sense of movement in sheared rocks." Geological Society of America Bulletin 94(11): 1281-1288.

72. **Spear, F. S., et al. (1999).** "P-T paths from anatectic pelites." Contributions to Mineralogy and Petrology 134(1): 17-32.

73. **Spicer, E. M., et al. (2004).** "The low-pressure partial-melting behaviour of natural boron-bearing metapelites from the Mt. Stafford area, central Australia." Contributions to Mineralogy and Petrology 148(2): 160-179.

74. **Steltenpohl, M. G. and J. M. Bartley (1988).** "Cross folds and back folds in the Ofoten-Tysfjord area, north Norway, and their significance for Caledonian tectonics." Geological Society of America Bulletin 100(1): 140-151.

75. **Stipp, M., et al. (2002).** "The eastern Tonale fault zone: a 'natural laboratory'for crystal plastic deformation of quartz over a temperature range from 250 to 700 C." Journal of structural geology 24(12): 1861-1884.

76. **Stipp, M., et al. (2010).** "A new perspective on paleopiezometry: Dynamically recrystallized grain size distributions indicate mechanism changes." Geology 38(8): 759-762.

77. **Stipp, M. K. (2001).** "Dynamic recrystallization of quartz in fault rocks from the Eastern Tonale Line (Italian Alps)."

78. **Sturt, B., et al. (1978).** "The Finnmarkian phase of the Caledonian orogeny." Journal of the Geological Society 135(6): 597-610.

79. **Torsvik, T., et al. (1996).** "Continental break-up and collision in the Neoproterozoic and Palaeozoic—a tale of Baltica and Laurentia." Earth-Science Reviews 40(3): 229-258.

80. **TWISS, R. J. and E. M. MOORES (2007).** "Structural Geology." Freeman.

81. **Van Hinsberg, V. J., et al. (2011).** "Tourmaline: an ideal indicator of its host environment." The Canadian Mineralogist 49(1): 1-16.

82. **Vernon, R. H. and G. L. Clarke (2008).** "Principles of metamorphic petrology." Cambridge University Press.

83. **Von Goerne, G., et al. (1999).** "Hydrothermal synthesis of large dravite crystals by the chamber method." European Journal of Mineralogy 11(6): 1061-1077.

84. **Werding, G. and W. Schreyer (1984).** "Alkali-free tourmaline in the system MgO-Al_2O_3 -B_2O_3 -SiO_2 -H_2O " Geochimica et Cosmochimica Acta 48(6): 1331-1344.

85. **Zwaan, K., et al. (1998).** "Geologisk kart over Norge, berggrunnskart TROMSØ, M 1: 250.000." Norges geologiske undersøkelse.

86. **Zwaan, K. and D. Roberts (1978).** "Tectonostratigraphic succession and development of the Finnmarkian nappe sequence, North Norway", Universitetsforlaget.

7 ANNEXE

List of the samples mentioned in this thesis. Rock type and GPS coordinates are given.

Sample reference	Rock type	GPS coordinates
RB 3	Mafic gneiss (high grade)	N 69°25'22" ; E 020°09'22"
RB 16B	Garnet-sillimanite gneiss (high grade)	N 69°23'21" ; E 020°06'51"
RB 16E	Garnet-kyanite-mica gneiss (high grade)	N 69°23'21" ; E 020°06'51"
RB 25	Phyllite	N 69°40'48" ; E 020°15'38"
RB 26	Garnet-kyanite-mica gneiss	N 69°40'43" ; E 020°15'57"
RB 27	Garnet-kyanite-mica gneiss	N 69°40'38" ; E 020°16'00"
RB 28	Garnet-kyanite-mica gneiss	N 69°40'37" ; E 020°16'00"
RB 33	Garnet-sillimanite gneiss (high grade)	N 69°38'53" ; E 020°18'30"
RB 38	Metamafic lens	N 69°36'17" ; E 020°19'17"
RB 39B	Garnet-kyanite-mica gneiss	N 69°36'14" ; E 020°19'11"
U1	Leucosome	N 69°36'02" ; E 020°18'43"
K1	Phyllite	N 69°40'49" ; E020°15'44"
K2	Garnet-kyanite-mica gneiss	N 69°40'43" ; E020°15'57"
K4	Garnet-kyanite-mica gneiss	N 69°40'43" ; E020°15'57"
K5	Garnet-kyanite-mica gneiss	N 69°40'38" ; E020°15'60"
K7	Leucosome	N 69°38'52" ; E020°18'40"
K8	Garnet-kyanite-mica gneiss	N69°37'25" ; E020°20'49"
K9	Metamafic lens	N69°37'25" ; E020°20'49"